

University of Alberta

**Pitch Production Using Solvent Extraction of Coal:
Suitability as Carbon Anode Precursor**

by

Mehdi Mohammad Ali Pour

A thesis submitted to the Faculty of Graduate Studies and Research
in partial fulfillment of the requirements for the degree of

Master of Science
in
Chemical Engineering

Chemical and Materials Engineering

© Mehdi Mohammad Ali Pour
Fall 2009
Edmonton, Alberta

Permission is hereby granted to the University of Alberta Libraries to reproduce single copies of this thesis and to lend or sell such copies for private, scholarly or scientific research purposes only. Where the thesis is converted to, or otherwise made available in digital form, the University of Alberta will advise potential users of the thesis of these terms.

The author reserves all other publication and other rights in association with the copyright in the thesis and, except as herein before provided, neither the thesis nor any substantial portion thereof may be printed or otherwise reproduced in any material form whatsoever without the author's prior written permission.

Examining Committee

Rajender Gupta, Chemical and Materials Engineering, University of Alberta

Arno de Klerk, Chemical and Materials Engineering, University of Alberta

Amit Kumar, Mechanical Engineering, University of Alberta

ABSTRACT

Albertan coal has been used to produce extracts as precursor for production of anode coke. Coal extractability was studied using digestion with Tetralin in a 500 ml reactor. Different operating conditions were tried and optimum conditions were chosen for runs with coal-derived solvents. Extracts from runs with coal-derived solvents and their hydrotreated versions were distilled and heat treated to produce pitches as coke precursors. Coking experiments were performed using a molten salt bath furnace. Coal, solvents, pitches and cokes were characterized to study the effects of process chemistry on coke anisotropy. Coke anisotropy was studied using image analysis of polarized light optical micrographs and x-ray diffraction. Aromaticity of the pitch was found to be the key parameter controlling coke anisotropy. Solvent was found to be the most important factor contributing to pitch aromaticity. Heat treated products of high aromaticity yield the highest coke conversion and anisotropy.

ACKNOWLEDGEMENTS

This research was made possible through the financial as well as technical contribution from Sherritt technologies. This work was part of a large scale project for production of carbon anode materials from coal.

The author would like to thank his research supervisor Dr. Rajender P. Gupta for his encouragement, guidance and support. Additionally, many thanks to other group members of the solvent extraction project: Sun Ping, Hassan Katalambula, Shahnaz Begum and John Peter for their great contribution in different aspects of the project from conducting the digestion runs to the characterization part.

The author also wishes to thank Center for Oil Sand Innovation especially Professor Murray Gray and Mr. Arash Karimi for providing the coking facility and assistance in conducting the coking experiments.

TABLE OF CONTENTS

CHAPTER1 – INTRODUCTION	1
1.1. RESEARCH OBJECTIVE	4
CHAPTER 2 – BACKGROUND	6
2.1. Carbon and Carbonaceous Materials	6
2.2. Carbon Materials in Anode Manufacture	8
2.3. Pitches	10
2.4. Coke.....	12
2.5. Carbonization and Carbon Anisotropy	14
2.6. Coal : A Source of Carbon	18
2.7. Coal Processing for Carbon Production.....	21
2.7.1. Pyrolysis.....	21
2.7.2. Indirect Liquefaction	22
2.7.3. Direct Liquefaction	23
2.7.4. Direct Liquefaction Mechanisms	24
2.7.5. Direct Liquefaction Parameters	28
2.8. Coking and Development of Anisotropic Structure.....	34
2.9. Characterization of Coke Anisotropy.....	38
2.9.1. Polarized Light Optical Microscopy.....	38
2.10. X-ray Diffraction (XRD)	47
2.10.1. XRD Fundamentals.....	47
2.10.2. XRD in Study of anisotropy in Carbon Materials	50
2.11. Summary of Background Remarks.....	53
CHAPTER 3 – EXPERIMENTAL PROCEDURE	54
3.1. Materials	55
3.2. Equipments	57
3.3. Liquefaction Reactions	59
3.3.1. Reactor Preparation.....	59
3.3.2. Reactor Charging	60
3.3.3. Coal Digestion / Liquefaction	60
3.3.4. Reactor Washout	61
3.3.5. Filtration	61
3.3.6. Soxhlet Extraction	62
3.3.7. Distillation	63
3.4. Operating Parameters of Coal Liquefaction.....	65
3.5. Coking Experiments.....	70
3.6. Calcination Experiments	75
3.7. Analytical Testing	76
3.7.1. Elemental Analysis	76

3.7.2. Softening Point	76
3.7.3. Proton NMR	77
3.7.4. Ash Test	77
3.7.5. Optical Microscopy	79
3.7.6. X-ray Diffraction	80
3.7.7. X-ray Line Profile Analysis	80
CHAPTER 4 – RESULTS AND DISCUSSION	83
4.1. Solvent Characterization.....	83
4.2. Effect of Liquefaction Parameters	85
4.3. Coking Yields.....	97
4.4. Image analysis of Coke Micrographs	100
4.5. X-ray Diffraction Studies	108
CHAPTER 5 – CONCLUSIONS AND RECOMMENDATIONS	112
5.1. Conclusions	112
5.2. Recommendations	115
REFERENCES	118
APPENDIX A: MASS BALANCES	124
APPENDIX B: SELECTED OPTICAL MICROGRAPHS.....	130
APPENDIX C: TYPICAL X-RAY DIFFRACTION CALCULATIONS	135

LIST OF TABLES

Table 2.1. Characteristics of Various Commercial Pitches	12
Table 2.2. ASTM Standard D388-5 for Coal Rank Classification	19
Table 2.3. Elemental Analysis of Various Coal Ranks	20
Table 2.4. Fundamental properties important in coal liquefaction	28
Table 2.5. Optimum solvent parameter ranges for effective dissolution	33
Table 2.6. Optical texture classification according to Marsh et al	40
Table 2.7. Classification of anisotropic texture in green coke according to Mochida et al	41
Table 2.8. Classification of anisotropic texture in Calcined coke according to Mochida et al	41
Table 2.9. (OTI) values for use in equation 2.2	42
Table 3.1. Analysis of coal valley	55
Table 3.2. Solvent Hydrotreatment Conditions	56
Table 3.3. Liquefaction Parameters for Tetralin Runs	66
Table 3.4. Distillation conditions for different batches of Tetralin runs	67
Table 3.5. Liquefaction conditions for runs using CTD as solvent	67
Table 3.6. Distillation Conditions for Coal Extracts of CTD Runs	68
Table 3.7. Liquefaction conditions for runs using hydrotreated CTD and other solvents	69
Table 3.8. Distillation Conditions for Coal Extracts of CTD Runs	70
Table 4.1. Elemental and NMR analysis data for solvents	84

LIST OF FIGURES

Figure 2.1. Crystal structures of carbon	7
Figure 2.2.A. Hall- Héroult cell	9
Figure 2.2.B. Söderberg Cell	9
Figure 2.3. Polarized light optical textures of isotropic and anisotropic cokes	14
Figure 2.4. Macromolecular model of carbon precursors	15
Figure 2.5. Sketch of Coronene and dicoronene	15
Figure 2.6. Liquid crystal textures of various orders	17
Figure 2.7. Solvolysis Mechanism of Coal Liquefaction	25
Figure 2.8. Dependence of coal liquefaction yield on hydrogen transfer abilities of different solvents	26
Figure 2.9.A. Free radical model of coal liquefaction	26
Figure 2.9.B. Solvent-mediated hydrogenolysis model of coal liquefaction	26
Figure 2.10. Reaction pathways for bituminous and subbituminous coals	29
Figure 2.11. Dependence of liquefaction conversion on reactive maceral content of coal	30
Figure 2.12. Conversion of a subbituminous coal vs. its Ash Content	31
Figure 2.13. Yield of different liquefaction product fractions vs. consumed hydrogen in solvent hydrotreatment	34
Figure 2.14. Temperature and Composition Effects of Structural Evolution	35
Figure 2.15. Carbonization Scheme of Delayed Coking	36
Figure 2.16. Stages of increasing order during Carbonization	38
Figure 2.17. Conversion steps in image analysis of coke texture	45
Figure 2.18. Pixel pattern used in calculation of fiber index	46
Figure 2.19: Fiber index and mosaic index values calculated for cokes with different levels of anisotropy	47
Figure 2.20. Evolution of crystal order in a carbonaceous material as evidenced by x-ray diffraction	52
Figure 3.1. Flow diagram showing the outline of experimental procedure	54
Figure 3.2. 500 ml reactor used in liquefaction experiments	57
Figure 3.3. Control console of the reactor	57
Figure 3.4. Filtration unit and Soxhlet Condenser	57
Figure 3.5. Distillation assembly	58
Figure 3.6. Molten salt bath container	59
Figure 3.7. Molten salt bath container and coking setup.....	59
Figure 3.8. Figure 3.8. Bags of residue in Soxhlet	62
Figure 3.9. Detailed view of Experimental Procedure.....	65
Figure 3.10. Schematic View of the coking setup	71
Figure 3.11.A. The quartz tube used for coking the pitch	72
Figure 3.11.B. vacuum fitting used for sealing	72

Figure 3.12. Quartz tube and Nitrogen flow rate during purge stage	73
Figure 3.13. Violent devolatilization in the start of coking experiment.....	74
Figure 3.14. Temperature profile used for calcination of selected cokes	75
Figure 3.15. Muffle furnace and the crucibles used for ash measurements	78
Figure 3.16. (002) Line profile analysis of commercial graphite	82
Figure 4.1. wt% of Nitrogen and Sulfur in hydrotreated solvents	84
Figure 4.2: Effect of digestion temperature on conversion for Tetralin runs	85
Figure 4.3. Effect of Hydrogen Pressure on Conversion.....	86
Figure 4.4. Effect of residence time on conversion for Tetralin Runs	87
Figure 4.5. Effect of liquefaction solvent on conversion	88
Figure 4.6. Effect of reaction gas on coal conversion for Tetralin	89
Figure 4.7. Effect of Solvent H/C ratio on Coal Conversion	90
Figure 4.8. Effect of Solvent aromaticity on Coal Conversion	91
Figure 4.9. Effect of digestion temperature on H/C and aromaticity of pitch for Tetralin runs	92
Figure 4.10. Effect of solvent on Pitch aromaticity	93
Figure 4.11. Effect of distillation severity on Pitch aromaticity	95
Figure 4.12. Effect of heat treatment on Pitch aromaticity	95
Figure 4.13. Effect of distillation severity on Pitch softening point	96
Figure 4.14. Softening Point – Aromaticity correlation for various pitches	96
Figure 4.15. Dependence of coke yield on pitch aromaticity	97
Figure 4.16. Effect of Heat Treatment on Dependence of coke yield on pitch aromaticity	98
Figure 4.17. Relationship between coke yield and softening point of Pitch	99
Figure 4.18. Coke micrograph – Pitch#11B2	100
Figure 4.19. Coke Micrograph – Pitch #9B2	100
Figure 4.20. Coke micrograph – Pitch#23B2	100
Figure 4.21. Coke micrograph – Pitch#30B2	100
Figure 4.22. Conversion steps in image analysis of one of the cokes	101
Figure 4.23. Graphical user interface of the computer program developed for calculation of image analysis indices	103
Figure 4.24. Dependence of Coke Fiber Index on Pitch Aromaticity	104
Figure 4.25. Dependence of Coke Mosaic Index on Pitch Aromaticity	105
Figure 4.26. Dependence of Coke Fiber Index on Pitch H/C	106
Figure 4.27. Dependence of Coke Mosaic Index on Pitch H/C	106
Figure 4.28. Dependence of Coke Anisotropy Indices on FLMO of Pitch	107
Figure 4.29. X-ray Diffraction Patterns of coal and residue	108
Figure 4.30. Composition of minerals in low temperature ash of coal and residue	109
Figure 4.31. Crystal structure evolution of carbon from pitch to calcined coke	109
Figure 4.32. Relation between crystallite height (L_c) and Fiber index	111
Figure 4.33. Relation between crystallite height (L_c) and Mosaic index	111

CHAPTER 1

INTRODUCTION

Carbon has been an important part of human civilization from its early use as the major component in traditional fuels like wood and charcoal to its widespread existence in modern materials like polymers, pharmaceuticals and other carbonaceous artifacts derived from natural occurring resources like petroleum, coal, etc. Carbon industry is an important section of modern technological society whose main focus is to provide carbonaceous materials of different types and properties to industries relying on these materials for their relevant purposes. In recent years, the carbon products industry has been going through a major period of change and adaptation mostly with respect to its source materials.

The most common uses of carbonaceous materials are as fuels from natural resources like petroleum, coal, natural gas that have deposits scattered in different areas of the world. Petroleum is also the major source of carbon used in petrochemical products, coke, tars, asphalts, etc. There are, however, some problems associated with the traditional use of these materials. Coal-fired power plants are generally seen as environmentally unfavorable and the quality of petroleum derived carbons can no further satisfy the requirements of the consuming industries mostly due to the increasing tendency of refineries for

processing of crudes with high level of impurities like sulfur, nickel, vanadium and other mineral matter.

Coal has shown a great potential for replacement of petroleum in production of different types of carbon materials. Coal is an abundant resource which is quite inexpensive compared to average price of petroleum in the past few years. Coal has already been used for non-fuel purposes in production of metallurgical coke, coal tars, pitches and activated carbons. However, all of these are either direct or indirect product of metallurgical coking. The high level of green house gas emissions produced by coking ovens of metallurgical coke production has led to creation of another incentive for finding an alternative process for production of these materials. Coal tar pitch, the heaviest fraction of coal tar distillation, is the most important by product of coking ovens. It is used as a binder in production of carbon anodes for aluminum industry, as an impregnator for increasing density and strength of carbon products and also for production of nuclear-grade graphite and carbon foams. This material can also be produced from petroleum (petroleum-pitch) and through synthesis of coal in solvent extraction processes. Pitches can also be coked to be used in manufacture of anodes.

Metal production industries greatly rely on carbon-based materials as a feedstock for production of electrodes used in their different processes. Electrodes used in electric arc furnaces of scrap-based steel making and prebaked anodes used in electro-winning cells are all carbonaceous materials synthesized from a variety of natural resources.

Delayed coke, a by-product of petroleum refining process, is usually used for the production of anodes used in aluminum industry. Anodes are usually made of 60-70% of coke as filler, 10-15% coal tar pitch as binder and anode butts (spent anodes) as recycled materials. Due to increasing percentage of contaminations, only a small fraction of delayed cokes are now suitable for production of anodes as result an alternative method for production of anode coke is greatly desired.

Coal to liquid conversion processes like solvent extraction and liquefaction can produce a mineral free organic material that has the required properties for use as a precursor to anode coke. Liquefaction can be done directly or indirectly. In indirect liquefaction, coal is converted to a syngas mixture ($H_2 + CO$) and tar byproducts. Syngas is then used to produce variety of hydrocarbon liquids by syngas-to-methanol or Fisher-Tropsch technologies. Direct liquefaction bypasses the syngas formation stage and coal liquid is directly produced using thermal treatment of a mixture of coal and solvent usually under high pressure of hydrogen gas. Usually hydrogen-donor solvents are used to break the macromolecular structure of coal and produce lower molecular weight organic species.

Tetralin (1, 2, 3, 4-tetrahydronaphthalene) and NMP (N-methyl-2-pyrrolidone) are the common solvents used in liquefaction research. These are very effective liquefaction solvents but they have a number of disadvantages which make their commercial use rather unpractical. The high price is the main reason. In addition, Tetralin as a hydrogen donor solvent loses its hydrogen and becomes naphthalene therefore solvent recycling requires a hydrotreatment stage

which is a very expensive process. In case of NMP removal of used solvent and purification stages makes the process more costly.

Industrial byproduct liquids like coal and petroleum-derived oils can be used to replace the expensive commercial solvents. A mineral-free organic feed can be obtained by separating the soluble and insoluble fractions. Here part of the solvent is incorporated into the coal structure and the mixture is co-processed into a pitch-like feed suitable for coke making. Another advantage is that the liquefaction process can be done under much milder conditions compared to standard liquefaction processes because the average molecular weight required for coke precursor is quite higher than those observed in liquefied fuel products.

As the delayed petroleum coke quality decreases, the consumption of carbon electrode and consequently CO₂ evolution per ton of aluminum produced increases. This leads to higher cost of aluminum production and more emission of green house gases. Subbituminous coals of low sulfur content are abundantly available in the province of Alberta. Considering the needs of aluminum industries in North America, it is of great interest to develop processes to use these coals for production of coke precursor feedstock.

1.1. RESEARCH OBJECTIVE

In this work, the objective is to investigate the suitability of feedstock produced by solvent extraction of the Albertan subbituminous coal for use in anode coke production. Effect of digestion conditions, type and chemistry of solvents used for

extraction, solvent hydrogenation on the properties of produced feedstock are investigated. A narrow range of digestion conditions were tried as the optimum conditions for this type of process are available from previous works of different researchers. Digestion experiments were performed using a 500 ml stirred reactor and the products extracted using Tetrahydrofuran (THF). Vacuum filtration was used to separate the insoluble parts. Conversion was calculated using the THF-insoluble fraction. The digested feedstocks were coked to evaluate their suitability for use as anode precursor. For this purpose, a number of characterization techniques like optical microscopy, x-ray diffraction and thermogravimetric analysis were used.

CHAPTER 2

BACKGROUND

2.1. Carbon and carbonaceous materials

Carbon is the sixth element of the periodic table. It is one of the least abundant elements in the earth's crust but the fourth most abundant element in the universe by mass after hydrogen, helium and oxygen. It exists in all known forms of life and is the second most abundant element in human body after oxygen [1].

Its extraordinary ability to combine with itself and other chemical elements is the basis of organic chemistry and life. This chemical adaptability has also caused a great diversity in structural forms of solid carbon. Different numbers of the carbon-carbon bond can give the materials a range of different properties. A compound with one or two of these bonds can exist in the vapor phase like ethane, ethylene whereas the existence of hundreds or thousands of the same bond gives rise to polymeric materials like polyethylene, nylon [2].

The unique ability of carbon to bond with itself via sp^3 , sp^2 and sp hybridization has resulted in an immense variety of possibilities to form allotropes. In its natural elemental form, Carbon exists in three different allotropic structures of Graphite, Diamond and Fullerene (Figure 2.1). Diamond is the tetrahedral crystalline form of Carbon which forms as a result of high temperatures and pressures over long periods of time and is considered a very

precious stone. Fullerene is the arrangement of carbon atoms in a soccer ball shaped sphere with varying number of carbons ranging from C_{60} to C_{70} . Graphite is the most abundant naturally occurring form of Carbon which has a hexagonal crystal structure. The basis of the crystal structure is the graphene or carbon layer plane i.e. an extended hexagonal array of Carbon atoms with sp^2 σ and delocalized π bonding. Hexagonal graphite consists of stack of planes arranged in ABABAB... sequence. These planes are held together using van de Waals' forces. The same type of binding and atomic forces is true for the rhombohedral graphite which follows the ABCABCABC ... sequence but is much less common compared to hexagonal graphite [3]. The crystal structure of graphite gives it a number of mechanical and physical properties that makes it a valuable commodity. This includes electrical and thermal conductivity, hardness and porosity.

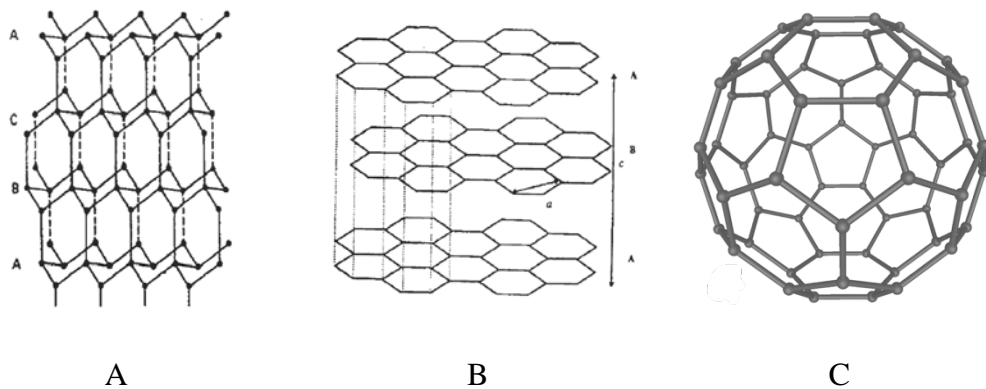


Figure 2.1. Crystal Structures of Carbon: A) Cubic Diamond, B) Hexagonal Graphite, C) Fullerene [4]

Most of the Carbon materials are based on the graphite structure and therefore understanding the properties of graphite are important for controlling the

properties of these materials. One of the main features of graphite that is crucially important is the concept of anisotropy. Anisotropy of graphite originates from the difference in carbon-carbon bonding parallel and perpendicular to graphene layers. A carbonaceous material can therefore have anisotropic properties with level of anisotropy going higher as the crystal structure gets closer to that of graphite. In practice carbons can be graphitizable or non-graphitizable with graphitizability defined as the ability to develop graphite structure upon heating up to 3000°C. Graphitizable carbons are usually named as Soft Carbons whereas Hard Carbon is used to describe the non-graphitizable ones [5].

2.2. Carbon Materials in Anode Manufacture

Manufacture of anodes for use in electrowinning of aluminum is one of the large scale uses of carbon materials. This is a \$33 billion business in United States alone. Nowadays, all commercial production of aluminum is done in Hall-Héroult cell. Two major types of cells are currently in use: those employing prebaked carbon anodes (Figure 2.2.A) and those employing self-baked Söderberg anodes (Figure 2.2.B). The prebaked anode cell is much more preferred because creation of anode from liquid pitch in Söderberg process involves emission of high amounts of pollutants. In both type of cells, aluminum recovery is achieved from a molten electrolyte of alumina and cryolite. The electrochemical process uses the anode as a source of carbon and the carbon is sacrificially converted to carbon dioxide according to equation 2.1 [6].

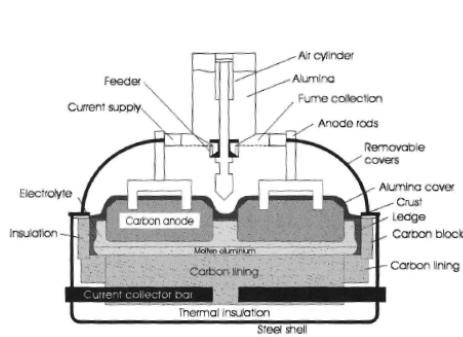
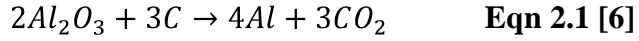


Figure 2.2.A: Hall- Héroult cell [7]

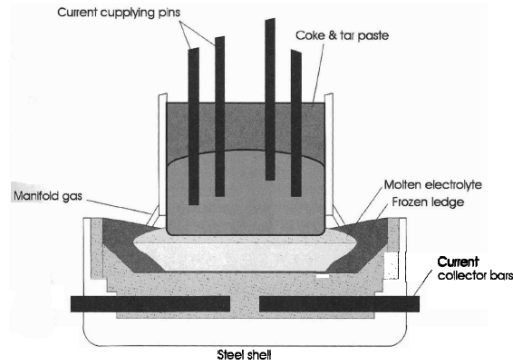


Figure 2.2.B: Söderberg Cell [7]

Production of 1 million tons of aluminum consumes up to 500 tons of anode and since the production of aluminum is considerable, huge quantities of anode material are required each year. Because ash from carbon can contaminate either the aluminum produced or the electrolyte, high purity carbon is required. Certain impurities such as vanadium are harmful in that they catalyze air burning of the carbon. High sulfur is also harmful in that it can affect the life of the anode by increasing the puffing tendency which is the irreversible expansion of the materials due to release sulfur and nitrogen compounds. Sulfur is also known to affect the reactivity of anodes. Other impurities such as phosphorous can accumulate in the electrolyte and undergo cyclic redox reactions consuming the electric current without producing product. Petroleum coke is the traditional choice for carbon anodes if it can satisfy the low level impurities required. Prebaked electrodes may be of two types: graphitized and carbonaceous. Carbonaceous electrodes have higher specific resistance ($\sim 40 \mu\Omega\text{m}$) than graphite electrodes ($\sim 10 \mu\Omega\text{m}$), but bear higher compression loads. Delayed coke

produced at 500°C is calcined at 1200°C to remove volatile constituents and increase its density before it is blended into the anode mix. After calcinations, the coke is ground and mixed with crushed spent anodes and sufficient coal tar pitch to allow molding into anode blocks by pressing or by vibrating. Blocks are baked at 1000-1200°C, causing pitch to carbonize, and forming strong carbon blocks. Electrodes after this stage are sometimes called green and are ready for use. For graphitized electrodes, an additional graphitization stage at temperatures above 2700°C exists to make highly graphitic bodies. These blocks are made with one or more sockets into each of which is fastened a steel stub by pouring cast iron around it. These stubs both conduct electric current into the anode and support the anodes in the cell. The cost of petroleum coke for prebaked carbon anodes in the United States was about \$0.20/kg in 1996 [7].

2.3. Pitches

Pitch is one of the chief compounds in manufacture of all carbonaceous materials including carbon anodes. It's been used as the main choice of binder in fabrication of electrodes used in aluminum and steel industries. Like tars, pitches are also considered a member of the bituminous materials family with coal and petroleum as other members but what distinguishes the pitches is that they're made through a destructive distillation process of organic precursors. These precursors can virtually be any organic material including wood, coal and petroleum. Each tar or pitch is distinct due to the distinct nature of the precursor

even coals of different mines can produce different tars and pitches. Pitch is the heavy fraction that remains after the distillation of tars and removal of the volatile matter and is a complicated mixture of organic compounds mostly made up of polycyclic aromatic hydrocarbons [8].

In carbon anode manufacturing process, coal tar pitch is the type of pitch that has the most widespread use as a binder. Coal tar pitch is a byproduct of metallurgical coking ovens. In recovery coke ovens, volatiles are collected along with any tar like materials. Coal tar is then distilled to remove some of the lighter compounds which are used to make tar acids/bases, creosotes and naphthalenes. The heavy matter left after distillation is called coal tar pitch a residue with a typical softening point of 110°C. Depending on the application for which the pitch is produced, further modifications can be done using thermal treatment, air blowing and solvent fractionation. Using careful thermal treatment, a specific type of pitch called mesophase pitch can be produced. Mesophase is a liquid crystalline phase of poly-aromatic hydrocarbons which occurs as result of molecular rearrangement during thermal treatment. Depending on duration of thermal treatment, percentage of mesophase can vary for a constant temperature. A pitch with 100% mesophase or bulk mesophase has the properties of an ordered solid and a fluid liquid state. This type of pitch is used extensively in for production of carbon fibers. In case of pitches used as binders or impregnators in carbon anode production, very low mesophase content if not no mesophase at all is required. This has implications in texture development during coking and

calcination which will be discussed later [9]. Table 2.1 lists the characteristics of some commercial binder and impregnation pitches.

	Binder Pitch			Impregnation Pitch		
Feedstock	Coal Tar	Coal Tar	Coal Tar	Petroleum	Coal Tar	Coal
Supplier	Allied	Aristech	Koppers	Ashland	Kawasaki	Mitsubishi
Softening Point(°C)	109.1	109.8	110.3	121.1	99.5	95.3
Coking Value (wt%)	58.5	57.6	58	49.1	50	44.3
Ash Content (wt%)	0.17	0.16	0.21	0.03	0	0.003
Sulfur (wt%)	0.61	0.62	0.59	3.1	0.41	0.43
Carbon (wt%)	93.84	92.84	93.83	91.25	92.7	92.49
Hydrogen (wt%)	3.66	4.42	3.92	5.08	4.44	4.27
% H_{aromatic}	85.4	85.8	86	55.5	86.1	82.8

2.4. Coke

Coke is the second major component in production of anode carbons as well as a few other carbonaceous materials. Coke has been used as a vital component of steel making technology since the very early years of this industry. Coking ovens produce the metallurgical coke from coal as the main feedstock. Modern coking ovens can have yields of up to 70% and they facilitate the recovery of volatile matter to produce a range of by-products as the main supplier of coal-derived feedstock used in carbon industry. These ovens are generally considered as environmentally and economically unfavorable with the present standards. That's why an alternative source for coal-derived feedstock seems quite necessary. Another type of coke, delayed coke is produced from petroleum-derived feedstock. Delayed coking is a thermal process designed to generate

distillates at high temperatures (~ 500°C) from heavy fractions of petroleum over long periods of time (12 to 36 h). It is a combination of continuous and batch processes to produce gas, gasoline, gas oils and coke. Coke yield of the process varies from 20 to 40% and about only 20% of the coke produced is suitable for the production of anodes in the aluminum industry. Provided the coke has the required composition i.e. low sulfur and metal content, the factor that greatly affects the suitability of coke for use in anode production is its level of anisotropy or degree of long range crystalline order in the carbon structure of the material. This is generally determined using optical microscopy with polarized light. Anisotropic cokes show large domains of flow texture under polarized light while isotropic phases are usually known by very fine textures (Figure 2.3) [11].

In addition to feedstock properties, the quality of delayed coke depends on the location in the coker drum where the final stage of coking occurs. Bottom and wall cokes usually do not have the required level of anisotropy. These cokes, also known as fuel and shot cokes are generally used as cheap fuels for cement kilns and utility industry. Worldwide about 80% of the coke produced is from these two types. Sponge coke is the type of coke that is calcined and sold to the aluminum industry. Needle coke is a highly anisotropic form of coke which is obtained from highly aromatic feedstock like FCC decant oil or solids-free coal tar pitches and is primarily used in fabrication of graphite electrodes used in electric arc furnaces of steel industry [12].

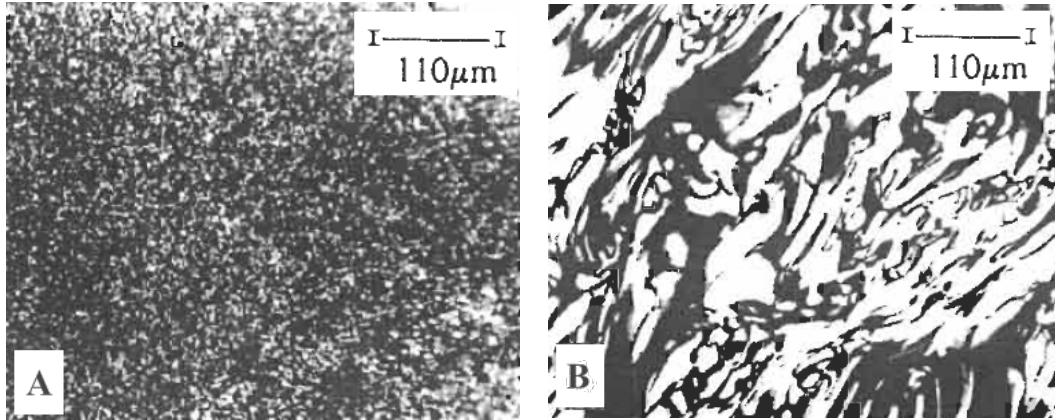


Figure 2.3. Polarized light optical texture of A) Isotropic and B) Anisotropic Cokes [11]

2.5. Carbonization and Carbon Anisotropy

The property that makes most of the carbonaceous materials suitable for application in different technologies like carbon anodes is the microstructural anisotropy. Anisotropy is defined as the directionality of properties in materials. Among crystalline solids, graphite has one of the highest degrees of anisotropy. For carbonaceous materials, degree of anisotropy is dependent upon the level of graphitization in them. To reach the graphitic structure, carbonaceous materials should undergo carbonization ($T < 2000^{\circ}\text{C}$), followed by graphitization ($2000^{\circ}\text{C} < T < 3000^{\circ}\text{C}$). Carbonization is a thermal process that involves compositional and structural changes in bituminous materials to attain the pre-graphitic structure. Any organic matter being made of C, H, O, N, S, it provides pure carbon by heteroatom release. During primary carbonization a part of heteroatom is released as volatiles, among which mostly hydrocarbons evaporate with a violent out gassing (defined as oil window). In most of organic materials, this process coincides with an increase in average molecular weight leading to

solidification which marks the end of primary carbonization. During secondary carbonization, only non condensable gases are produced (CH_4 , H_2) by aromatic CH group loss (defined as gas window). Various carbon precursors experience different reaction paths during carbonization depending on their H/C and O/C ratios. From a structural point of view however no classification can be made because none of the carbonaceous materials are truly amorphous and all have a two dimensional crystalline structure. Very low rank coals, kerogens, oil derivatives such as refinery residues, asphaltenes and pitches are described as macromolecules made of polyaromatic molecules. These molecules are connected into a continuum by various functional groups and they may or may not be stacked (Figure 2.4) [13].

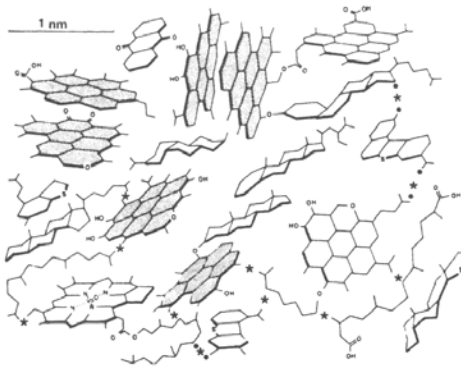


Figure 2.4. Macromolecular model of carbon precursors [13].

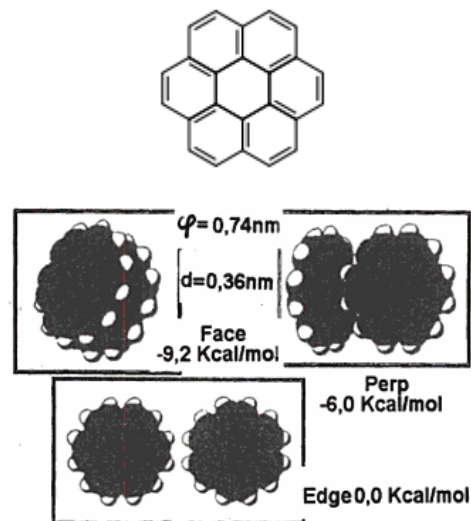


Figure 2.5. Sketch of Coronene and dicationene [14]

Carbonization starts with a marked softening which is due to breakage of the macromolecular structure. This breakage converts the material to a suspension of random elemental units in a light medium. These elemental units also called basic structural units (BSU) are the foundations of anisotropy in carbonaceous materials. BSU are made of two to four piled-up polyaromatic molecules less than 1 nm in diameter. Coronene is an example of the type of polyaromatic molecule that can take part in BSU and dicoronene is the smallest BSU possible (Figure 2.5) [15]. Ordering of BSU leads to formation of liquid crystals. Liquid crystals are the intermediate between liquid and crystals. Several models have been proposed for liquid crystals depending on the type of order that exists. Figure 2-6 shows the columnar, distorted columnar and nematic order of disc like units (mesogens) in liquid crystals with different columnar structure has the highest order while nematic is the least ordered structure. Mesogens associate into homogeneously oriented volumes limited by spherical or digitized contours. These associations are usually known under the name of local molecular orientation (LMO). Liquid crystals demix and coalesce during primary carbonization leading to a minimum in viscosity before the start of solidification. Upon solidification mesophase coalescence stops irreversibly to form mosaic bands that can be observed under optical microscope with polarized light as shown in Figure 2.3 [16].

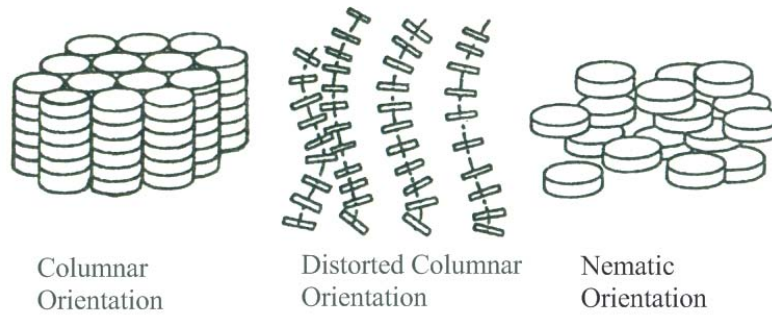


Figure 2.6. Liquid crystal textures of various orders [16]

Liquid crystals and their resultant LMO domains form the microstructural basis for anisotropy in carbonaceous materials. Like any other phase transformation, this ordering of molecules also follows the rules of thermodynamics and kinetics. If the conditions for coalescence and growth of LMO domains are created in the material system, the resultant microstructure will be coarse domains of high anisotropy [17]. This is very important when considering the carbonization (coking) technique in the manufacture of carbon artifacts. This way, different coke qualities from delayed coker can be explained in terms of heat transfer and fluid mechanics parameters. For a fixed feedstock composition, high cooling rates and lower residence time at high temperatures results in finer textures as it is the case for shot and fuel cokes where as sponge and needle coke form at areas where the longer residence times at favorable temperature, effective mass transfer due to turbulent conditions promote the coalescence and growth of LMO domains and therefore coarser and more anisotropic textures can be obtained. These effects are best reflected in polarized light micrographs of polished sections of carbonaceous materials. Scattering

technique like x-ray diffraction can also be used to study these microstructural effects [18, 19].

2.6. Coal: A Source of Carbon

Petroleum has been the main source material for production of carbon artifacts; however the trend in carbon industry is now in a transition to replace petroleum. Although petroleum still remains a chief competitor, Coal is the preferred option. As this study is focused on production of coke precursor from coal, knowledge of coal and coal processing techniques for production of carbonaceous materials is necessary.

Coal is an abundant yet complicated natural resource. The complexity arises from the high level of pollution that is associated with its utilization. The main focus of coal utilization technology has been on overcoming this environmental liability. Coal is the end product of a sequence of complex biological processes. As organic sediment, it is formed from partially decomposed (and subsequently metamorphosed) plant debris. The trace various plant species are identifiable in coal. Considering the wide variety of plant life, it's not surprising that coal differs markedly in composition from one point to another to such a high degree that pronounced differences in coals from one particular seam are not uncommon. In addition to wide variety of plant debris, many different chemical reactions that can occur during coal formation (coalification) also have a significant effect. The initial material formed from the plant debris is called peat. The progression of coal matter generally follows the following diagram [20]:

Peat → Lignite → Sub-Bituminous Coal → Bituminous Coal → Anthracite

Different levels of this diagram are different ranks of coal. Peat and lignite have the lowest degree of coalification and the lowest carbon content (60% - 70%). Bituminous coals usually have around 85% carbon which has lost a significant amount of oxygen in the molecular structure of the original material. Subbituminous coal has properties between lignite and bituminous. Anthracite as the highest rank coal has the highest degree of coalification and carbon content as high as 95%. ASTM standard specifies the following property values for different ranks of coal [21]:

Table 2.2. ASTM Standard D388-5 for Coal Rank Classification [21]				
Class	Group	Fixed Carbon ^a	Volatile Matter ^b	Heating Value ^c
Anthracite	Meta-anthracite	>98	<2	
	Anthracite	92-98	2-8	
	Semi-anthracite	86-92	8-14	
Bituminous	Low-Volatile	78-86	14-22	
	Medium-Volatile	69-78	22-31	
	High Volatile A	<69	>31	>32.557
	High Volatile B			30.232-132.557
	High Volatile C			26.743-30.232
Sub-Bituminous	Sub-Bituminous-A			>26.743
	Sub-Bituminous-B			24.418
	Sub-Bituminous-C			22.09
Lignitic	Lignite A			14.65 - 19.30
	Lignite B			<14.65

a. Dry, mineral matter-free basis, b. Dry, mineral matter-free basis, c. Mj/kg

Microscopically, coals can be classified into groups called macerals. Three main types of macerals are vitrinite, exinite and inertinite. Vitrinite macerals are typically derived from more woody tissues, while exinites come from the resins, fatty secretions, cuticles and spores from the plants. Inertinites are derived from the plant matter that has been partially carbonized during the peat stage of coalification. The maceral content of the coal the determination of which is the subject of petrographic classification has an important effect on coal processing through control over the convertible or soluble portions of the material [22].

Coal is a carbonaceous material but it contains hydrogen, oxygen, sulfur and nitrogen (heteroatoms) as well as inorganic mineral matter. Higher ranks coals generally have high carbon content and low heteroatom (O₂ in particular) while the reverse is true for low rank coals (Table 2.3).

Sample	Element, %wt (dry, ash free basis)				
	C	H	O	N	S
Meta-Anthracite	97.90	0.21	1.70	0.20	0.00
Anthracite	95.90	0.89	1.80	0.30	1.80
Semi-anthracite	90.50	3.90	3.40	1.50	0.70
Low Volatile Bituminous	90.80	4.60	3.30	0.70	0.60
Medium Volatile Bituminous	89.10	5.00	3.60	1.70	0.60
High Volatile Bituminous A	84.90	5.60	6.90	1.60	1.00
High Volatile Bituminous B	81.90	5.10	10.50	1.90	0.60
High Volatile Bituminous C	77.30	4.90	14.30	1.20	2.30
Sub-Bituminous A	78.50	5.30	13.90	1.50	0.80
Sub-Bituminous B	72.30	4.70	21.00	1.70	0.30
Sub- Bituminous C	70.60	4.80	23.30	0.70	0.60
Lignite	70.60	4.70	23.40	0.70	0.60

Mineral matter content of coal is measured using proximate analysis. This is usually done by converting the coal to ash and measure the weight percent remaining. Proximate analysis also gives the moisture and volatile content of the coal. Various standards exist for these measurements to make the results comparable and useable for practical applications [22].

2.7. Coal Processing for Carbon Production

Currently metallurgical coke is the largest non-fuel use of coals, primarily bituminous coals. Use of coal-derived liquids like tars and pitches is another major application. Reports are also available on use of mainly anthracites for production of activated carbons and graphite. For production of carbon materials however the major methods are Pyrolysis and liquefaction.

2.7.1. Pyrolysis

Pyrolysis is the heating up of coal at high temperatures in the absence of oxygen. This process drives-off the volatiles which can later be collected as a hydrogen-rich liquid and leaving a carbon-rich solid residue (either char or coke). Pyrolysis involves a breakage of the molecular structure of coal. First at around 400°C, aromatic clusters are broken apart, at higher temperatures (~ 450°C) aliphatic side chains and lower molecular weight fragments start to break apart.

These aliphatic compounds become the tar and gases that evolve during the process. The collected condensed matter is the pyrolysis product useable for carbon manufacture. The solid residue usually has higher mineral content than those required by most carbon product like anode-grade coke. Because high liquid yield is desired in these processes high heating rates are usually used. Rapid heating as is used in the flash pyrolysis method has been shown to considerably increase the total volatile matter for a constant temperature although the exact mechanism is not known yet [23]

2.7.2. Indirect Liquefaction

As the name implies, liquefaction is the process of liquefying the coal. This can be done directly which is by addition of a solvent or indirectly which is by production of synthesis gas (H_2 and CO) and then recombining into liquids. Indirect liquefaction of coal has long been used in the Fisher-Tropsch process for production of fuels. The process supplied most of the fuel required by the war machine of Nazi Germany. Conversion of syn-gas into liquids occurs in the presence of the Fisher-Tropsch catalyst. Fisher-Tropsch catalyst allows the process to be selective toward different hydrocarbons that can be produced. This includes gasoline, kerosene, diesel fuel, fuel oil, methanol or acetone. The produced liquids have the advantage of having minimal amounts of mineral matter. The chief disadvantage of the process is the production of a variety of by-products. This is due to fact that the gasification of coal is typically done with

steam and oxygen. In addition, as the process involves destruction of the original coal structure, it is considered an expensive process in terms of thermal efficiency [24].

2.7.3. Direct Liquefaction

There are two methods available for direct liquefaction of coal. Liquid conversion can either be done by catalytic hydrogenation of the coal or by dissolution of coal in an organic hydrogen donor solvent which is sometime also called solvent extraction. The first method shares the same disadvantages with indirect liquefaction and is more suitable for production of liquid fuels. The second method a commercial example of which is the Exxon Donor Solvent (EDS) process is more economically viable and has the flexibility of producing the desired product which in this case is heavy liquids suitable for coking. Direct liquefaction involves dissolution of the coal into an organic solvent which is usually a hydrogen-donor too. Once heated up to a high enough temperature and stirred, the solvent in the slurry can disperse the coal particles, break down the coal molecules, donate hydrogen, transfer hydrogen from gaseous atmosphere and therefore promoting the liquefaction of coal. The role of hydrogen is to stabilize the free radicals which are created as a result of heating and dissolution. The product of direct liquefaction is a liquid and solid residue. Solid residue is rich in mineral matter and it also contains some unconverted organic matter which is high molecular weight coal fragments that are not broken during the process.

Rather mild liquefaction conditions are usually used in the production of carbon precursors as an extensive break down of the original structure is not usually desired. Severe liquefaction conditions leads to production of the oil and gas fractions which is more desirable for fuel-related applications [25].

2.7.4. Direct Liquefaction Mechanisms

A vast literature exists on solvent extraction of coal dealing for the most part with the effect of solvent chemistry and coal structure on the mechanisms. Various mechanisms have been proposed to explain different effects observed in experiments. However as the process involves complicated components (solvent and coal) a universal mechanism that can rationalize the liquid conversion is not available yet. Most of the proposed mechanisms rely on the interaction of free radicals and hydrogen during the process [26].

When coal is mixed and stirred in a solvent at high temperature, a number of physical and chemical phenomena take place a combination of which leads to the final dissolution of coal. Dispersion of colloid particles of coal in the solvent can be considered as the initial stage of liquefaction process. At lower temperatures where thermal decomposition of coal is not possible, the physical processes play an important role. At these stages physical properties of coal may play an important role in the coal solubilization, the rate of diffusion of reagents into the matrix, the rate of diffusion of products out of the coal matrix, and the heat transfer to particles. Physical processes at higher temperatures may also

affect the chemical processes but as the temperature is increased chemical interactions become more important. Changes in particle size, surface area, viscosity and pore structure which occur during dissolution can all have important effects. The processes causing the major physical changes include thermal expansion of coal, adsorption of solvent, swelling caused by solvent, fragmentation and plasticization of coal, mass transfer and chemical reactions between coal and solvent.

Chemical reactions between coal and solvent play the major role at higher temperatures (350– 450°C). As use of hydrogen-donor solvent is of particular importance from a technological point of view, in most of the proposed mechanism hydrogen transfer and hydrogen interactions have a central role, The term “Solvolysis” that is usually used to describe these processes imply the thermal degradation and dissolution that occur during the liquefaction process. Solvolysis can be summarized in the set of reactions listed in Figure 2.7.

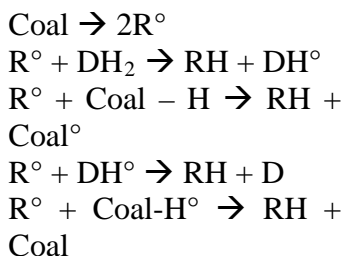


Figure 2.7. Solvolysis Mechanism of Coal Liquefaction [27]

In this mechanism, first reaction which is the generation of free radicals (R°) is believed to be the rate-determining step. These radicals can then abstract

hydrogen from the donor solvent (DH₂), from the coal and from the free radicals that are produced by each of these steps [27].

In the free radical model described above, free radicals are generated as a result of thermal pyrolysis (thermolysis) and the solvent mainly serves to stabilize them. In this view, solvent is not involved in bringing about the bond scission which is inconsistent with the observed liquefaction abilities of various solvents at a constant temperature (Figure 2.8) [28].

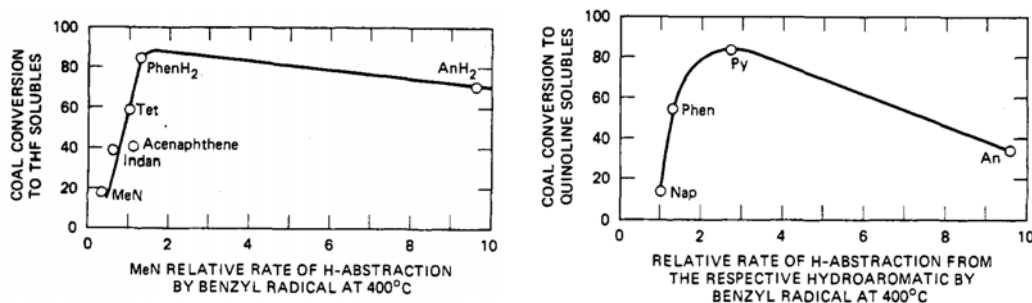


Figure 2.8. Dependence of coal liquefaction yield on hydrogen transfer abilities of different solvents [28]

Hydrogenolysis is a modification of the conventional thermal pyrolysis that considers the role that solvent plays not only in the stabilization of radicals after the breakage of the coal but also the effect that it has during the degradation stage. This can be described by a consideration of Figures 2.9.A and 2.9.B

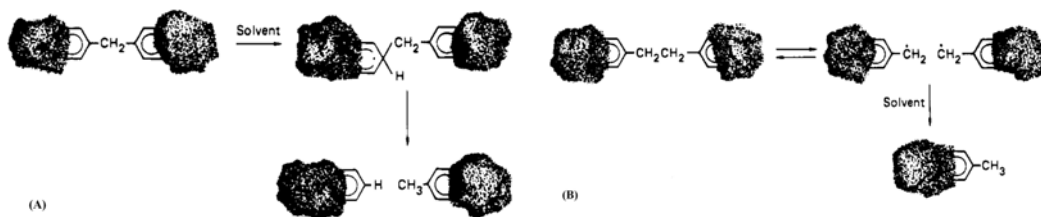


Figure 2.9. A. Free radical and B. solvent-mediated hydrogenolysis Models of Coal Liquefaction [29]

The Hydrogenolysis is based on the hypothesis that while there is a free radical mechanism involved in the coal liquefaction, it does not account for all the coal conversion that occurs in the process. In this mechanism, it is assumed that solvent donates a hydrogen atom into a particular position on a large coal molecule and this hydrogen atom causes the strong bond to be cleaved which leads to creation of additional radicals.

Hydrogenolysis occurs through a complicated set of regressive and progressive reactions but the whole process can be broken down into two parts:

1. *Coal solubilization*, which depends on the nature and intensity of pyrolytic and Hydrogen transfer reactions in the reactant system.
2. *Hydrogenation*, which depending on the particular reaction conditions, drives the liquefaction process toward lower-molecule weight liquids.

Ideally the process should convert the coal into lower molecular weight liquids like oils but simultaneous existence of polymerization and condensation reactions produce a combination of different products of varying molecular weight like Carbenes, Carboids, Asphaltenes and Preasphaltenes which can be characterized based on their solubility in different solvents. High fraction of oils are highly desired in fuel-related applications but for carbon product applications, a combination of asphaltenes and oils suitable as coke precursors are the goal for which the reaction conditions should be selected [30].

2.7.5. Direct Liquefaction Parameters

Selection of operating conditions for liquefaction reaction is crucially important in generation of a product suitable as coke precursor. Coal properties are among the first parameters that can affect the quality of liquefaction product. Table 2.4 lists some the fundamental properties of coal that can affect the quality of liquefaction in terms of conversion efficiency [31].

Property	Influence	Desired Level
Rank	Liquids Yield	Medium
Ash Content	Operations and handling	Low
Moisture Content	Thermal Efficiency	Low
Hydrogen Content	Liquids yield and hydrogen consumption	High
Oxygen Content	Gas make and hydrogen consumption	Low
Extractability	Liquids yield and quality	High
Aliphatic character	Liquids yield and quality	High
Particle Size	Operations	Fine/ very fine

There is a general agreement that coals of high rank give lower liquefaction yields but for coals of higher rank a correlation cannot be established. Coal rank is however believed to affect the pathway through which the liquefaction happens. For bituminous coals, two stages are involved: For increasing reaction severity, conversion starts to increase with an increase in the production of asphaltenes and Preasphaltenes while the production of gas and oil remains constant. In the second stage where a maximum in conversion is achieved the Preasphaltenes and asphaltenes begin to be converted to oils and gases. For

subbituminous coal, the only difference is that oil and gas production in the first stage also has an increasing trend. These pathways are described in Figure 2.10 in which severity index (S.I.) is defined as $S.I. = \theta/\theta_R \exp\left[\frac{30000}{1.986}\left(\frac{1}{T_R} - \frac{1}{T}\right)\right]$ where θ is reaction time in minutes, θ_R is a reference time (5 min), T is the reaction temperature (K) and T_R is the reference temperature (598 K) [32].

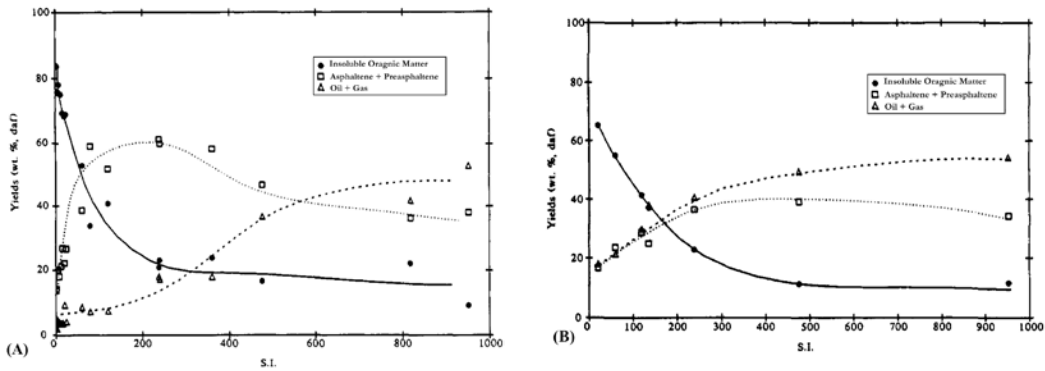


Figure 2.10. Reaction pathways for (A) Bituminous, (B) Subbituminous Coals [32]

Another coal parameter that affects the liquefaction quality is its maceral content or petrographic classification. Vitrinite and exinite are commonly considered to be the reactive macerals from which coal liquids are derived. A linear relationship has been shown to exist between liquefaction yields of subbituminous coal and its vitrinite and exinite content (Figure 2.11).

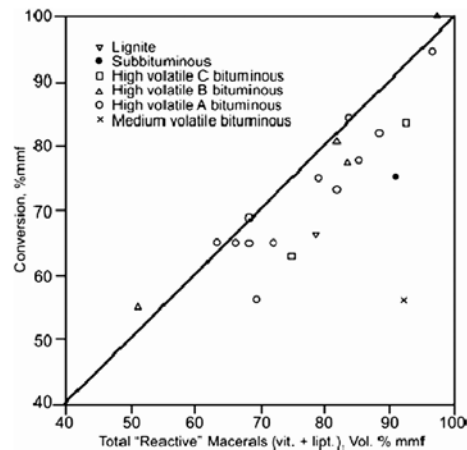


Figure 2.11. Dependence of liquefaction conversion on reactive maceral content of coal [33]

Exinites are generally found to be soluble and dissolve more readily regardless of coal rank. Vitrinite is readily liquefied but degree of solubility depends on rank. Vitrinite is the major source of liquid hydrogenation products. Inertinites are usually insoluble [34].

Effect of elemental composition and inorganic constituents can be superimposed on the previous two parameters. Mineral matter, particularly iron is also Important. Pyrite would be expected to be reduced to pyrrhotite or even metallic iron under liquefaction conditions. Titanium containing minerals and Kaolinite can also have catalytic effects. The catalytic effects can be during dissolution and coal liquefaction. Primary role of catalyst in the liquefaction process is to hydrogenate the solvent and upgrade the dissolved coal. Minerals are less likely to catalyze the hydrogen transfer reactions from either molecular hydrogen or a hydrogen donor solvent to coal, since both mineral and coal species are in solid form. Mineral matters can also generate hydroaromatic donors from

solvent components having three or more rings. The combined effect is usually to increase the conversion for coals of higher mineral content (Figure 2.12).

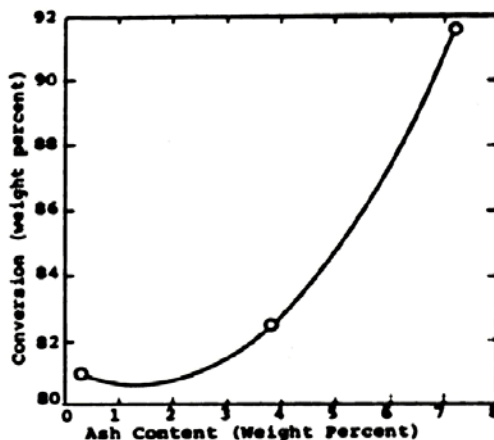


Figure 2.12. Conversion of a subbituminous coal vs. its Ash Content [35]

After coal, solvent is the major component in coal liquefaction to affect the process parameters and product properties. Pure solvents with high conversion values and favorable product properties are available but for a conversion process to be commercially useful, the solvent must be derived from the coal itself. Such process-derived solvents are complex mixtures of compounds.

Coal liquefaction solvents can be classified in four distinct categories based on their effects on coals. These are specific, non-specific, degrading and reactive solvents. Most liquid solvents belong to either of the specific or non-specific groups. For these solvents, extraction is performed at low temperature (<200°C) and therefore physical effects predominate. These solvents are able to dissolve 20 to 40% of the coal at the temperature range of interest. These solvents are electron donors and their dissolution of coal is a physical process. Pyridine and NMP (N-methyl-2-pyrrolidone) are the most common examples of this type

of solvents. For the other two categories, chemical processes are important in extraction at higher temperatures. Solvents of the latter category are those more commonly used in the liquefaction process [30].

Degrading solvents can extract up to 90% of the coal at temperatures up to 400°C. After extraction, the solvents can be almost totally recovered from the solution. Since thermal degradation of coal occurs at these temperatures, the action of degrading solvents is presumed to depend on thermal action which produces smaller and more soluble fragments. Phenanthrene, diphenyl, phenanthridine and anthracene oil are examples of degrading solvents. Tar oil fractions are often used as degrading solvents. They contain a variety of chemical compounds but are not always recovered unchanged from the coal solution. This may be a sign that some reactive solvent species are also present. Polymerization is a feature of extraction with degrading solvents. Use of molecular hydrogen can prevent this by stabilization of coal fragments by dissolved hydrogen gas. Degrading solvents can also act as hydrogen transfer agents or hydrogen shuttlers. Hydrogen shuttling is the process in which hydrogen is abstracted from the solvent by the thermally produced coal radical. The solvent radical then abstracts hydrogen from another part of the coal fragment yielding another coal radical. This way, non-donor solvents like some polyaromatic compounds can also participate in hydrogen shuttling and aid in the redistribution of hydrogen in coal fragments [36].

Coal extraction by reactive solvents has been referred to as extractive chemical disintegration [36]. Reactive solvents dissolve coal by reacting

chemically with it often at high temperatures. The reaction can be detected by studying changes in the recovered solvent. The residue and extract often weigh more than the original coal even after solvent recovery which indicates that some solvent remain chemically bound in the extract. Hydrogenolysis is the dominant mechanism through which coal dissolution by reactive solvents occurs. The hydrogen donor power of a solvent depends on its molecular structure. Hydroaromatic member of a heterocyclic pair is a more effective hydrogen donor than the aromatic member [37]. Exxon-Mobil has defined a solvent quality index for ranking the effectiveness of coal liquefaction solvents. The details of index definition are Exxon's proprietary information but it seems to vary with degree of solvent hydrogenation. [26]. Table 2.5 shows the optimum solvent parameter ranges for effective dissolution.

Solvent Parameter	Range	Optimum Value
Hydrogen content (wt %)	8.00 - 9.60	8.80
Atomic C/H ratio	0.78 – 0.97	0.87
Degree of partial hydrogenation	Higher 0.65	--
Infrared ration in CCl ₄	0.25 – 0.42	0.30
Aromatic hydrogen (wt %)	2.75 – 4.3	3.55
α Hydrogen (wt %)	1.60 – 2.25	1.88
β Hydrogen (wt %)	1.60 – 3.55	2.55
γ Hydrogen (wt %)	0.60 – 1.25	0.90
average chemical shift (ppm)	3.15 – 4.55	3.80

Solvent hydrotreatment has therefore been reported to be an effective way in increasing product yield of coal liquefaction process. Total conversion and yields of different fractions in liquefaction of a subbituminous coal has been shown to be dependent on the amount of hydrogen consumed during hydrotreatment of the solvent (Figure 2.13).

In production of coke precursor for carbon manufacture, larger fractions of high molecular and highly aromatic components are more favorable but this sometimes can be sacrificed for higher total conversion yield because further heat treatment of liquefaction products before coking can shift the oil to asphaltene and preasphaltene fractions to compositions more desirable for coking. In this work, a combination of distillation and heat treatment is used for this purpose.

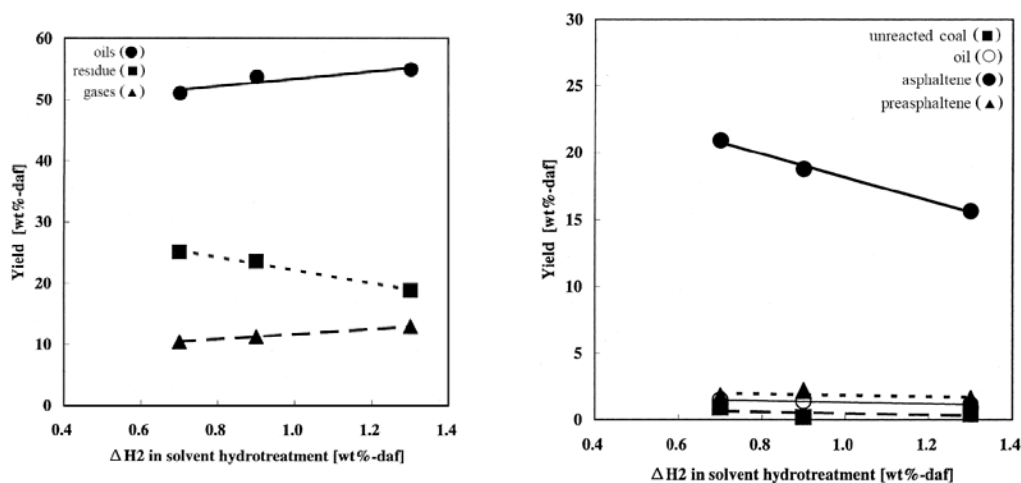


Figure 2.13. Yield of different liquefaction product fractions vs. consumed hydrogen in solvent hydrotreatment [39]

2.8. Coking and Development of Anisotropic Structure

Anisotropy is the most desired property in carbon materials for anode manufacture. The coking technique and the carbonization phenomena occurring during this process greatly determine the extent and morphology of anisotropic structure in the final product. Mesophase formation, growth of mesophase spheres and their coalescence into coke is the foundation of anisotropy in carbon

materials. Development of anisotropy which needle coke represents its highest level in pre-graphitic carbons requires a specific carbonization scheme that provides the thermodynamic and kinetic requirements for creation of such properties.

An understanding of the structure evolution during liquid phase carbonization and its dependence on processing and materials parameters is necessary for microstructure engineering of these materials. Carbonization involves compositional changes in a material that interchangeably affects the structure. This phenomenon can be described by a consideration of Figure 2.14. The phase diagram in this Figure shows the possible structural phases present in a carbonaceous material over a range of temperature and composition.

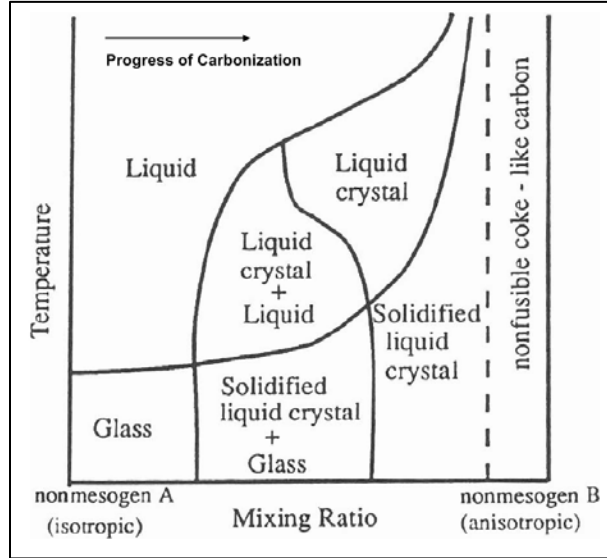


Figure 2.14. Temperature and Composition Effects of Structural Evolution [40]

Anisotropic structure development requires liquid crystal formation and growth. As a result the regions of phase diagram containing liquid crystal phase is

the range over which carbonization and coking should be performed. Carbonization at this temperature range leads to anisotropic structure as result of liquid crystal formation prior to solidification. Very low or high temperatures lead to isotropic structure due glass stability at low temperatures and limited stability of liquid crystal at higher temperatures [40].

Delayed coking as the traditional source of anisotropic carbon has a specific phenomenology which should be kept in mind before one can develop a carbonization technique for production of anisotropic carbons. This can be summarized in 6 steps as shown in Figure 2.15.

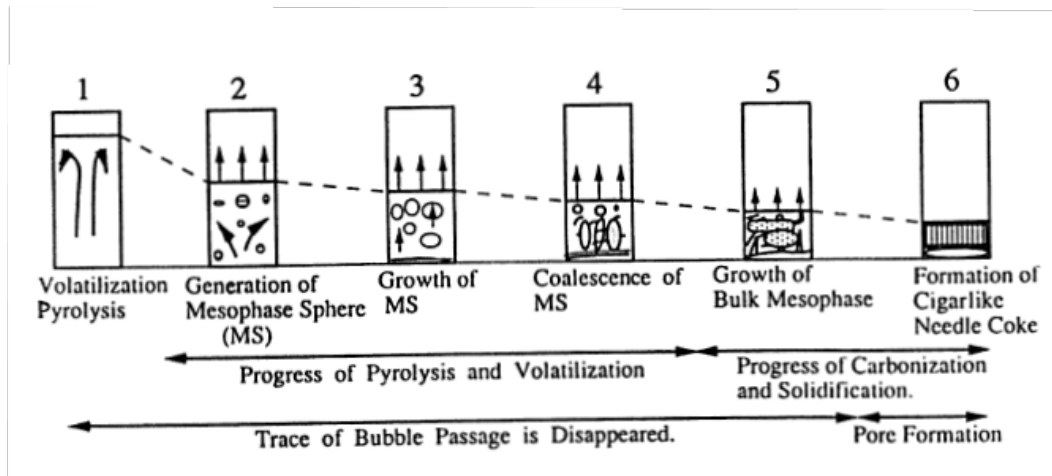


Figure 2.15. Carbonization Scheme of Delayed Coking [41]

Process starts with volatilization pyrolysis which is a kind of destructive distillation. This shifts the composition to the left side of the phase diagram of figure 2.14. The composition or the concentration of mesogens is now at a suitable range for nucleation of the mesophase spheres. Carbonization continues with growth and coalescence of mesophase spheres while at the same time

volatilization of lighter compounds still continues. At stage 3 mesophase spheres grow in size and fall down to the bottom of the drum due to their higher density. Coalescence of mesophase continues at stages 4 and 5 leading to bulk mesophase formation which can grow at the bottom of the drum leading to coke at stage 6 [42].

Three major factors determine the quality of anisotropic coke at this process. Anisotropic developments, viscosity of the bulk mesophase and gas evolution are these parameters that are themselves strongly influenced by the carbonization temperature and pressure as well by the structure and reactivity of the intermediates. Stage 5 has a key role in development of a highly oriented anisotropic texture during which Rearrangement of mesophase planar molecules into a uniaxial structure occurs. That is why the timing and amount of gas evolution at solidification of the mesophase is said to determine the extent of orientation in the resultant coke. Further stages of Carbonization occurring at temperatures above 1200°C involves further heteroatom release and carbon diffusion to reach to graphite structure which occurs at temperatures above 2600°C [43]. Figure 2.17 outlines different stages of secondary carbonization to reach to graphite structure in carbonaceous materials.

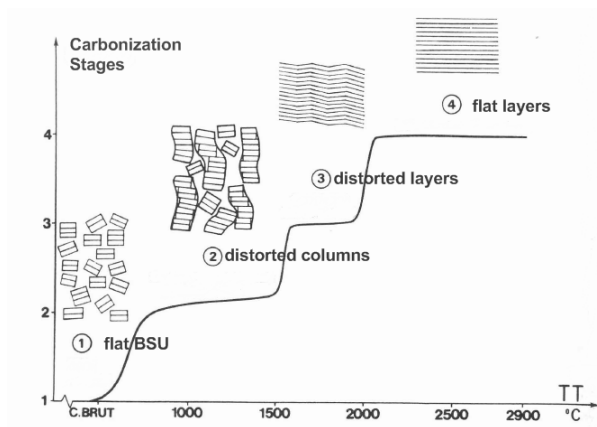


Figure 2.16. Stages of increasing order during Carbonization [13]

2.9. Characterization of Coke Anisotropy

Anisotropy is defined as the dependence of material's properties on direction. At a macroscopic level, this phenomenon is usually understood by measuring the considered properties at different directions. In case of coke and other carbonaceous materials where anisotropy exists at a microscopic level, measurement of anisotropy requires tools that respond to changes in atomic configuration. Optical microscopy by polarized light and x-ray diffraction are of the most important tools used for this purpose. In this section, a brief review of these two techniques is presented to clarify some of the coke properties measured in this work using these two techniques.

2.9.1. Polarized Light Optical Microscopy

Optical microscopy by polarized light is the most commonly used technique in determining the textural component of coke broadly defined as either

isotropic or anisotropic. A material is considered to be isotropic when; being viewed under a polarized microscope, the incident light reflected from the surface suggests only one refractive index such that the light intensity is the same in all directions from which it is being measured. This is commonly referred to as having lack of optical activity. The reflected beam from an anisotropic material, however, suggests different refractive indices. They display different colors associated with reflection, double refraction or no refraction at certain wavelengths.

Carbons are classified into isotropic and anisotropic based on their optical activity. This property can be used to classify carbons into graphitizable and non-graphitizable. Texture in anisotropic carbons is generally inherited from the coalescence of mesophase. Mesophase can still exist when it is not visible under polarize light. Mesophase particles $< 0.5 \mu\text{m}$ in diameter appear to be isotropic in optical microscopy. Such coke can be described as isotropic with limited graphitizability; therefore the size, shape and distribution of the isochromatic areas are important characteristics of the resulting coke and may influence the quality of the final carbon product [44].

Currently no standard classification of carbon textures based on mutual agreement exists in the scientific community. Different authors have developed different classifications based on the type of research they were performing and also the class of carbonaceous material being studied.

Marsh and his coworkers were among the first to develop a classification for anisotropic textures in carbonaceous materials. This classification is slightly different from one publication to the other and has been modified by different authors. Table 2.6 shows the classification for polished surfaces of coke according to Forrest and Marsh. Both isotropic and anisotropic components and have been categorized and anisotropic parts have been subdivided according to size, shape and alignment [45].

Table 2.6. Optical texture classification according to Marsh et al [45]		
Optical Texture Component	Abbreviation	Size (μm)
Isotropic	I	No optical activity
Very fine-grained mosaics	VMF	< 0.5
Fine-grained mosaics	Mf	< 0.1, < 0.5 in diameter
Medium-grained mosaics	Mm	< 5.0, > 1.5 in diameter
Coarse-grained mosaics	Mc	<10.0, > 5.0 in diameter
Supra-mosaics	Ms	Mosaics of anisotropic carbon orientate in the same direction to give a mosaic area of isochromatic color
Medium flow anisotropy	MFA	< 30 in length, < 5 in width
Coarse flow anisotropy	CF	< 60, > 3 in length; < 10, > 5 in width
Acicular flow domain anisotropy	AFD	> 60 in length, < 5 in width
Flow domain anisotropy	FD	> 60 in length, < 10 in width
Small domains	d	< 60, > 10 in diameter
Domains	D	> 60

Isao Mochida is one of the authors with a huge number of publications in the area of carbon and studies on origins of anisotropy in these materials. Two classification schemes for anisotropic textures in carbonaceous materials have been developed by Mochida and his coworkers. For green cokes he has used a point counting technique to classify the texture according to shape characteristics. He has used a total number of points above 400 to classify the isochromatic areas of coke texture into spherical and elongated areas. This classification (Table 2.7) has been developed to study the suitability of various feedstocks as precursors in

production of needle coke but it can be used to characterize anisotropy in other types of anisotropic carbons as well. For calcined cokes, the same approach (point counting) has been used however the classification is different in terms of the size of domains as shown in Table 2.8. Classification is fairly straightforward and does not include the isotropic areas.

Table 2.7. Classification of anisotropic texture in green coke according to Mochida et al [46]		
Anisotropic texture	Abbreviation	Size(μm)
Spherical Units		
Mosaic	M	Diameter < 60
Domain	D	Diameter > 60
Elongated Units		
Short Flow	SF	Length < 300, Width < 60
Long Flow	LF	Length > 300, Width < 60
Flow domain	FD	Length > 300, Width > 60

Table 2.8. Classification of anisotropic texture in Calcined coke according to Mochida et al [46]		
Anisotropic texture	Abbreviation	Size(μm)
Ultra fine mosaic	UMf	< 1.0
Fine mosaic	Mf	1.0 -5.0
Coarse Mosaic	Mc	5.0 – 20.0
Flow type	F	20.0 – 60.0
Flow domain	FD	> 60.0

Oya et al [47] have used a modified version of Marsh classification to calculate an optical texture index (OTI) according to equation 2.2.

$$OTI = \frac{\sum f_i \times (OTI)_i}{100} \quad \text{Eqn 2.2 [47]}$$

In equation 2.2, f_i is the percentage of each anisotropic unit and (OTI) is the specific factor of each isochromatic unit assigned according to isotropic-anisotropic properties and the size and the shape of each anisotropic unit. Table 2.9 lists the (OTI) values for different optical texture type based on a modified version of Marsh classification.

Description of Optical Texture	Abbreviation	Size (μm)	(OTI)
Isotropic	I	No optical activity	0
Fine-grained mosaics	MF	< 1.5	1
Medium-grained mosaics	Mm	1.5 – 5.0	3
Coarse-grained mosaics	Mc	5.0 – 10.0	7
Supra-mosaics	Ms	Aligned mosaics	10
Small domains	SD	10.0 – 60.0	20
Domains	D	> 60	30
Medium-flow anisotropy	MFA	< 30 in length, < 5 in width	7
Coarse-flow anisotropy	CFA	30 – 60 in length, 5- 10 in width	20
Flow domain anisotropy	FD	> 60 in length, < 10 in width	30

A few other classifications are also available which are mostly based on Marsh classification or a modification of it. All these techniques share a common feature that they rely on partitioning of texture into different classes and then statistical studying of them. This means a manual approach and therefore user-error makes the reproducibility an issue.

In this work, a procedure, developed by Rørvik et al [48] to overcome the common flaw of the previous techniques and facilitate an automatic analysis of coke texture, is used. The technique uses an image analysis procedure to extract the gradient lines in optical domains of the texture to calculate a mosaic index and a fiber index. The idea behind the technique is based on the optical principles according to which an optical microscope operates.

In a typical metallurgical microscope, light produced by a usually halogen lamp is first plane polarized before going through the optics and reaching the

sample surface. In plane polarized light, oscillation is limited to a single plane perpendicular to direction of propagation of the wave. When analyzing the polished surface of a coke samples, the plane of polarization is changed after the light is reflected form the surface. The change in plane polarization depends on the angle of intersection of the coke (graphene) planes with the surface. The reflected light is then passed through a second polarizing filter which is crossed at 90° relative to the first filter. A half-wave retarder then shifts the phase of the retarder one half wavelengths. This causes interference in the visible light range which produces different colors depending on the angle of intersection of graphene layers. Planes in east-west direction are seen in magenta color, southwest-northeast (SW-NE) in yellow and southeast-northwest in cyan.

Optical domains are defined as areas of the sample with the same color which in turn means same direction of the graphene planes. In coke, graphene planes show a gradual change in direction resulting in a transition in color between domains therefore a well-defined border between color domains does not exist. In previous techniques, domain size is the main parameter used for classification; therefore an inherent error due to gradual color change exists in all of those techniques adding to their lack of accuracy as discussed earlier. In the current technique, the boundaries between domains and not the domains themselves are used for used to minimize this error. There is no need to emphasize that like any other computation, this technique is also prone some errors but as the technique can be automated, the results have been shown to be repeatable [49].

Gradient lines are extracted by thresholding a grayscale image of the coke texture micrograph. Thresholding is a standard image analysis procedure in which all pixels having a gray level above certain gray color are changed to black and those below the proposed level are considered as white. This produces a black and white gradient image which is then thinned to produce a skeletonized image. Skeletonized image is an image in which width of the gradient lines is thinned to one pixel. This is the image used for pixel counting and calculation of the two indices introduced earlier.

Figure 2.18 outlines this conversion process of the image from grayscale to the skeletonized one. Thresholding stage is the only step that can produce some discrepancy in the process as the threshold value to create the highest level of contrast may be different for different samples. This error can be minimized by considering the same threshold level in analyzing different samples in a study. This error and the similar problems that exist in other texture classification techniques exhibit a maturing of this area of carbon science and a need for a universal standard in such analysis.

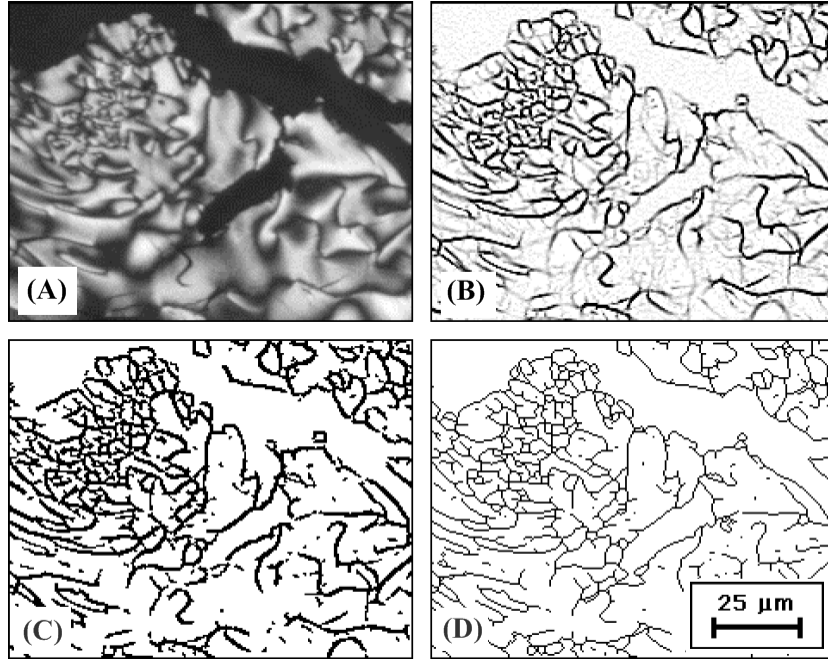


Figure 2.17. Conversion steps in image analysis of coke texture:
(A) Grayscale image, (B) Gradient image, (C) Thresholded gradient image and
(D) Skeletonized image [48]

Texture analysis is performed on the skeletonized image. The procedure after this stage basically involves pixel counting and simple arithmetic. Mosaic index (Equation 2.3) is calculated by finding the relative ratio between the number of gradient pixels in the skeletonized image (Figure 2.17.D) and the total number of carbon pixels. Carbon pixel means the total number of pixels in the sample minus the number of pixels in the pore areas. Pores are usually characterized by their dark circular or oval shapes in the texture and can easily be diagnosed in the raw image form the microscope. The mosaic index is a relative number between 0 and 1, where finer textures will give a higher value.

$$Mosaic\ Index = \frac{Line\ Pixels}{Total\ Area - Pore\ Area} \quad \text{Eqn 2.3}$$

Fiber index (Equation 2.4) is calculated as the ratio between the number of pixels having neighbors in the four respective directions. The pixel patterns of directions used in equation 2.4 is shown in Figure 2.19. For an extremely fine texture where the number of pixels in all directions is relatively the same, the fiber index will be zero. For flow textures where some directionality exists in the pixel pattern, number of pixels in one direction will be higher than the other than the others and the fiber index will be greater than zero. A texture with higher directionality in flow pattern gives a higher fiber index and for ideally parallel planes, fiber has its maximum value of 1.

$$Fiber\ Index = 2 \times \frac{\max(h, v) + \max(d_1, d_2)}{sum(h, v, d_1, d_2)} - 1 \quad \text{Eqn 2.4}$$

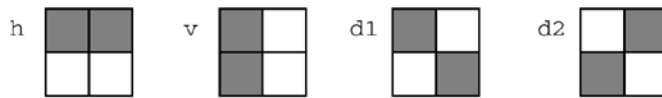


Figure 2.18. Pixel pattern used in calculation of fiber index [48]

Figure 2.19 shows an example of fiber index and mosaic index values calculated by Rørvik et al for different types of coke known to have different levels of anisotropy. Needle coke which is usually characterized by highly directional flow texture has the highest fiber index and the lowest mosaic index whereas shot coke shows the reverse trend. Petroleum coke shows values between those of the two extreme cases.

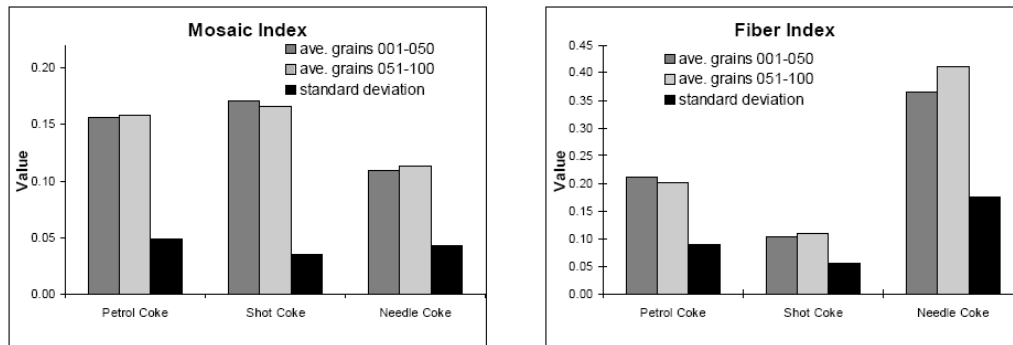


Figure 2.19. Fiber index and mosaic index values calculated for cokes with different levels of anisotropy [49]

2.10. X-ray Diffraction (XRD)

X-ray diffraction is a material characterization technique developed in the early twentieth century by Laue's discovery of diffraction phenomena in crystals and its relation with materials structure. Its initial use was limited to determination of crystal structure but later on it was used to deal with diverse problems such as chemical analysis, stress measurement, particle size measurement and crystal orientation studies.

2.10.1. XRD Fundamentals

In XRD, a beam of X-rays is incident on a specimen and is diffracted by the crystalline phase in the specimen. The intensity of the diffracted X-rays is measured as a function of the diffraction angle (2θ). Bragg equation (Equation 2.5) gives the relationship between the wavelength of the X-ray beam (λ), the

angle of diffraction (2θ), and the distance (d) between each set of atomic planes of the crystal lattice. (n) in Bragg equation represents the order of diffraction.

$$n\lambda = 2d \sin \theta \qquad \text{Eqn 2.5 [50]}$$

Diffraction obeys the general physical laws of scattering. When X-rays or any other kind of photons are incident on a crystal, they are scattered in all directions around the material. The periodic array of atoms leads to constructive scattering in specific directions. These are the directions or angles that satisfy the Bragg equation and usually known as Bragg angles.

Bragg law puts very stringent conditions on λ and θ for a given crystal. With a single wavelength of X-ray radiation, an arbitrary setting of a single crystal in a beam of x-rays will not in general produce any diffracted beams. Some way of satisfying the Bragg law must be devised, and this can be done by continuously varying either λ or θ during experiment. Depending on the way in which these quantities are varied, diffraction techniques have been developed. Powder method is the most commonly used of these techniques in which a monochromatic X-ray beam of single wavelength is used to characterize the specimens and angles are varied by random orientation of the powder particles.

XRD patterns are usually presented as plots of Intensity versus diffraction angle. Bragg angles appear as peaks on this type of graphs. Position (2θ), intensity and shape of these peaks are used to study the structure of materials. The Peak positions are usually used to calculate the lattice spacing using the Bragg law and they key parameter of peak shape i.e. the full width at half maximum

(FWHM) which is used in Scherrer equation (Equation 2.6) to calculate the extent of crystallinity in a material from the values crystallite size(L). In Scherrer equation, Θ is half of the Bragg angle, β is the FWHM, λ is the wavelength and K is a constant for each family of Bragg lines.

$$L = \frac{K\lambda}{\beta \cos \Theta} \quad \text{Eqn 2.6 [51]}$$

Scherrer equation only considers crystallite size as the physical origin of the broadening. In reality, other factors also contribute to peak broadening. The other significant factor contributing to the peak broadening is micro-strain. Different models have been developed to consider this factor in addition to the crystallite size in analyzing the effects of broadening.

Integral breadth analysis provides relations for calculating crystallite size and strain effects in peak broadening. This analysis can be applied to multiple peaks of the same family or single strongest peak in a family. Simultaneous determination of crystallite size and micro-strain using a single peak was developed by Keijser et al [52]. In this approach, the experimentally measure peak, h , is considered the combination of a structurally broadened profile, f , and the standard profile, g . The g profile is usually used for correcting the instrumental broadening. The experimental profile is assumed to be a convolution of f and g profiles and each of these profiles are assumed to follow a pseudo-Voigt type of distribution. Pseudo-Voigt is a distribution function which itself is a convolution of Cauchy and Gauss distributions. The reason for choosing these distribution types is the resemblance of Cauchy and Gauss distribution functions

to broadening effects due to crystallite size and strain respectively. Using the above assumptions, the crystallite size and micro-strain can be calculated using equations 2.7 and 2.8 respectively

$$D = \frac{K\lambda}{\beta_C^f \cos \theta} \quad \text{Eqn 2.7} \quad [52]$$

$$e = \frac{\beta_G^f}{4 \tan \theta} \quad \text{Eqn 2.8} \quad [52]$$

In these equations, K (usually 0.9) is the same constant used in Scherrer equation, λ is the wavelength of X-ray radiation, θ is half the Bragg angle of the peak under consideration and β_C^f and β_G^f are the FWHM values of Cauchy and Gauss components of the experimentally measured profile after correction for instrumental broadening.

2.10.2. XRD in Study of anisotropy in Carbon Materials

Graphite was one the first materials to be studied by X-ray diffraction [53]. X-ray diffraction has also been extensively used to characterize the structure of coal and other carbonaceous materials. Works of Franklin, Diamond and Warren [55, 55, and 56] are all based on the interpretation of diffuse X-ray diagrams of carbon-based materials to understand the atomic arrangement of Carbon in its different degrees of crystallinity.

X-ray diffraction being a technique sensitive to changes in atomic configuration and crystallinity in materials makes it a useful tool in studying the atomic-level anisotropy that exist in coke and other carbonaceous materials. Carbons with higher levels of anisotropy measured by optical texture analysis are more easily graphitized and show higher crystalline order [47]. X-ray diffraction therefore seems to be an interesting candidate for studying anisotropy in Carbon materials.

Diffraction pattern of the hexagonal Graphite is usually used as a basis in XRD studies of Carbon materials. Hexagonal graphite has the highest degree of crystal order and pregraphitic Carbons like anode coke all have lower crystallinity compared to it. However, the patterns are all the same which means the approximate location of peaks and their relative intensities remain close to that of Graphite during the carbonization process. Development of crystallinity is indicated by development of (002), (004) and (101) of the graphitic structure (Figure 2.21). (002) is the miller index for basal plane in the graphite structure or in case of pregraphitic carbons considered here, it represents the stack of graphene sheets. (002) can readily be seen in all pregraphitic carbons. This is quite obvious because the two dimensional order exists in all forms of carbon as planes of hydroaromatic carbons. With progress of carbonization, (002) peak becomes stronger i.e. its intensity increases and its width decreases which is an indication of crystal growth. (004) and in the same manner (006) peaks are basically higher order diffractions of the (002) plane and their appearance that usually occurs at higher degrees of carbonization like calcined cokes is a sign for development of

three dimensional order. Figure 2.20 when combined with the schematic depiction of carbonization stages shown in Figure 2.16 gives a complete view of structural changes during carbonization and graphitization. These points and other diffraction parameters should be considered when this technique is used for studying anisotropy in carbonaceous materials.

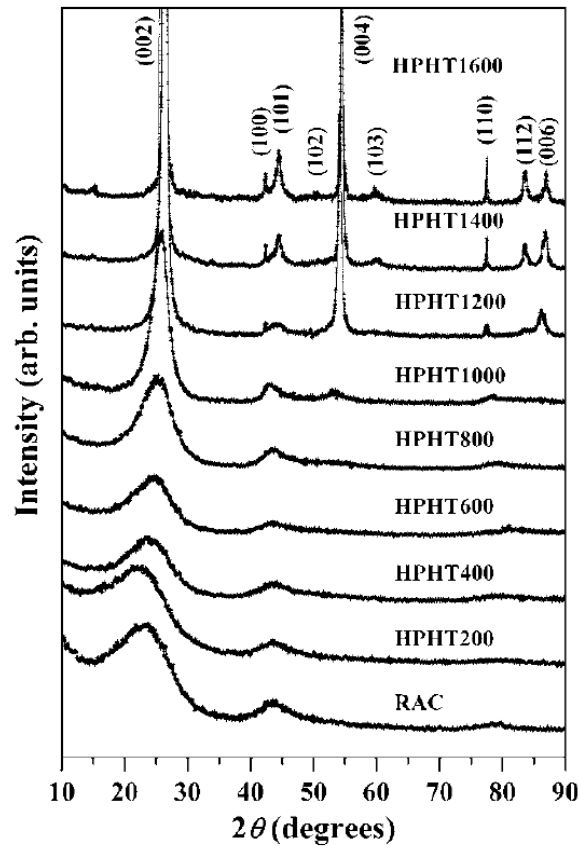


Figure 2.20. Evolution of crystal order in a carbonaceous material as evidenced by x-ray diffraction [57]

2.11. Summary of Background Remarks

Use of coal to produce coke precursor for production of anode grade coke is the main focus of this work. Special requirements of this type of carbonaceous

material necessitate direct liquefaction as the choice of coal utilization technique. Production of a carbon artifact from liquefaction products using coal byproducts and industrial streams as solvents has huge economic incentives.

Characterization of processes leading to anisotropic carbons from coal should be chosen based on the nature of different stages involved. Coal liquefaction requires techniques to reveal the chemical changes whereas in the secondary carbonization stages where structural changes are more pronounced techniques detecting these changes seem to be more helpful.

Understanding physical and chemical processes behind the evolution of coal to the final product is necessary in developing a sustainable process for use over a considerably long period of time. The high market demand for coke precursor in aluminum anode manufacture necessitates such long-term sustainability.

CHAPTER 3

EXPERIMENTAL PROCEDURE

This chapter provides a discussion on all the materials and equipments used in conducting the experiments. Type of coal and solvents used in liquefaction reactions, experimental conditions of these reactions, the treatments performed on liquefaction products, coking and calcination experiments used to produce the coke precursor and relevant details about them are among the discussed items. Figure 3.1 gives a summarized process diagram of different steps of the experimental procedure from coal to the final coke precursor product.

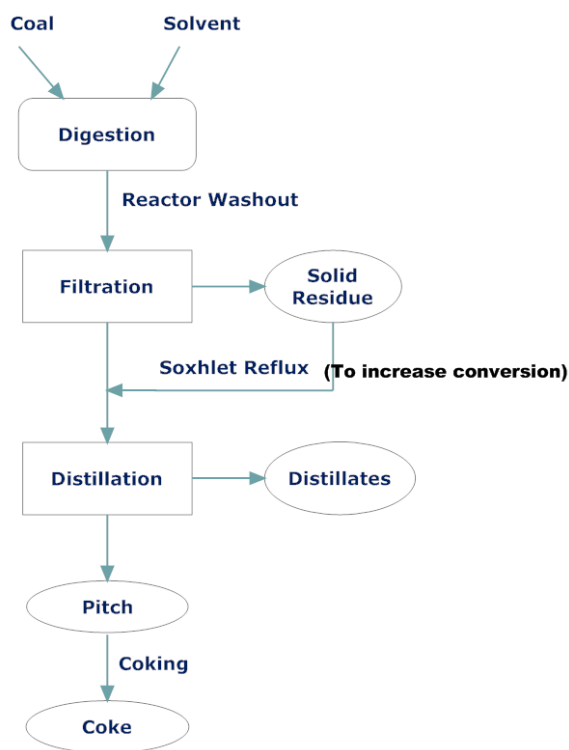


Figure 3.1. Flow diagram showing the outline of experimental procedure

3.1. Materials

A beneficiated subbituminous coal produced in Alberta was used in this thesis. Crushed coal was supplied in large plastic buckets. The coal was ground using ball-milling with still balls. The ground coal was then sieved to separate different sizes. Ground coal was stored in plastic bags and placed in sealed metallic containers. Metallic containers were kept in a cold place to prevent oxidation. For most of the liquefaction experiments performed in this work, the size range of 53-75 mm or 45-75 mm was used. The coal used is a subbituminous coal with the ultimate and proximate analysis given in table 3.1.

Ultimate Analysis					Proximate Analysis		
%C	%H	%N	%S	%O	%Moisture	%Ash	%Volatile
63.16	4.06	0.96	0.23	17.68	3.71	10.32	19.16

CTD (Coal Tar Distillate) supplied by a commercial coal tar refinery was the main industrial solvent used in this research work. It is a highly viscous dark liquid with typical tar odor. The same liquid was later hydrotreated to provide another set of solvents. Information on hydrotreatment will be provided later in this section.

1,2,3,4 Tetrahydronaphthalene (Tetralin) was acquired from Sigam-Aldrich Company with 97% purity. It was used as solvent in trial liquefaction runs of this work.

Tetrahydrofuran (THF) – Lab grade was acquired from Fisher Scientific. THF was used in all product extractions. This includes reactor washout and Soxhlet reflux.

Pyridine – 99.0% pyridine D5 was acquired from Fisher Scientific. This reagent was the main solvent used in preparing pitch solutions for proton NMR measurements.

H₂ and N₂ supplied in 99.99% purity by PRAXAIR were the gases used in conducting liquefaction experiments.

Hydrotreated Solvents were supplied by Sherritt. Solvents labeled CTD and CTD2 were hydrotreated at different conditions to provide a set of solvents with different hydrotreatment levels. Hydrotreatment conditions are reported by Sherritt are shown in Table 3.2. According to Sherritt, Ni-Mo catalyst has been used for all of the hydrotreatments.

Solvent	T	P	Time (min)	Other description
HT-CTD-1	350 °C (623 K)	700 psi (4.83 MPa)	60	Batch
HT-CTD-2	350 °C (623 K)	700 psi (4.83 MPa)	60	Batch
HT-CTD-3	350 °C (623 K)	700 psi (4.83 MPa)	120	Batch - two repeated cycles
HT-CTD-4	350 °C (623 K)	700 psi (4.83 MPa)	60	Batch
HT-CTD-5	350 °C (623 K)	700 psi (4.83 MPa)	60	Batch
HT-CTD-N	350 °C (613 K)	1000 psi (6.89 MPa)	Continuous feed	Continuous reactor

3.2. Equipments

HP/HT Stirred Reactor designed and manufactured by Parr instruments was in the core of experimental work in this research. All coal liquefaction experiments were performed in this 500 ml reactor (Figure 3.2) supplied with a control panel for temperature profile programming and adjustment of stirring speed. Reactor has a maximum operating temperature of 500°C and maximum operating pressure of 2500 psi. Heat is supplied using a programmable resistant-heater (Figure 3.2) and an automatic valve is used to pump cooling water into cooling loop for the purpose of maintaining temperature during reaction. The reactor assembly was placed in a ventilated enclosure for protection against vapors and odors during reactor washout.



Figure 3.2. 500 ml reactor used in liquefaction experiments



Figure 3.3. Control console of the reactor

Vacuum Filtration was the stage immediately after liquefaction. A glass filtration unit (Figure 3.4.A) was used for this purpose. Vacuum was provided through the utility line of the lab's building. For filtration, vacuum level was set to a level high enough to pass the often viscous liquid through the filter paper.

Soxhlet Condenser (Figure 3.4.B) was used for THF extraction of insoluble fractions from the filtration stage. Tap water was used as the cooling medium to fill the condenser of the apparatus.

Distillation assembly was the combination of several glass parts including flasks of various sizes, condenser, column, thermocouple and a heating mantle (Figure 3.5). Fiber glass was used to insulate the hot parts.



Figure 3.4. Filtration unit and Soxhlet Condenser



Figure 3.5. Distillation assembly

Molten Salt Bath Coker was used for coking experiments. Design of the coker provides advantage in terms of coking mechanism which will be discussed in the

relevant section. The molten salt bath furnace (Figures 3.6 & 3.7) is composed of a container filled with a mixture of NaCO_3 and MgCO_3 connected to a resistant heater with single set point controller. Salt mixture melts around 300°C and constant temperatures up to 1200°C can be easily obtained with it



Figure 3.6. Molten salt bath container



Figure 3.7. Molten salt bath container and coking setup

3.3. Liquefaction Reactions

All liquefaction reactions of this work were performed in the 500 ml reactor. For all runs, a coal particle size of 53-75 mm and solvent to coal ratio of 3:1 was used. High temperatures and pressures involved and the use of a highly combustible gas like hydrogen required high safety measures as result reactor preparation and charging steps had to be done most cautiously.

3.3.1. Reactor Preparation

The 500 ml reactor, made by Parr Instruments, was first pressure tested to ensure it would hold the proper pressure. A trial run using water was first

performed to leak test the reactor and the connected tubing. Leak test was a vital step of each of the runs.

3.3.2. Reactor Charging

Solvents and coal were separately weighed using a Mettler-Toledo PR 5002 scale. The solvent was first loaded into the reactor to prevent any caking effect on the coal at the bottom of the reactor. After the reactor was fully loaded with coal and solvent, the bottom part was raised to close the gap between the upper and lower compartments. Graphite gaskets were placed in the space provided in the upper part for sealing. Final sealing was performed using a flange the bolts of which were tightened using a torque wrench. The reactor was then 3 times purged with nitrogen. After purging, the reaction gas (hydrogen or nitrogen) was loaded in the reactor and pressurized to high pressure usually 40 to 60 bars and then left for fifteen minutes to monitor possible pressure loss and leaks. The above steps were performed for each of the liquefaction runs.

3.3.3. Coal Digestion / Liquefaction

If there is no pressure drop or leak in the charging stage, reaction could be started by setting the desired temperature and heating rate using the controller software of the reactor. The impeller was usually turned on to 1000 RPM and the reactor heated up to the desired reaction temperature. The reactor temperature and

pressure were monitored during the usually one hour reaction time. At the end of reaction time, the heater was turned off and the impeller was left on while the reactor cooled down.

3.3.4. Reactor Washout

Once the reactor cooled down to an acceptable temperature, the pressure was released by the gas release valve after which the reactor was opened by loosening bolts. All of these were performed under the fume hood since there would likely be noxious fumes as the products were still at a slightly elevated temperature (~ 100°C). THF was then used to dilute the often viscous product solution. This was done after the reactor has cooled down to room temperature. A certain amount of THF was weighed in a glass beaker and poured into the reactor. The mixture was stirred with the reactor's impeller to clean walls and corners. Depending on the product's thickness and viscosity, this was repeated a couple of time before the solution was transferred to a filtration unit.

3.3.5. Filtration

0.5 µm filter papers were used to separate the dissolved products from mineral matter and unreacted coal. The THF – product mixture was poured on the upper part of the filtration unit and vacuum was used to pass the mixture through the filter, the dissolved products were collected in the bottom flask and the residue

over the filter paper. The dissolved products were stored in a separate flask and the filter paper was dried at 105°C before the residue can be collected for Soxhlet extraction.

3.3.6. Soxhlet Extraction

Weight of the dried residue was measured by finding the difference between weight of the filter paper before and after filtration. The collected residue was then placed in plastic bags and weighed. 300 ml of THF was poured into a flat-bottom flask. The flask was fitted to the bottom of the Soxhlet and this was then placed onto a heating mantle (Figure 3.4.B). Residue bags were placed into the Soxhlet extractor (Figures 3.4.B and 3.8). The top of Soxhlet was fitted with a water cooled condenser. The cooling water and the heating mantle were then turned on to start the reflux process. Once the THF started to boil the heating mantle dial was fixed and left the same for the period of time (~ 24 h) over which the THF extraction was done.



Figure 3.8. Bags of residue in Soxhlet

After the Soxhlet extraction, THF soluble collected in the bottom flask were weighed and transferred to another flask for storage before moving to the next stage. Bags were removed from the Soxhlet and weighed after drying. This weight of the residue after as measurement is used to calculate the conversion. In this calculation (Eqn. 3.1) it is assumed that all THF-insoluble portions would have come from the coal and not from the solvent.

$$\%Coal\ Conversion\ (daf) = \frac{W_{coal\ (daf)} - W_{THF\ Insolubles\ (daf)}}{W_{Coal\ (daf)}} \times 100 \quad \text{Eqn. 3.1}$$

The low boiling point of THF (~66°C) has the advantage that its removal doesn't cause any significant change in the products whereas use of a solvent like NMP (N-methyl Pyrrolidone) with a boiling point (~202°C) close to a number of light hydrocarbons can lead to serious changes or even product loss at its removal.

3.3.7. Distillation

The THF-soluble part collected from the Soxhlet bottom plus the solubles from the reactor is used as the feed for distillation. For most of the runs, distillation was done in three separate parts. THF-recovery was the first stage of distillation that was done to remove the THF used in reactor washout and Soxhlet extraction section. Normal boiling point of THF (66°C) was used as the baseline for temperature control during this stage of distillation.

Temperatures above 66°C were used in the second stage of distillation. In this stage temperature was chosen according the type of solvent used in the

liquefaction reaction and the feedback that was received from the characterization of the produced coke precursors (pitches). For many runs, vacuum levels as high as 730 mmHg was applied to increase the severity of distillation.

Third stage of the distillation was in fact a heat treatment process i.e. the final product was soaked at a constant temperature in the same flask as was used for distillation. This heat treatment was shown to have important effects on the properties of products like softening point, coking value and the anisotropic content of the resultant coke.

Distillation can be considered as the last part of coal liquefaction reaction. Two major products were collected at this stage. The residue, which is the part remaining after distillation, is the coke precursor or pitch whose properties and its suitability as a feedstock for carbon production was the subject of this thesis. Distillates are the byproducts of distillation.

Distillates and their properties can have important implications in the study of coal liquefaction process. In this research, these liquids were only weighed to calculate the mass balance. However all of the liquids obtained from the distillation have been kept for later studies. Characterization of these liquids can show what part of solvent incorporates into the final product and also their suitability as recycle solvent. This is very important if a process similar to Exxon Donor Solvent is going to be used for pilot scale production of the pitch.

3.4. Operating Parameters of Coal Liquefaction

Figure 3.8 shows a more detailed view of the experimental procedure, consideration of which is useful before introducing the coking experiments

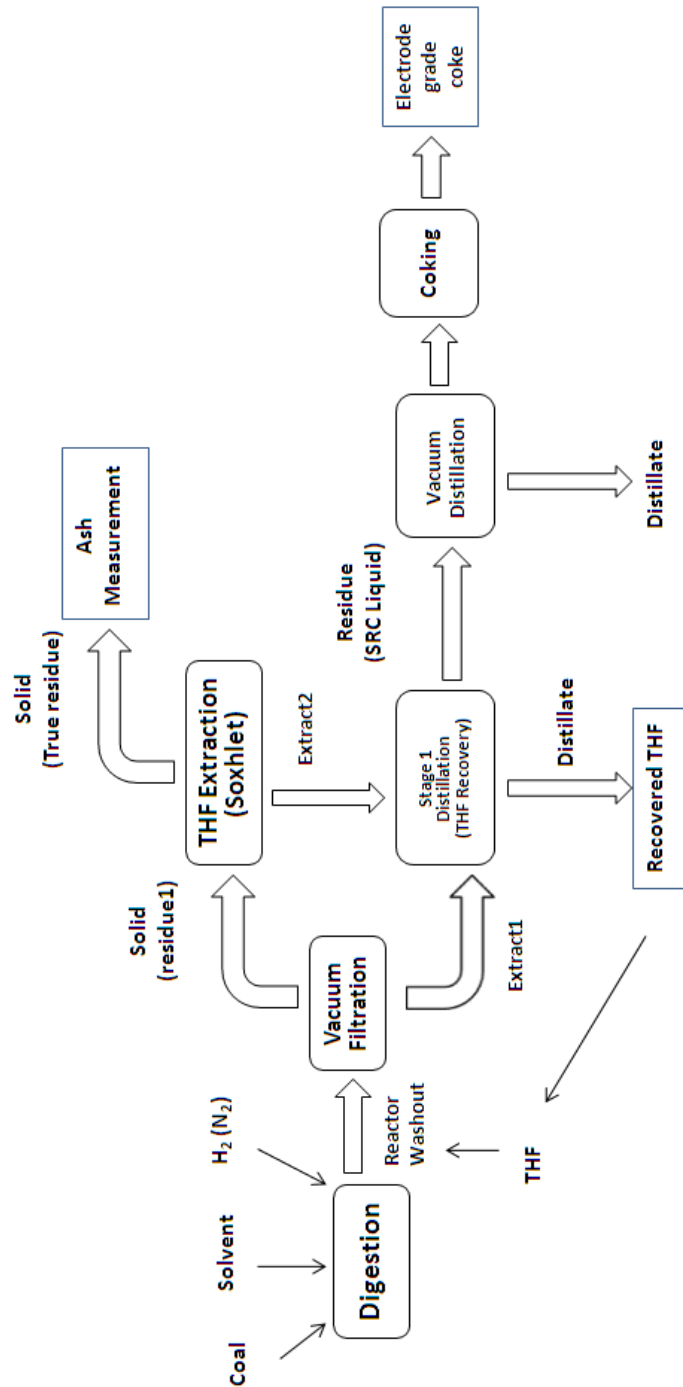


Figure 3.9. Detailed view of Experimental Procedure

A total of 50 digestions were performed using the 500 ml reactor. For 18 runs, Tetralin was used as the solvent. These runs were mostly trials to evaluate the extractability of the coal before using the industrial solvents. Digestion and distillation conditions of the rest of the main runs were based on the results of Tetralin runs. The liquefaction conditions for these runs are listed in Table 3.3.

Run#	Atmosphere	Temperature	Cold Pressure	Time (min)
1	N ₂	250°C (523 K)	30 bar (3 MPa)	60
2	N ₂	300°C (573 K)	40 bar (4 MPa)	60
3	N ₂	350°C (623 K)	40 bar (4 MPa)	60
4	N ₂	400°C (673 K)	60 bar (6 MPa)	10
5	N ₂	400°C (673 K)	60 bar (6 MPa)	60
6	N ₂	400°C (673 K)	60 bar (6 MPa)	30
7	H ₂	400°C (673 K)	60 bar (6 MPa)	60
8	H ₂	400°C (673 K)	40 bar (4 MPa)	10
11	H ₂	400°C (673 K)	60 bar (6 MPa)	30
13	H ₂	400°C (673 K)	60 bar (6 MPa)	30
14	H ₂	400°C (673 K)	40 bar (4 MPa)	30
15	H ₂	375°C (648 K)	60 bar (6 MPa)	30
16	H ₂	425°C (698 K)	60 bar (6 MPa)	30
17	H ₂	400°C (673 K)	60 bar (6 MPa)	30
18	H ₂	400°C (673 K)	60 bar (6 MPa)	30
19	N ₂	400°C (673 K)	60 bar (6 MPa)	30
20	N ₂	400°C (673 K)	40 bar (4 MPa)	30

Except for run #1 in which a solvent to coal ratio of 2 was used, the other runs digested 60 g of coal with a solvent ration of 3 to 1. To remove the Tetralin from then product based on the normal boiling point of Tetralin (~ 210°C), a temperature of 250°C was used. The liquefaction extract of Run #11 and runs 13-20 were divided into equal batches and for each, different distillation conditions were used to investigate the effect of these parameters on the quality of final product. Distillation conditions for these batches are listed in table 3.4

Batch #	T	P
1	250°C (523K)	710 mmHg (0.1 MPa)
2	350°C (623 K)	710 mmHg (0.1 MPa)
3	400°C (673 K)	710 mmHg (0.1 MPa)
4	400°C (673 K)*	710 mmHg (0.1 MPa)
5	250°C (523K)	150 mmHg (0.02 MPa)

* soaked at 400°C for 1 hr

CTD was the solvent of choice for main runs beginning with run #9. The liquefaction conditions for runs using CTD as solvent are listed in Table 3.5.

Run#	Atmosphere	Temperature	Cold Pressure	Time (min)
9	H ₂	400°C (673 K)	40 bar (4 MPa)	60
10	H ₂	400°C (673 K)	60 bar (6 MPa)	60
21	H ₂	400°C (673 K)	60 bar (6 MPa)	30
22	H ₂	400°C (673 K)	60 bar (6 MPa)	30
23	H ₂	400°C (673 K)	60 bar (6 MPa)	30
24	H ₂	400°C (673 K)	60 bar (6 MPa)	60

The high viscosity of CTD caused a number of operating problems for these runs. This was most severe for run #10 in which product recovery was not possible because of the rigorous foaming of the product during reactor opening. This was most probably as a result of jamming of the gas release lines during pressure discharge due to a sudden expansion of the reactor's content. Filtration of these runs was also quite a demanding task. Larger amounts of THF for reactor washout improved the problems associated with the filtration problems due to high viscosity of the products. The reduction of coal amount to 50 g with keeping the same solvent to coal ratio was also helpful in alleviating the problem. The distillations for these runs are shown in Table 3.6. For these runs, coal extract was

divided into two batches for distillation. In the following table, B1 and B2 following the run number denote batches 1 and 2 respectively

Table 3.6. Distillation Conditions for Coal Extracts of CTD Runs		
Run#	Temperature	Pressure
9B1	350°C (623 K)	760 mmHg (0.1 MPa)
9B2	350°C (623 K)*	760 mmHg (0.1 MPa)
21B1	250°C (523 K)	30 mmHg (0.004 MPa)
21B2	350°C (623 K)	710 mmHg (0.095 MPa)
22B1	250°C (523 K)	30 mmHg (0.004 MPa)
22B2	350°C (623 K)	710 mmHg (0.095 MPa)
23B1	300°C (573 K)	30 mmHg (0.004 MPa)
23B2	250°C (523 K)	150 mmHg (0.02 MPa)
24B1	250°C (523 K)	30 mmHg (0.004 MPa)
24B2	300°C (573 K)	30 mmHg (0.004 MPa)

* soaked at 350°C for 1 hr

The hydrotreated solvents and petroleum-derived solvents were the next set of solvents to be used for liquefaction experiments. The liquefaction conditions for runs 25 to 50 which have used these solvents are listed in Table 3.7. Operation of liquefaction reaction using these solvents again faced a number of problems. This time in addition to the type of problem that occurred in run #10, solidification of the coal slurry during the reaction was another problem. In these cases, a very hard coke like solid had accumulated around the cooling loop and the impeller which was very hard to scratch. These problems made product recovery and obviously rest of the experimental procedure for runs 27, 29, 33, 34, 35 and 36 impossible. As of the day this thesis is being written, the author has not been able to find an explanation for the second type of problem but speculations will surely continue as the reason and remedy to this problem is necessary for sound and smooth operation of the liquefaction experiments.

Run#	Atmosphere	Temperature (°C)	Pressure	Time (min)	Solvent
25	H ₂	400	60 bar (6 MPa)	60	HT-CTD1
26	H ₂	400	60 bar (6 MPa)	60	HT-CTD3
28	H ₂	400	40 bar (4 MPa)	60	HT-CTD3
30	H ₂	400	40 bar (4 MPa)	60	HT-CTD2
31	H ₂	400	40 bar (4 MPa)	60	HT-CTD2
32	H ₂	400	40 bar (4 MPa)	60	HT-CTD2
37	H ₂	400	40 bar (4 MPa)	60	Fr-HTCTD3*
38	H ₂	400	40 bar (4 MPa)	60	HT-CTD5
39	H ₂	400	20 bar (2 MPa)	60	HT-CTD5
40	H ₂	400	40 bar (4 MPa)	60	Fr-CTD
41	H ₂	400	40 bar (4 MPa)	120	HT-CTD5
42	H ₂	400	40 bar (4 MPa)	30	HT-CTD5
43	H ₂	400	40 bar (4 MPa)	60	HT-CTDN
44	H ₂	400	40 bar (4 MPa)	60	CTD2
45	H ₂	400	60 bar (6 MPa)	60	CTD2
46	H ₂	400	40 bar (4 MPa)	60	HT-CTD5
47	H ₂	400	40 bar (4 MPa)	60	HT-CTD4
48	H ₂	400	40 bar (4 MPa)	60	HT-CTD2
49	H ₂	400	60 bar (6 MPa)	60	HT-CTD2
50	H ₂	400	60 bar (6 MPa)	30	HT-CTD2

*"Fr" refers to fractionation of the solvent using distillation at 150°C and 30 mmHg. Lighter fraction of the distillation was used as the solvent.

For all of these runs, a solvent to coal ratio of 3 with 50 g of coal was used. The temperature was fixed at 400°C for all of the runs. This is the most common temperature range for liquefaction as cited in literature and corroborated by the Tetralin runs. For distillation conditions, more severe conditions compared to CTD runs were chosen. This includes higher temperatures and longer soaking times in the heat treatment. The temperature was however limited to 330°C to prevent the mesophase formation which usually happens over the temperature range of 350 to 550°C. This will be discussed in more detail in the next part which deals with the coking experiments. The distillation conditions for the last group of liquefaction products are listed in Table 3.8.

Table 3.8. Distillation Conditions for Coal Extracts of CTD Runs			
Run#	Temperature	Pressure*	Soaking Time (min)
25	300°C (573 K)	30 mmHg (0.004 MPa)	0
26	300°C (573 K)	30 mmHg (0.004 MPa)	0
28B1	300°C (573 K)	30 mmHg (0.004 MPa)	60
28B2	330°C (603 K)	30 mmHg (0.004 MPa)	60
30B1	330°C (603 K)	30 mmHg (0.004 MPa)	60
30B2	330°C (603 K)	30 mmHg (0.004 MPa)	60
31B1	300°C (573 K)	30 mmHg (0.004 MPa)	60
31B2	330°C (603 K)	30 mmHg (0.004 MPa)	0
32B1	330°C (603 K)	30 mmHg (0.004 MPa)	120
32B2	300°C (573 K)	30 mmHg (0.004 MPa)	60
37	330°C (603 K)	30 mmHg (0.004 MPa)	120
38P1	330°C (603 K)	30 mmHg (0.004 MPa)	120
39	330°C (603 K)	30 mmHg (0.004 MPa)	120
40	330°C (603 K)	30 mmHg (0.004 MPa)	120
41	330°C (603 K)	30 mmHg (0.004 MPa)	120
42	330°C (603 K)	30 mmHg (0.004 MPa)	120
43	330°C (603 K)	30 mmHg (0.004 MPa)	120
44	330°C (603 K)	30 mmHg (0.004 MPa)	120
45	330°C (603 K)	30 mmHg (0.004 MPa)	120
46	330°C (603 K)	30 mmHg (0.004 MPa)	120
47	330°C (603 K)	30 mmHg (0.004 MPa)	120
48	330°C (603 K)	30 mmHg (0.004 MPa)	120
49	330°C (603 K)	30 mmHg (0.004 MPa)	120
50	330°C (603 K)	360 mmHg (0.05 MPa)	120

* It is worthy to remind that for measuring the vacuum, a pressure gauge was used that the sound working of each was questioned after completion of the experiments; therefore the vacuum levels reported should be dealt with caution.

Final products of all of liquefaction runs were stored in plastic bottles and held at a cool and dark place. Samples were later taken from these products for characterization and coking.

3.5. Coking Experiments

The purpose of this research was to produce the coke precursors from coal liquefaction products. One of the best ways to evaluate the suitability of these products for the final application is to follow the same pathway as occurs in

industrial applications for production of carbon materials from coal liquefaction products. As described in chapter 2 delayed coke and binder pitch are the major components of prebaked carbon anodes for aluminum electrowinning. As discussed in chapter 2, delayed coking and the combination of processes that occur during delayed coke formation are essential for the creation of desired properties, the most important of which is anisotropy, in coke as a carbon anode material. This, the simplicity of coking setup and availability of the molten salt bath furnace were the main reasons for choosing the coking technique used in this work. Figure 3.10 shows a schematic view of the coking setup.

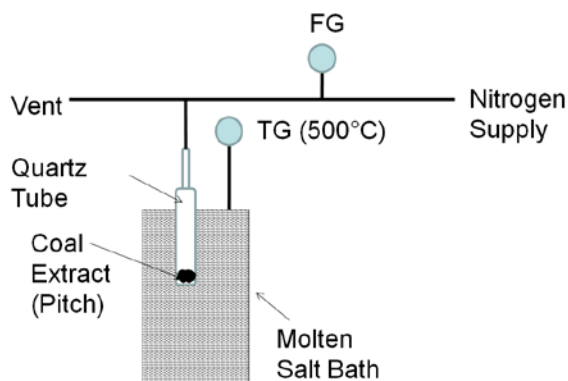


Figure 3.10. Schematic View of the coking setup

Coking requires heating of feedstock at high temperatures under an inert atmosphere to prevent oxidation of carbon. Nitrogen was used to provide the inert atmosphere in the coking experiments of this work. As the coking process requires removal volatile components, a batch process cannot be used and some mechanism is necessary to remove the released gases and liquid from the reaction vessel. On the other hand, maintenance of a certain level of viscosity is vital for

development of anisotropy in the structure. This creates a dilemma from an operation point of view. The current setup allows a compromise between both requirements with a level of sealing enough to take the air out of the coking flask.

Custom-made quartz tubes were used as the coking vessel in these experiments. For most of the experiments about 5 g of pitch was loaded into the tubes (Figure 3.11.A) and Swagelok[®] Ultra-torr vacuum fitting (Figure 3.11.B) was used to connect the tube to the nitrogen gas line. The Fluorocarbon O-ring/stainless steel ferrule combination provides the sealing required for coking the pitch.

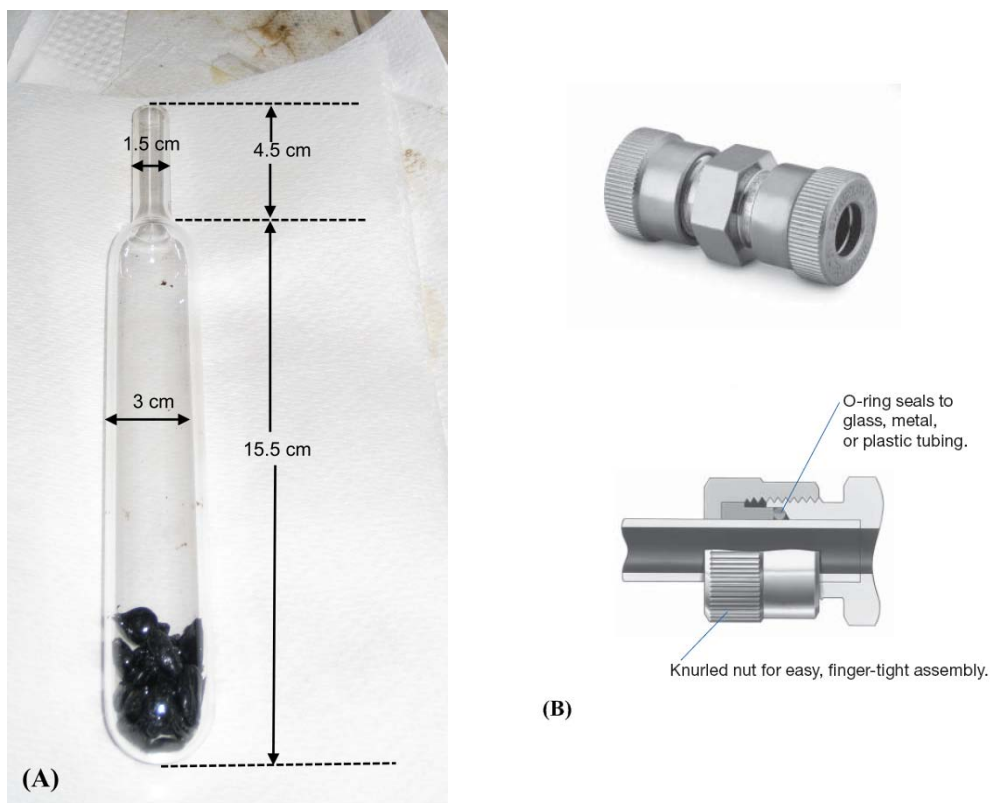


Figure 3.11 - A. The quartz tube used for coking the pitch, B. vacuum fitting used for sealing

Coking time and temperature were fixed at 1 hr and 500°C. This way, the coking properties of different products digested from coal could be tested. 500°C is the average operating temperature most delayed cokers and it lies within the temperature range of mesophase stability. This provides a favorable condition for mesophase nucleation, growth and conversion to anisotropic structure [41]

Each coking experiment performed involved a few steps which were more or less the same for about 20 pitches that were coked. After measuring the weight of the quartz tube and loading the required amount of pitch, the tube was connected to the nitrogen line (Figure 3.12) and the flow rate was fixed at 30 in rotameter units (~320ml/min) and monitored to make sure the system is sealed by blocking the exhaust pipe. Nitrogen was allowed to flow for 10 minutes to purge as much as the air is possible from the system.



Figure 3.12. Quartz tube and Nitrogen flow rate during purge stage

After purging, the quartz tube was lowered into the molten salt bath which marked the starting time of the coking. The tube was dipped into the molten salt bath for about half of its height. This was to allow a colder segment to facilitate the reflux of heavier volatiles back into the coking tube. The coking was usually starting with violent devolatilization and emission of white or sometimes yellow cloudy vapor (Figure 3.13) which were being vented into the exhaust line



Figure 3.13. Violent devolatilization in the start of coking experiment

Gas evolution was usually continuing up to about half of the coking period. Gas reflux could easily be seen on the walls of the quartz tube during this stage which was being followed by solidification or at least high increase in viscosity as no bubbles could be seen in the content of the quartz tube. After 1 hr, the tube was taken out and nitrogen was allowed to flow for a few minutes before opening the fittings and separating the tube from the coking setup. The outside of quartz tube had to be washed with water to wipe the solidified salt remaining on

it. Tube was then weighed to calculate the coke yield. Coke samples were then stored in glass bottles for characterization and calcination.

3.6. Calcination Experiments

Coke produced from the alt bath coker has properties close to that of the green coke produced by delayed coker that is it still has quite high amounts of volatile matter. This coke should be calcined to remove a portion of the volatile matter and improve its physical properties before being formed into prebaked anodes. A few green cokes produced by molten salt bath coker were chosen for calcination experiments. Calcinations were performed by an M&P Lab. Q600 TGA/DSC. The temperature profile shown in Figure 3.14 was used for all samples calcined this way.

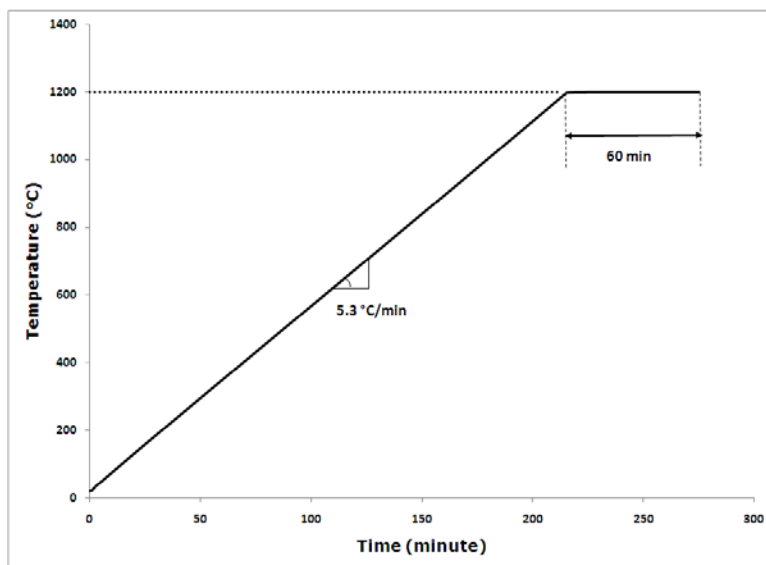


Figure 3.14. Temperature profile used for calcination of selected cokes

Calcined coke samples were stored in glass bottled for later characterization.

3.7. Analytical Testing

The properties of coal, solvents and coal liquids were evaluated to assess the changes occurring during the liquefaction process and to find a correlation between the properties of the feedstock and the resultant cokes. Elemental analysis of coal, solvents and pitches, softening point of selected pitches, proton NMR of solvents and pitches and ash content of coal and residues were the analytical tests that were performed in this work.

3.7.1. Elemental Analysis

This was performed for the coal and all of the solvents and pitches produced by digestion of coal. This test was done by Flash Elemental Analyzer in University of Alberta analytical lab. The machine uses a 2 to 3 mg sample size and measures the percentage of Carbon, Hydrogen, Nitrogen and Sulfur by converting them into their respective oxides (CO_2 , H_2O , NO_2 and SO_2). The gases pass through a chromatographic column where they are separated and analyzed. Oxygen is calculated difference.

3.7.2. Softening Point

Softening point is a measure of the temperature at which point the material will flow a particular distance [58]. This property is crucially important when binder and impregnation pitches are concerned. Pitch should be able to flow to fill

the pores within the coke structure. Proper wetting of the coke by pitch is also another important factor in the carbon anode manufacture. This is crucially important in the mixing stage before forming of the anodes. In this work, softening point of a few pitches was measured by monitoring the changes in droplet height between a delayed coke bed and the pitch sample.

3.7.3. Proton NMR

The molecular structure of solvents and their resultant products are crucially important in predicting the coal-digestion behavior and development of anisotropy during coking. The ratio of aromatic and aliphatic molecules is one property that can to some extent represent the molecular structure. Proton NMR is one of the techniques that can provide this type of information with relative ease and acceptable precision. In this work, proton NMR spectrum of all solvents and selected pitches were obtained from the pyridine-soluble fraction of these materials. NMR tests were performed using a VarianTM 500 MHz spectrometer in NANUC NMR facilities in Edmonton, Alberta.

3.7.4. Ash Test

The primary purpose of the ash test was to measure the ability of the solvent to remove or reduce the ash content in the original coal from the final digest product. This test was done according to ASTM D3174 on coal and residue

samples. Ceramic crucibles were heated to a red hot state at 900°C under a flow of air, to derive off any moisture or previous contamination and then placed into a desiccator to cool down. Once cool, they were weighed and the appropriate amount of sample was placed into the crucible (Figure 3.15). The crucible was placed into a programmable single set point muffle furnace (figure 3.15). The temperature was then ramped up to 750°C at 6.3°C/min and then held for 120 minutes under a 40 rotameter unit of air to ensure complete combustion and then the furnace was allowed to cool to room temperature. The crucible was carefully weighed, and the difference in weights (pre-heat less post-heat) was divided by the original sample weight to calculate the percent ash in the sample.



Figure 3.15. Muffle furnace and the crucibles used for ash measurements

3.7.5. Optical Microscopy

Optical microscopy by crossed polarized light of polished sections of coke is the main technique for evaluating anisotropy in this material. In this work, optical microscopy of selected green and calcined coke samples was performed elsewhere and the micrographs were provided to the author for image analysis. The following procedure was used to prepare samples for optical microscopy. Coke particles were ground using mortar and pestle and screened to a narrow fraction of 500-600 μm grain size. A few grams of this fraction were embedded in epoxy in 30 mm diameter cylindrical molds. The grinding and polishing were performed on a RotoForce-4 unit attached to RotoPolo-31 unit supplied by Struers. Three samples were mounted at the same time were mounted in a holder and ground and polished using silicon carbide paper. A force of 10 N per sample was applied and the rotation was 300 RPM. The grinding paper was continuously wetted by water and the grinding time was 30 seconds.

Fine grinding was performed using a fine grinding disc supplied by Struers. The disc was coated with a 9 mm diamond spray and continuously wetted by ethanol during the two minutes grinding time. The samples were then polished in three consecutive steps using 6 mm, 3 mm and 1 mm diamond spray on a polishing cloth wetted continuously by ethanol. For these steps, the grinding time was 5 minutes and, rotation speed 300 RPM and the force applied per sample was 20 N. The final polishing step was performed using a cloth soaked with a colloidal silica suspension. The force per sample was lowered to 10 N and opposite rotation direction for sample and polishing disc was used.

3.7.6. X-ray Diffraction

In coal studies, X-ray diffraction is generally performed to characterize the crystalline mineral content of the material. For this purpose, low temperature ash of the coal is produced using RF-plasma ashing. This type of analysis was performed on coal, residues from a few runs and their low temperature ashes to investigate the evolution of mineral content during the process.

X-ray diffraction was also performed on a number of coke samples to investigate their crystallinity. All X-ray diffraction experiments were performed on powdered samples using a RIGAKU (RU-200B Generator) rotating anode XRD system. A copper target at an accelerating voltage of 140 kV was used to generate X-rays and a graphite monochromator to generate the monochromatic radiation. The resultant X-ray diffraction patterns were used to calculate crystallite size as indication of anisotropic development in carbon precursors produced.

3.7.7. X-ray line profile analysis

(002) peak in the x-ray diffraction patterns of the cokes was analyzed to calculate the crystalline properties of these products. To perform single line analysis discussed in chapter 2, it is required that the line profile of each peak is fitted with a pseudo-Voigt distribution function. For this purpose, the equation developed by Wertheim et al [59] was used. The pseudo-Voigt function, $pV(2\theta)$ is defined according to equation 3.2.

$$pV(2\theta) = I_0[\eta L(2\theta) + (1 - \eta)G(2\theta)] \quad \text{Eqn 3.2 [59]}$$

In this equation, L and G are the Cauchy and Gauss functions respectively defined according to equation 3.3 and 3.4.

$$L(2\theta) = \left[1 + \frac{(2\theta - 2\theta_0)^2}{w^2} \right]^{-1} \quad \text{Eqn 3.3 [59]}$$

$$G(2\theta) = \exp \left[\frac{-(\ln 2)(2\theta - 2\theta_0)^2}{w^2} \right] \quad \text{Eqn 3.4 [59]}$$

In equations 3.2 to 3.4, $2\theta_0$ is the centroid position which represents the peak maximum for symmetrical profiles, η is the mixing parameter, which prescribes the fractions of Cauchy and Gauss components included, I_0 is the maximum intensity, and the $2w$ is the full width at half maximum (FWHM) for each of the profiles. The FWHM values calculated here were used in equations 2.7 and 2.8 to calculate the crystallite size and micro-strain.

MATLAB[®] curve-fitting toolbox was used for line profile analysis calculations. The toolbox uses the Trust-Region least-square analysis to solve the optimization problem. Figure 3.16 shows the results of line profile analysis on the (002) profile of a commercial graphite sample.

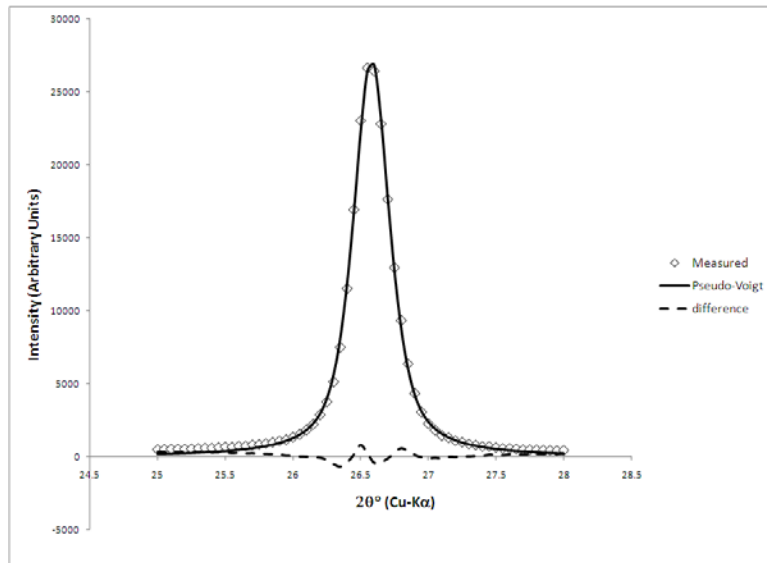


Figure 3.16. (002) Line profile analysis of commercial graphite

For higher accuracy in determination of the crystalline properties, it is required that the measured profile be corrected for a number of artifacts that exist in x-ray diffraction. Some of these artifacts are inherent in the diffraction process while others are caused by the diffraction instrument. In this work, the general guidelines proposed in the specification [60] developed by Japanese Society for Promotion of Sciences (JSPS) is used. The specification recommends test conditions as well as procedures for calculation of corrections and use of Si as an internal standard for correction of instrumental broadening. For all x-ray diffraction experiments, scanning steps of 0.01° at a rate of $1^\circ/\text{min}$ in accordance with the JSPS specification were used. Details of the line profile analysis for calculation of profile parameters and calculation of crystallite height and width and micro-strain for different atomic planes are given in appendix X.

CHAPTER 4

RESULTS AND DISCUSSION

This chapter covers the results of coal liquefaction runs and coking experiments. Effect of the operating conditions like temperature, pressure and type of solvent on liquefaction conversion and product properties are presented and discussed here. Pitch properties are then correlated with values obtained from optical microscopy and X-ray diffraction to make a connection between the properties of the final product and that of the original coal and solvent. Mass balances for various steps of the liquefaction experiment are also calculated to find the best conditions for this process.

4.1. Solvent Characterization

Elemental analysis and NMR were performed on all solvents used in this work. Table 4.1 summarizes these results for solvents. Figure 4.1 shows the sulfur and nitrogen content of different solvents used in this work. This value is important as these two elements are considered unfavorable in green coke used for carbon anode manufacture. Attention should be paid to variations in measured values for different hydrotreatments used in case of hydrotreated solvents. NMR values provide the fraction of aromatic and aliphatic fractions in different materials. For this calculation, total area of aromatic and aliphatic regions was

normalized to 100 and the individual integral values were divided by the total area to find the fractions.

Solvent	%C	%H	H/C ratio	%Aromatic
CTD	N/A	N/A	N/A	80
HT-CTD1	87.51	5.50	0.06284	66
HT-CTD2	91.67	5.70	0.06215	68
HT-CTD3	90.65	5.70	0.06288	63
HT-CTD4	91.20	5.61	0.06152	69
HT-CTD5	90.53	5.75	0.06353	66
HT-CTDN	N/A	N/A	N/A	73
Fr-CTD	N/A	N/A	N/A	79
Fr-HT-CTD3	N/A	N/A	N/A	60

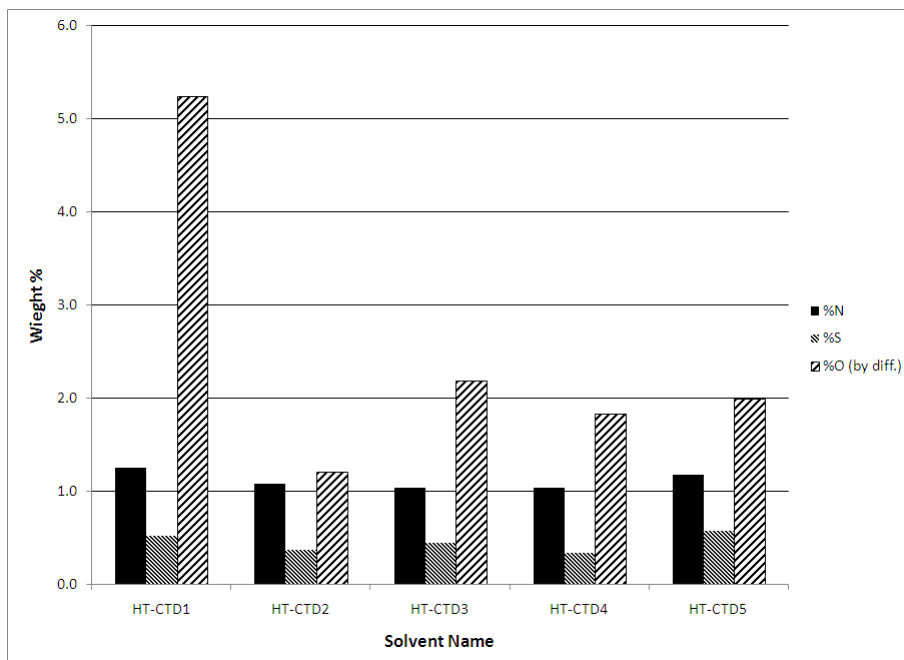


Figure 4.1. wt% of Nitrogen and Sulfur in hydrotreated solvents

4.2. Effect of Liquefaction Parameters

Coal digestion experiments were performed under varying parameters. This includes temperature, pressure, time, type of solvent and the reaction atmosphere. Conversion is one of the key parameters in coal liquefaction.

Figures 4.2 to 4.10 show the effect of different liquefaction parameters on conversion. It should be noted due to quite long heating and cooling times during reactor operation, these data are not kinetically reliable but they can still provide some insight.

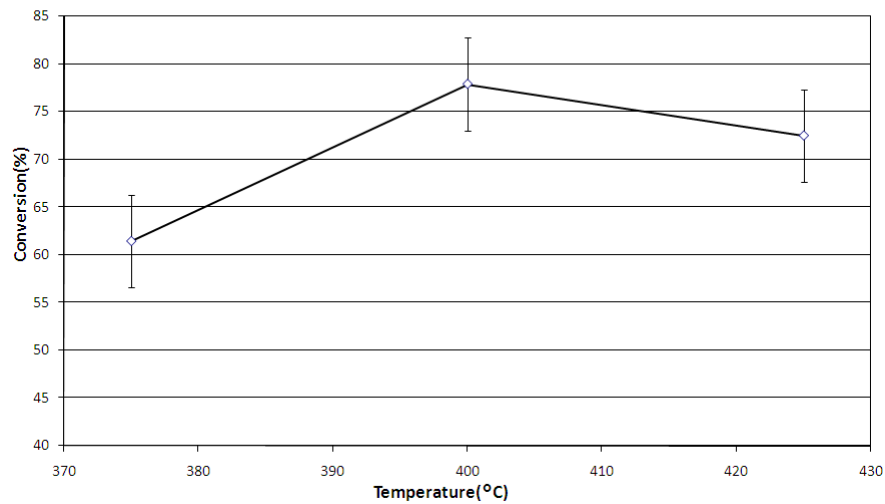


Figure 4.2. Effect of digestion temperature on conversion for Tetralin runs

($P_{H_2} = 60$ bars, $t = 60$ min)

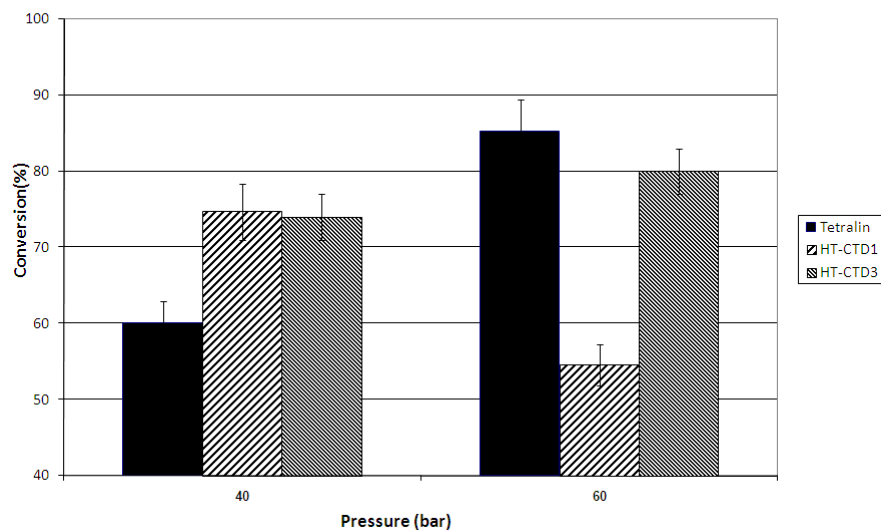


Figure 4.3. Effect of Hydrogen Pressure on Conversion
(T=400°C, t=60 min)

Figure 4.2 clearly shows the effect of temperature. Optimal conversion is achieved at 400°C. The lower conversion obtained below 400°C is due to an inability of solvent to thoroughly digest the coal, while the lower conversion achieved at higher temperatures is due to retrograde reactions (polymerizations, combinations) that occur at elevated temperature ($\geq 450^\circ\text{C}$).

Effect of hydrogen pressure is obvious for Tetralin runs but for other solvents, contradictory values can be seen. For industrial solvents which are not as good hydrogen donors as Tetralin, higher hydrogen pressure seems to either have no effect or even decreases the conversion. This point shows the need for more detailed studies on this effect for industrial solvents.

Residence time is another parameter than can affect the conversion of coal. In this most of the runs were performed with nominal residence times of 30 and 60 minutes as a result, affect of this parameter cannot be fully studied based on the current results; however some general trends can be seen in conversion data as shown in Figure 4.4. Tetralin has higher conversion compared to the industrial solvent for both of 30 and 60 min residence. Higher residence time has led to higher conversion for both of the solvents but the effect is stronger for Tetralin.

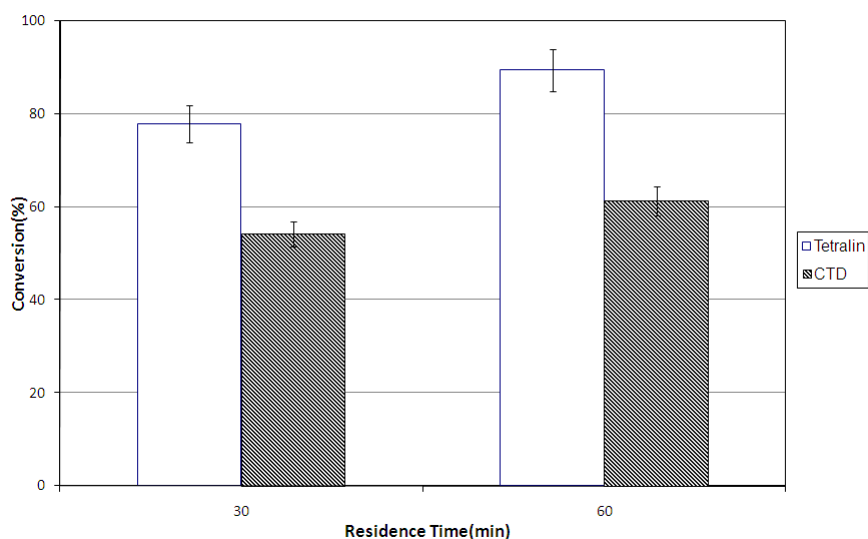


Figure 4.4. Effect of residence time on conversion

(T=400°C, P_{H2} = 60 bar)

Solvent is the main agent of coal dissolution in the liquefaction process. Different solvents were tried in this work with varying levels of aromaticity and hydrotreatment. The capability of solvents to transfer hydrogen has been shown to

be the most important factor on its ability to digest coal. Figure 4.5 shows different conversion values obtained using different solvents used for coal liquefaction. The most important information that can be obtained from this graph is the dependence of conversion on level of hydrogenation. Among the coal-derived solvents, CTD with no hydrotreatment has yielded the lowest conversion while HT-CTDN which is the solvent with the most severe hydrotreatment conditions (Table 3.2) has the highest coal conversion. Tetralin has the highest conversion but as will be seen later, cokes from coal digests using Tetralin are not highly suitable for carbon anode manufacture. The quality of pitch should also be considered when designing a liquefaction process for carbon anode applications.

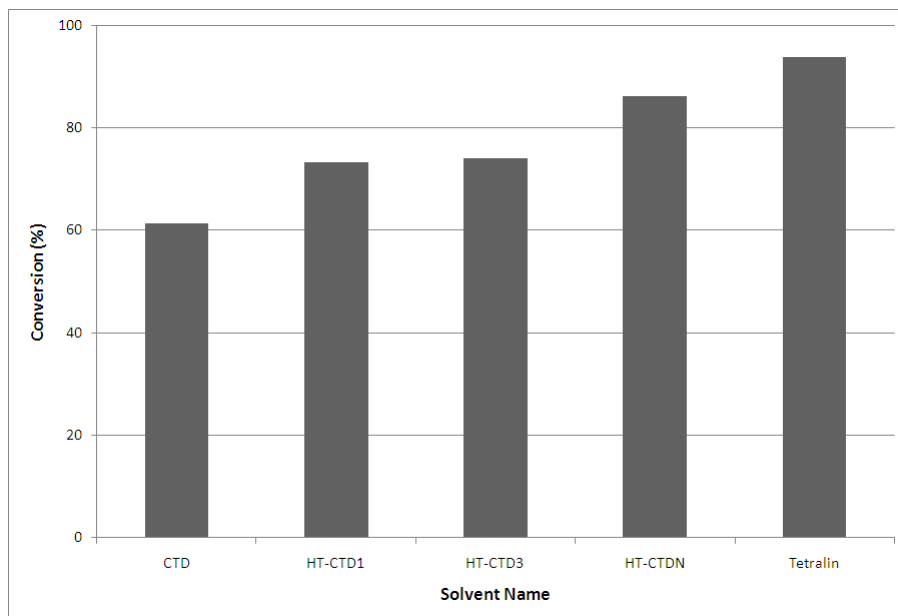


Figure 4.5. Effect of liquefaction solvent on conversion

(T=400°C, t = 60 min, P_{H2} = 60 bar)

Hydrogen and its transfer play an important in coal dissolution mechanisms. Solvents are different in terms of their ability to receive hydrogen from gas phase. Figure 4.6 shows the effect of atmosphere on conversion for Tetralin runs. Digestion of coal with Tetralin under hydrogen atmosphere has a higher conversion regardless of the residence time. This can be explained in the view of hydrogen transfer from gas phase by Tetralin. In other words, Tetralin donates its hydrogen to the coal and converts to naphthalene. After this stage the solvent acts by transferring hydrogen from gas phase. Using the current data, no judgment on the same effect for coal-derived solvents can be made.

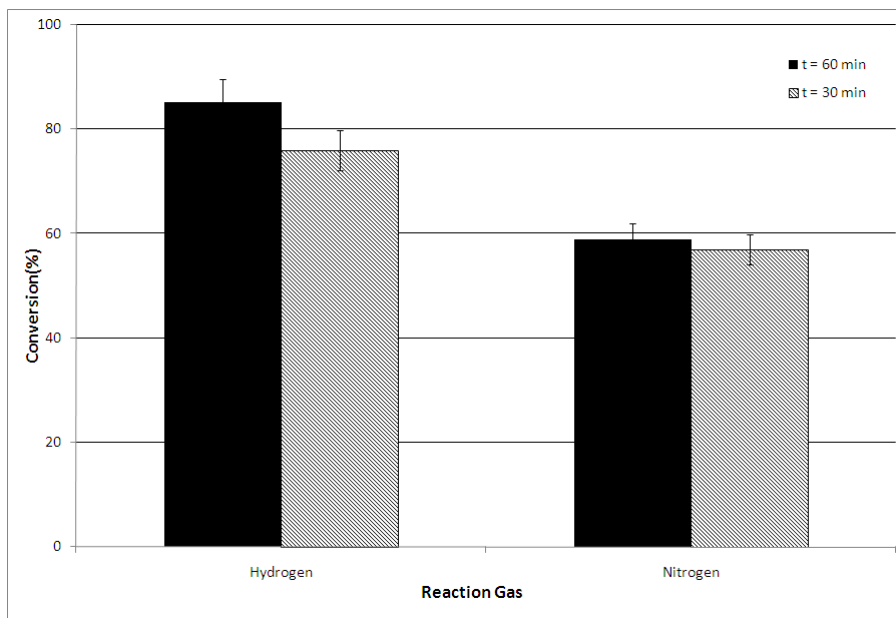


Figure 4.6. Effect of reaction gas on coal conversion for Tetralin

(T = 400°C, P = 60 bar)

One of the solvent properties that greatly affect coal digestion is its H/C ratio therefore studying this effect (Figure 4.7) can be used to choose optimum liquefaction solvents. In this study, a group of solvents of the same origin plus Tetralin as a commercial solvent were used for coal liquefaction. Because the H/C values are within a very small range for most of the solvents, a well-defined trend cannot be observed, however it is seen that solvent of higher H/C values have higher conversions too which is in agreement with the previous remarks on this effect.

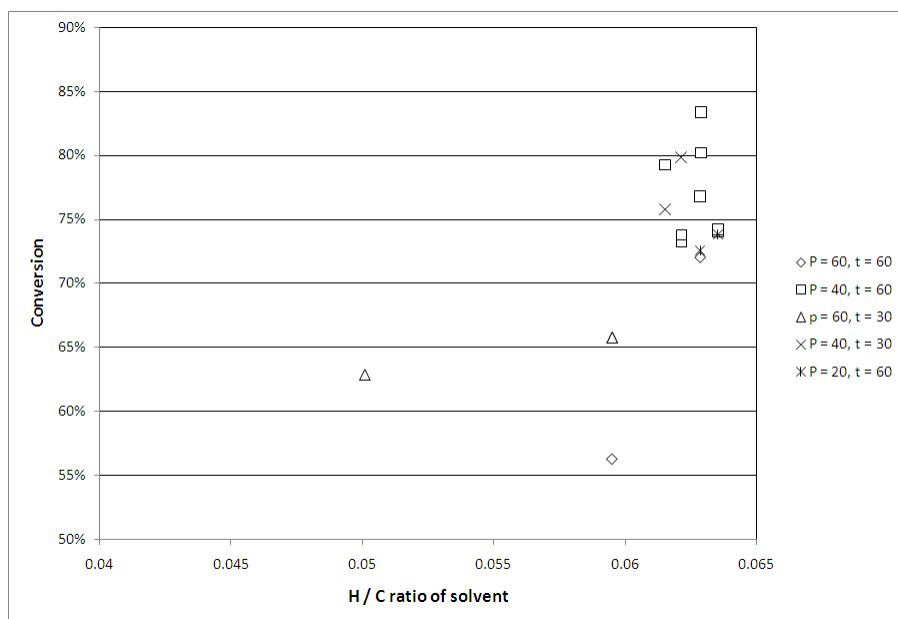


Figure 4.7. Effect of Solvent H/C ratio on Coal Conversion
(pressure (P)-bar, time(t)-minute)

In addition to the total amount of hydrogen present in the solvent, the types of hydrogen present may have an effect on the conversions observed in the

digestion. When conversion values are plotted against the ratio of aromatic hydrogen from NMR analysis (Figure 4.8), this effect becomes clear. Conversion shows an inverse relation with fraction of aromatic hydrogen. Although the trend here is relatively clearer, one should have this point in mind that the range of aromaticities studied are very narrow and therefore the results should be dealt with care. In terms of dissolution mechanisms, this effect can be explained in terms of higher rates for retrograde reactions in solvents of higher aromaticity. In other words, solvent itself may tend to polymerize and therefore reducing the conversion.

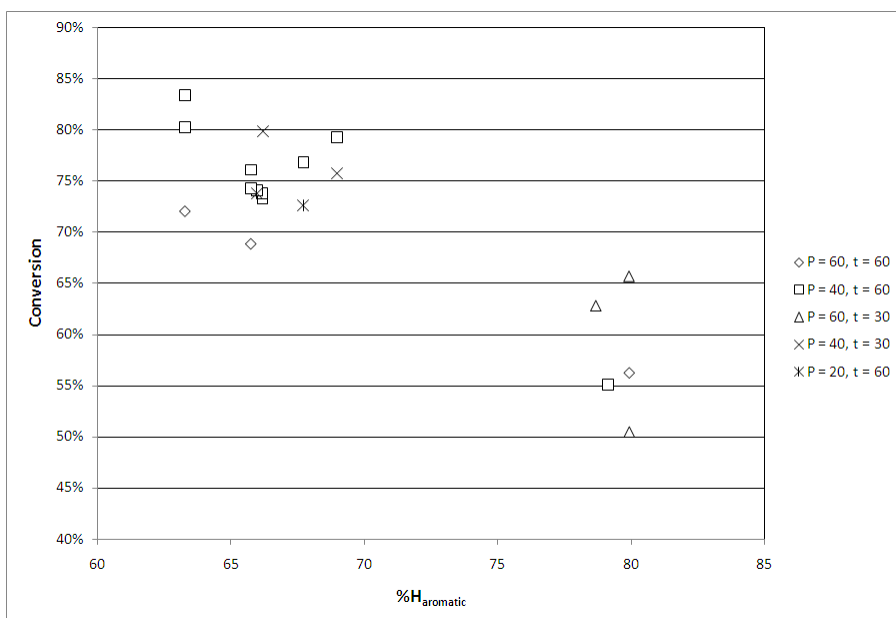


Figure 4.8. Effect of Solvent aromaticity on Coal Conversion
(pressure (P)-bar, time(t)-minute)

Conversion is the quantitative indication of coal liquefaction effectiveness. It is highly desired that the highest amount of coal organic matter is dissolved to

increase the amount of coke precursor produced per unit weights of coal and solvent consumed but one should not ignore the quality of the liquefaction products. As the purpose of this study was to use liquefied coal as coke precursor for carbon anode manufacture, products of quite high molecule size and aromaticity are required. This last factor is crucially important because hydroaromatic compounds are the foundation of anisotropy in carbonaceous materials. Other important factors in terms of product chemistry are its H/C ratio and its sulfur content.

The effect of temperature on H/C ratio and aromaticity for Tetralin runs are shown in Figures 4.9.A and 4.9.B. These two graphs when considered with tend observed for conversion (Figure 4.2) prove that the 400°C digestion temperature is the optimum condition for coal digestion because it gives the highest yield of a product with optimum quality.

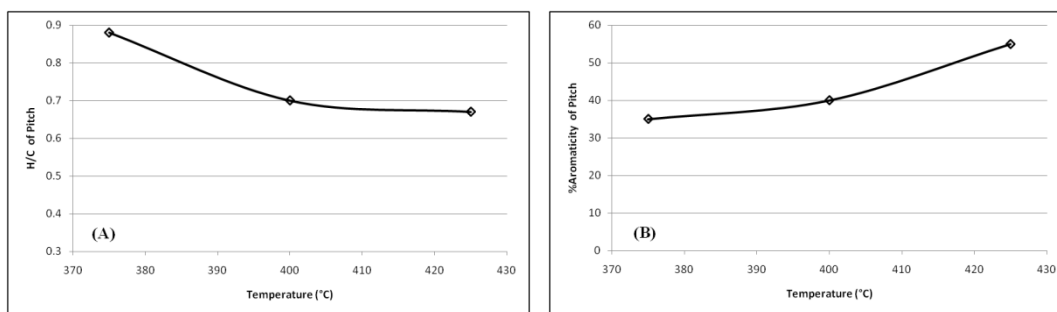


Figure 4.9. Effect of digestion temperature on (A) H/C and (B) aromaticity of pitch for Tetralin runs (Distillation: T = 250°C, P = 760 mmHg)

Tetralin recovery from the product can be done nearly completely using vacuum distillation as result, no residual solvent exist in the final pitch, the

condition is different when coal-derived solvents are used. These solvent react with coal and can never be completely removed from the final product as a result pitch properties is highly affected by their properties. Figure 4.10 compares the aromaticity of the pitches produced using different solvents. It is clearly seen that products from industrial solvents have higher aromaticity compared to those of Tetralin. This can be partially explained based on the residual solvent hypothesis discussed previously. The solvent incorporates in the final product structure and therefore is a major contributor to its properties although operating conditions like temperature are also important in terms of the final pitch properties.

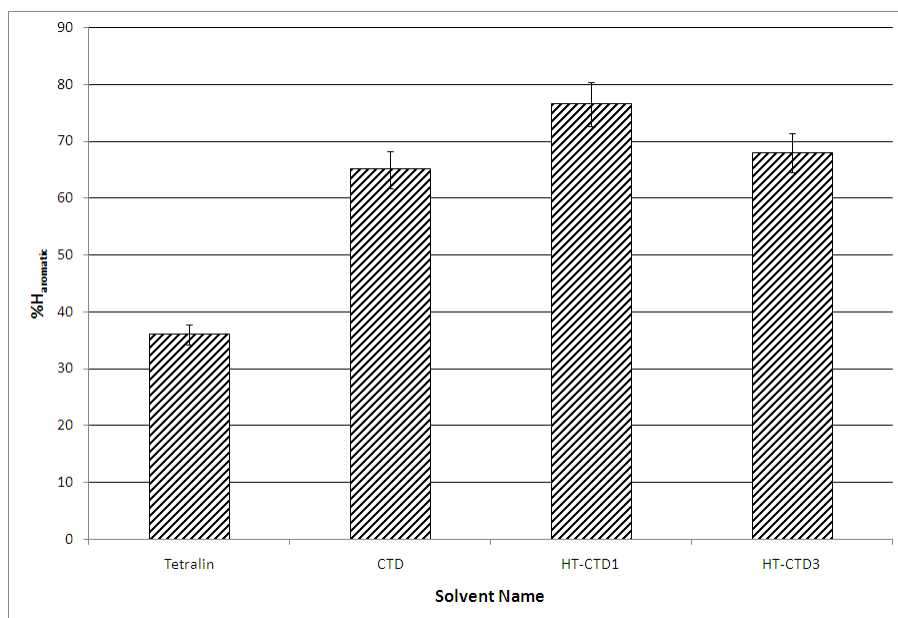


Figure 4.10. Effect of solvent on Pitch aromaticity
(Digestion: $P_{H_2} = 60$ bar, $T = 400^\circ\text{C}$)
(Distillation: $P = 760$ mmHg, $T = 330^\circ\text{C}$)

The coal extract is a complicated mixture of different organic compounds. These compounds can undergo further transformation even after the liquefaction.

Distillation conditions can greatly affect the chemical properties of the products through destruction or pyrolysis of these compounds. Figure 4.11 shows the effect of distillation severity of some coal extracts on the aromaticity of the resultant pitch. Higher vacuum levels have produced higher aromaticity products. Distillation severity is shown by correcting the distillation temperatures for reduced pressure values. For this correction, a polynomial equation introduced by Kurganova et al. was used [64]. The equation uses petroleum boiling point values as its basis, so the values presented here are only useful for showing the observed trend and no quantitative comparison with other liquids can be made. Vacuum tends to prevent reflux of lighter molecules during distillation and therefore leading to higher fraction of aromatic compounds and higher aromaticity.

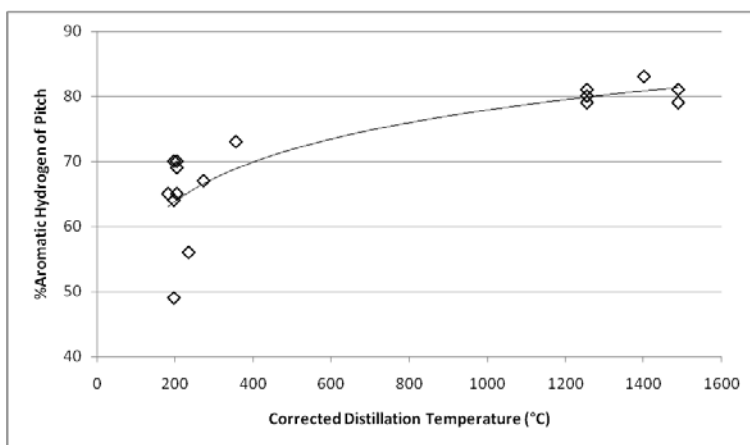


Figure 4.11. Effect of distillation severity on Pitch aromaticity

Contrary to the initial remarks on the effect of heat treatment, this process did not show any significant effect on the aromaticity of most of the pitches. This is shown in Figure 4.12 for a number of pitches produced by liquefaction using different solvents.

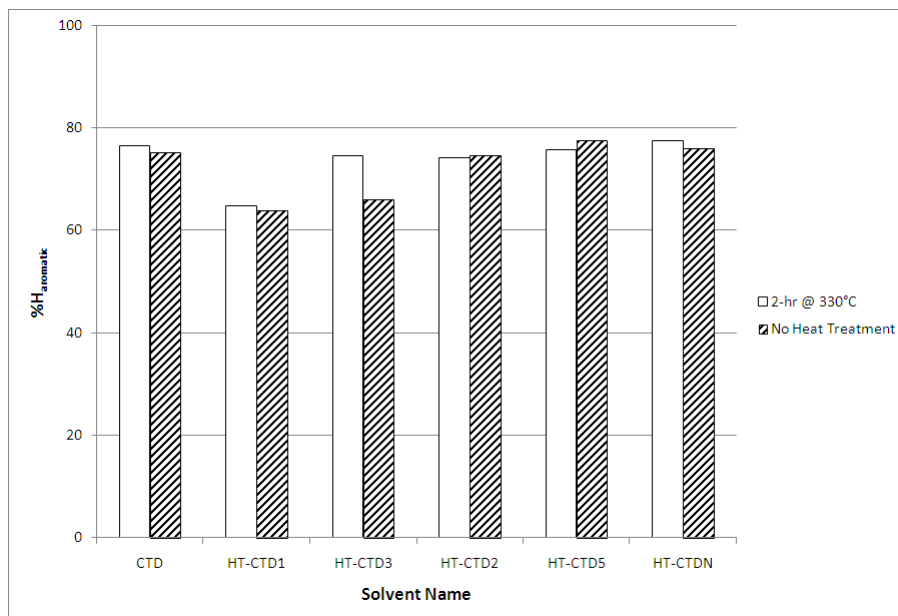


Figure 4.12. Effect of heat treatment on Pitch aromaticity
(Digestion: $P_{H_2} = 60$ bar, $T = 400^\circ\text{C}$)
(Distillation: $T = 330^\circ\text{C}$, $P = 30$ mmHg)

The only physical property of the pitch that was measured in this work was the softening point. The limited number of measurements performed shows a dependence of this factor on distillation severity. Most of the pitches studied for softening point are those produced using CTD as the liquefaction solvent. It is seen in Figure 4.13 that this factor increases with an increase in distillation severity. Distillation severity is highly sensitive to level of the vacuum applied. A high vacuum prevents the reflux of lighter compounds known to be responsible for the fluidity and therefore increasing the softening point of the pitch. This trend of course is based on a limited number of data points; therefore it should be dealt with care. Softening point of the pitch can then be correlated with its

aromaticity as shown in figure 4.14. For a better understanding of these property relations, molecular size has a high degree of importance. This property was not measured in this work as result the correlations are not highly acceptable because the analysis considers only part of the affecting parameters which is the aromaticity while ignoring the molecule size distribution.

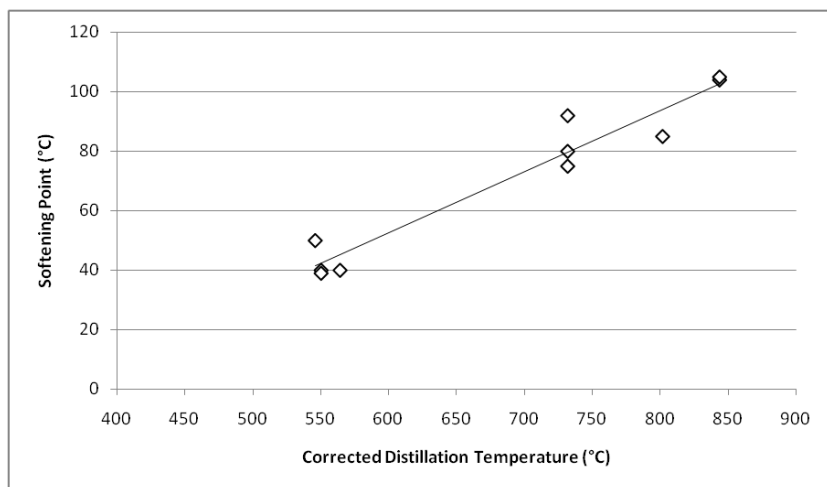


Figure 4.13. Effect of distillation severity on Pitch softening point

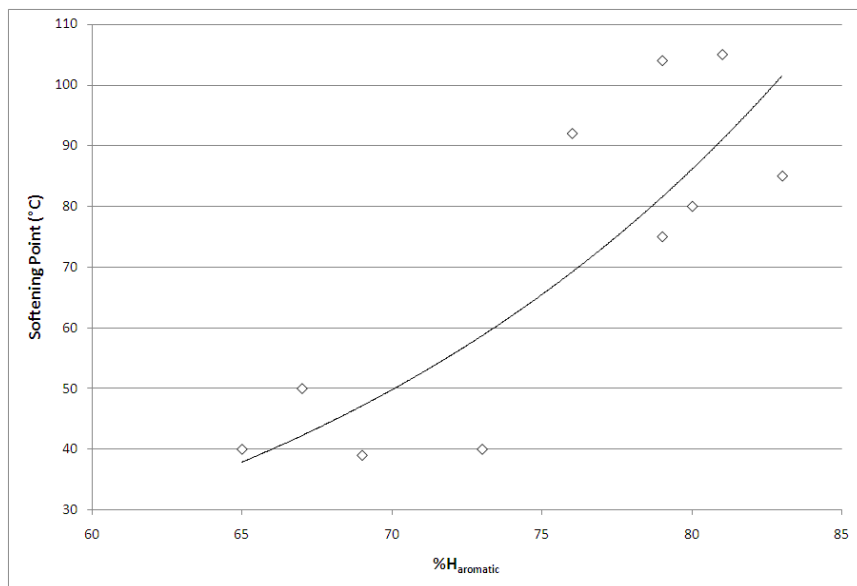


Figure 4.14. Softening Point – Aromaticity correlation for various pitches

4.3. Coking Yields

Nearly all of the pitches produced were coked using the salt bath coker. This part represents the correlations between coke properties and that of the pitch which can in turn be related to the liquefaction parameters. Coke yield is usually the first property to be studied. This is a quantitative indication of coking properties of different pitches. The yields calculated here are average values because only part of the pitch in the quartz tube usually converts to coke and some unreacted matter always exists, However because all of the coke yields were calculated in the same manner, the results should be good enough for the sake of comparison between different pitches.

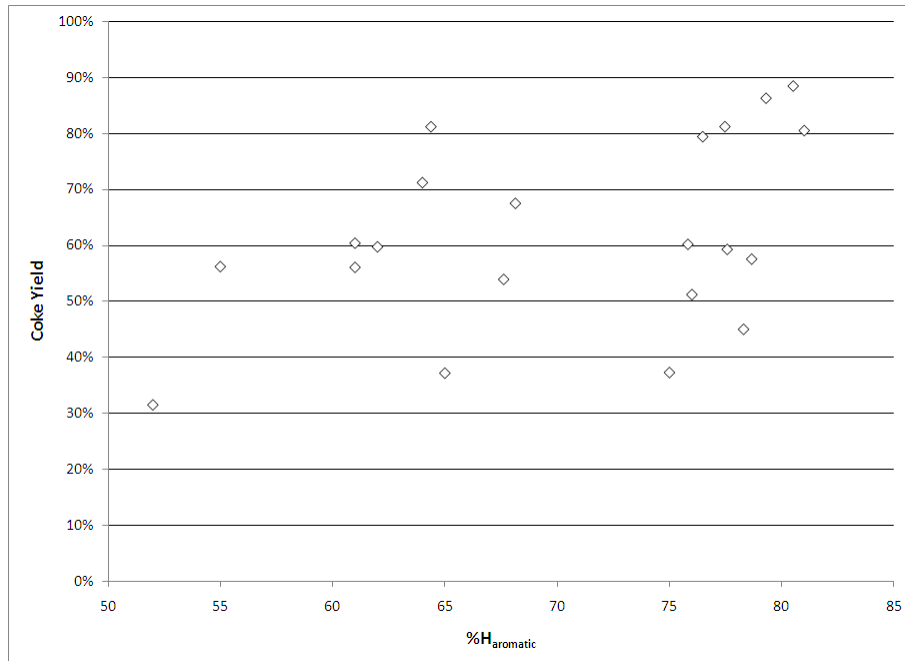


Figure 4.15. Dependence of coke yield on pitch aromaticity

Figure 4.15 shows the effect of pitch aromaticity on the coke yield. Although a general trend of increasing coke yield with aromaticity can be observed in this figure, the correlation is far from acceptable. This is another sign that aromaticity alone cannot be a suitable criterion for judgment on properties of the material.

Figure 4.16 shows the same data with data points shown separately based on whether they had heat treatment or not. Heat treated products generally have higher coke yield despite having the same aromaticity as the pitch without any heat treatment

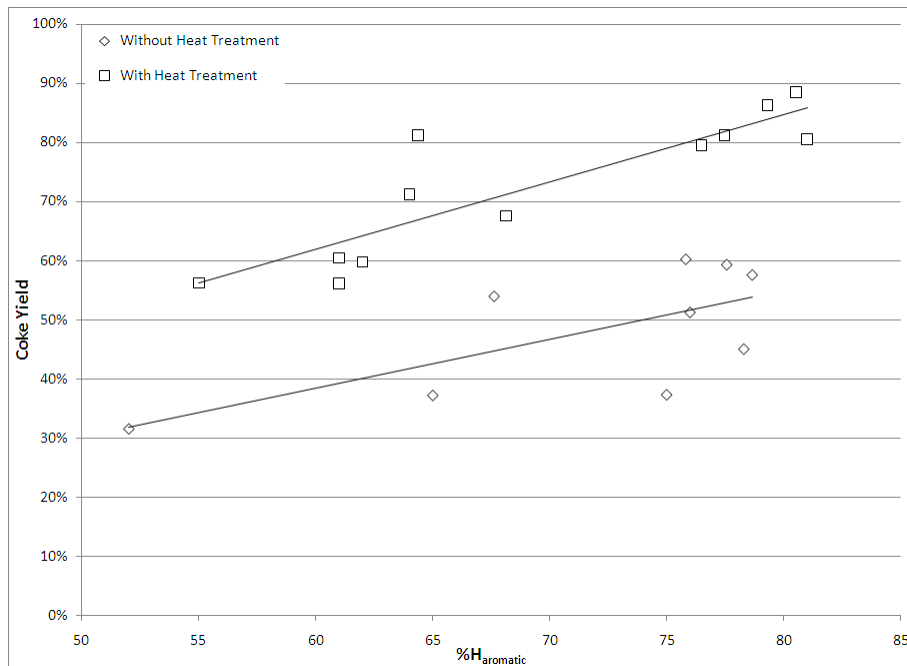


Figure 4.16. Effect of Heat Treatment on Dependence of coke yield on pitch aromaticity

Figure 4.17 shows the dependence of coke yield on the softening point of pitch. Although only a limited number of softening point measurements were

performed, a good correlation can be observed in this figure. The data of course represent pitches with lower coke yield, whether or not the same correlation can exist for other pitches cannot be understood based on the current set of data. This can prove the argument that aromaticity in combination with other pitch property, the most important of which is the molecular size distribution, should be used in such studies.

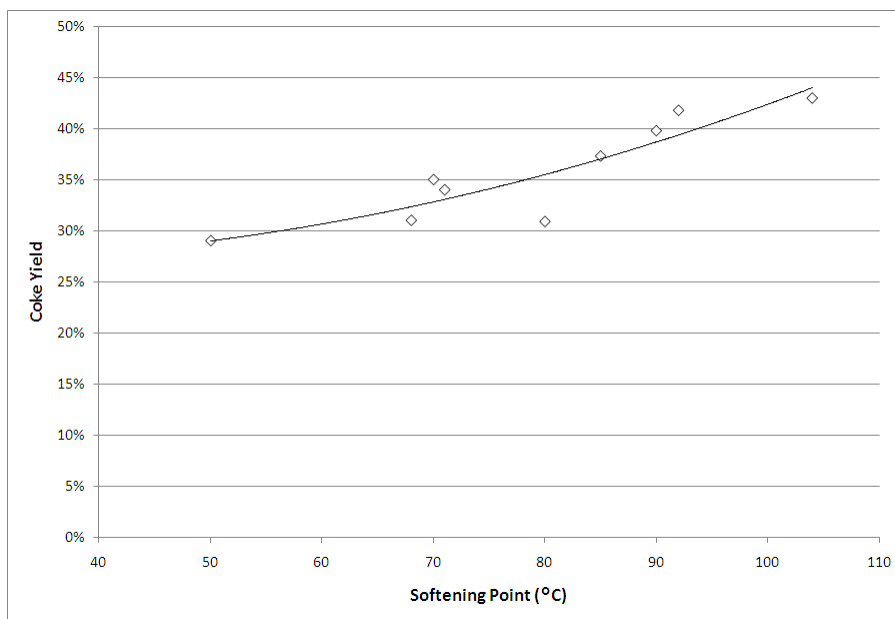
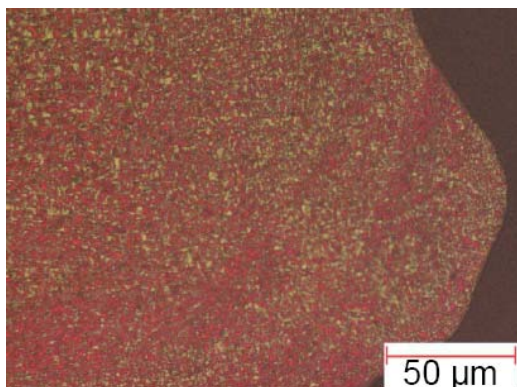


Figure 4.17. Relationship between coke yield and softening point of Pitch

In addition to coke yield, the quality of coke produced is also crucially important. Anisotropy and crystallinity are the two of the coke qualities vital to its applicability as a precursor for production of carbon anode materials. Optical microscopy and X-ray diffraction were the main techniques used to estimate these properties.

4.4. Image analysis of Coke Micrographs

For estimating the anisotropy using optical microscopy, the image analysis procedure introduced in Chapter 2 was used. For this purpose, available photomicrographs of cokes produced from different pitches were used as the input data. Most of the micrographs are from the cokes produced in thermobalance using N₂ as the inert gas and temperature profile of Fig. 3.13 by the third party supplier of the micrographs. Several micrographs of the cokes produced in the salt bath coker are also used for comparison and studying the effect of coking technique. Figures 4-18 to 4-21 show the micrographs of four of the cokes produced from pitches of different liquefaction solvents using the salt bath coker.



**Figure 4.18. Coke micrograph – Pitch#11B2
(Solvent = Tetralin)**

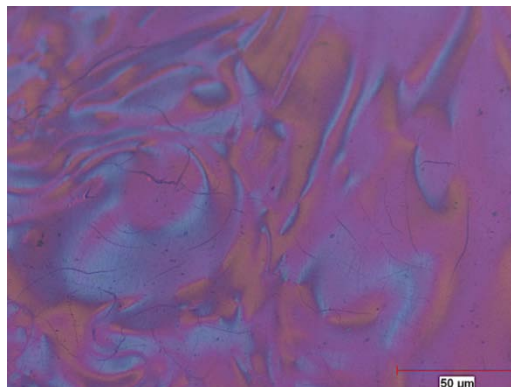


**Figure 4.19. Coke Micrograph – Pitch #9B2
(Solvent = CTD)**

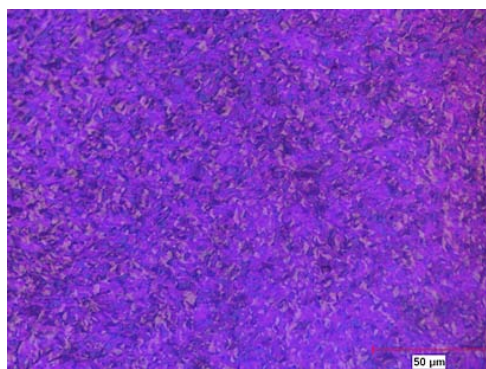


**Figure 4.20. Coke micrograph – Pitch#23B2
(Solvent = HT-CTD3)**

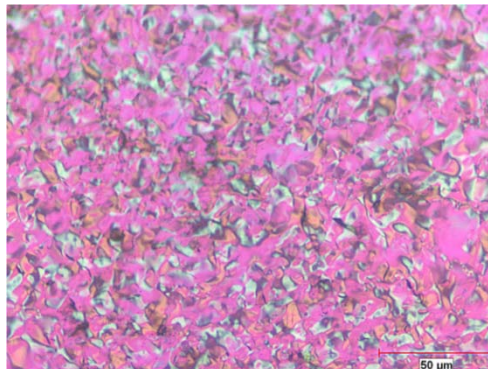


**Figure 4.21. Coke micrograph – Pitch#30B2
(Solvent = HT-CTD2)**

ImageJ, a public domain, java-based program developed by National Institute of Health [61] was used to process the micrograph images for calculating the indices discussed in Chapter 2. The type of process performed using ImageJ was mainly to produce the skeletonized image of the coke textures from the available micrographs. This task was performed in four steps. The available micrographs had to be converted into an 8-bit grayscale image before they can be used by the software for thresholding; outlining and later skeletonizing that produced the final bitmap image usable by the computer code for calculations. Figure 4.22 shows this process for the micrograph of one of the cokes.

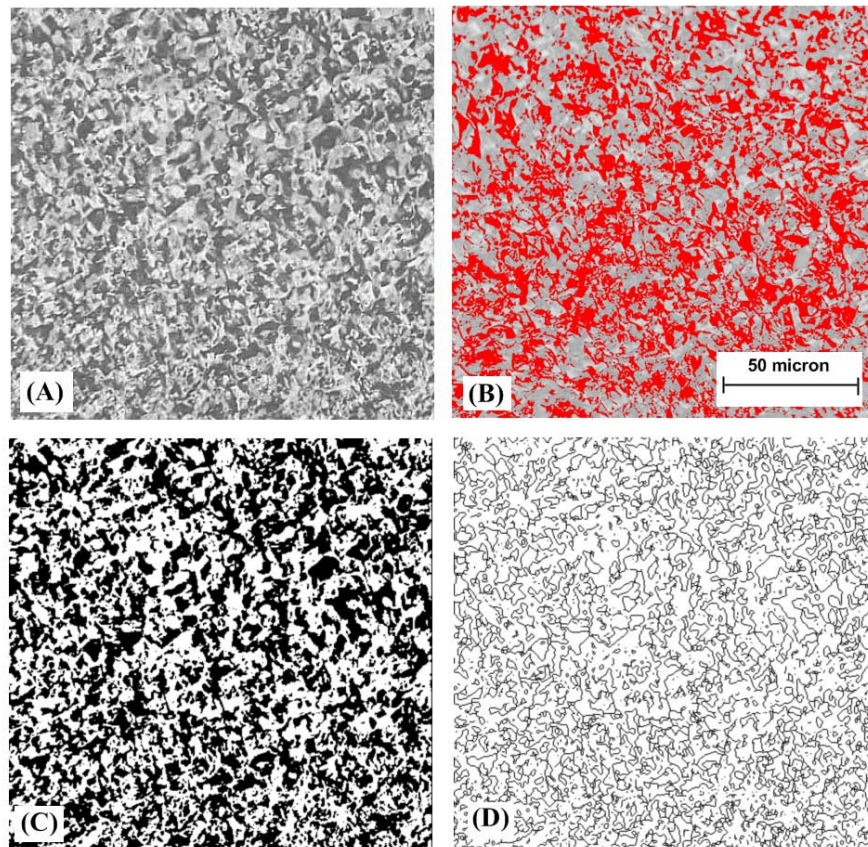


Figure 4.22. Conversion steps in image analysis of one of the cokes:
(A) Grayscale image, (B) Thresholded image, (C) Binary image and
(D) Skeletonized image

The grayscale image was produced by using the green channel of the original image. Green channel was chosen for this purpose because it produces the highest contrast among the three RGB channels [48].

The thresholded image is produced by the auto thresholding feature of the software. The program divides the image into objects and background. It does this by taking a test threshold and computing the average of the pixels at or below the threshold and pixels above. It then computes the average of those two, increments the threshold, and repeats the process. Incrementing stops when the threshold is larger than the composite average. That is, $\text{threshold} = (\text{average background} + \text{average objects})/2$ [62]. The thresholded image is then produced by converting the pixels above threshold to red and leaving those below unchanged or vice versa. This doesn't make a difference in the final results because the borders between these areas are only important in the analysis and not the areas themselves.

The thresholded image is then converted to a binary image by converting the red pixels to black and the rest to white. This binary image is used to construct the skeletonized image. ImageJ does the skeletonization by repeatedly removing pixels from the edges of objects in the binary image until they are reduced to single pixel wide skeletons [62].

The skeletonized image was processed to find the mosaic index and fiber index introduced earlier in chapters. This was done using a computer program written using visual basic. Figure 4.23 shows a snapshot of the graphical user interface of the program.

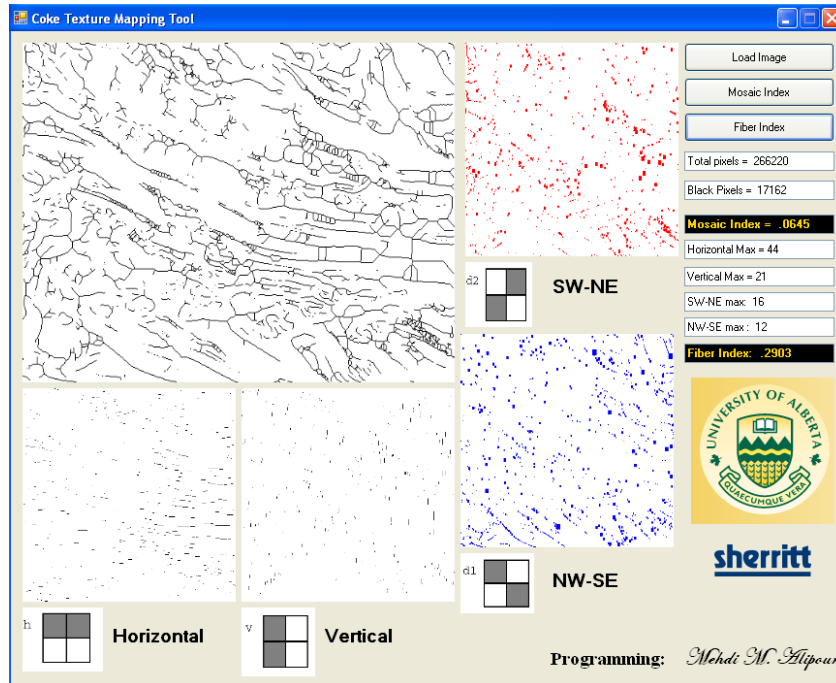


Figure 4.23. Graphical user interface of the computer program developed for calculation of image analysis indices

The code follows the ideas introduced in chapters, for calculating the Mosaic Index and Fiber Index. Simple pixel counting was used to calculate the ratio between black (0) and white (1) pixels which gives the mosaic index. To prevent the pore areas to be considered in the calculation, pores were already removed from the image using ImageJ in the previous stage. For calculation of Fiber Index, a subroutine was written to swipe the micrograph in the four directions required and count the pixels having the largest number of immediate black neighbors in that direction. This was used to produce directionally filtered images of the micrograph as shown by pictures labeled Horizontal, Vertical, SW-NE, and NW-SE in Figure 4.23. The two largest numbers of pixels with immediate black neighbors plus the summation of all four digits was then used to calculate the fiber index according to equation 2.4.

The calculated image analysis indices represent the degree of anisotropy in the coked product. Figures 4-24 to 4-27 can help to understand how pitch quality affects anisotropy in coke. High fiber index means a more directional texture and therefore higher anisotropy. Dependence of this index on pitch aromaticity is shown in Figure 4.24. This is in agreement with the previous understanding of the effect of aromaticity on anisotropy. The higher aromatic pitches can develop much better arranged structures compared to those with lower aromaticity.

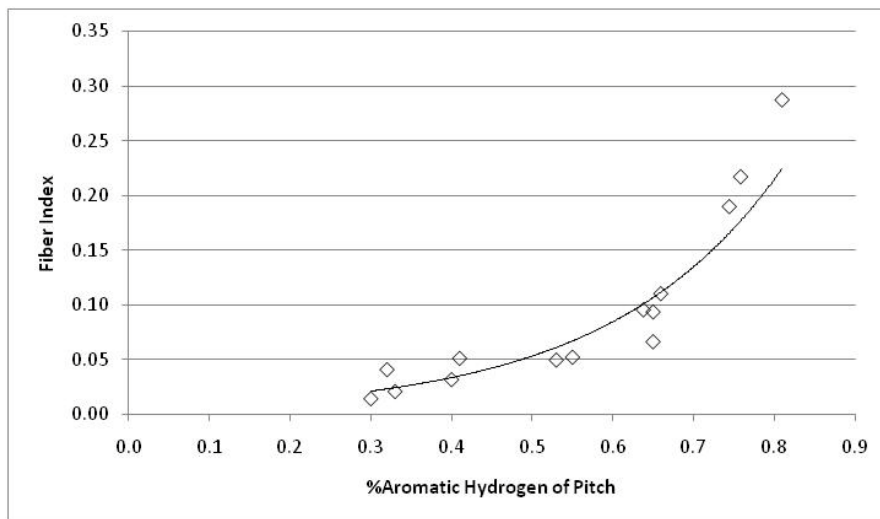


Figure 4.24. Dependence of Coke Fiber Index on Pitch Aromaticity

Mosaic index shows the reverse trend (Figure 4.25). In pitches of low aromatic content, although local arrangement to form mesophase spheres is possible but under the same heat treatment (coking) conditions coalescence of mesophase and formation of a bulk texture is out of reach. This leads to formation

of small crystallites which upon solidification form the fine texture morphologies represented by high values of mosaic index.

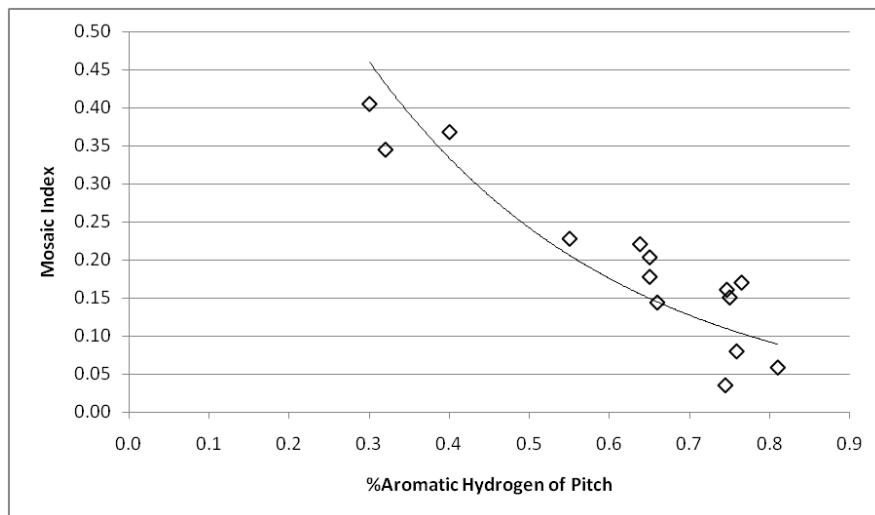


Figure 4.25. Dependence of Coke Mosaic Index on Pitch Aromaticity

H/C of pitch is another factor whose effect is worth studying. As expected from the aromaticity relations, cokes produced from pitches with high H/C generally show lower anisotropy (Figures 4.26 and 4.27). This can be explained in terms of the processes during coking too. Pitches with higher H/C usually tend to have lower molecular size distribution. This means that a higher fraction of smaller molecules of low boiling point exist in them which do not have the ability to take part in the polymerization process and are usually lost as volatile compounds during coking. This loss of components responsible for fluidity prevents the mesophase growth to bulk texture and results in cokes with fine textures as represented by high mosaic index.

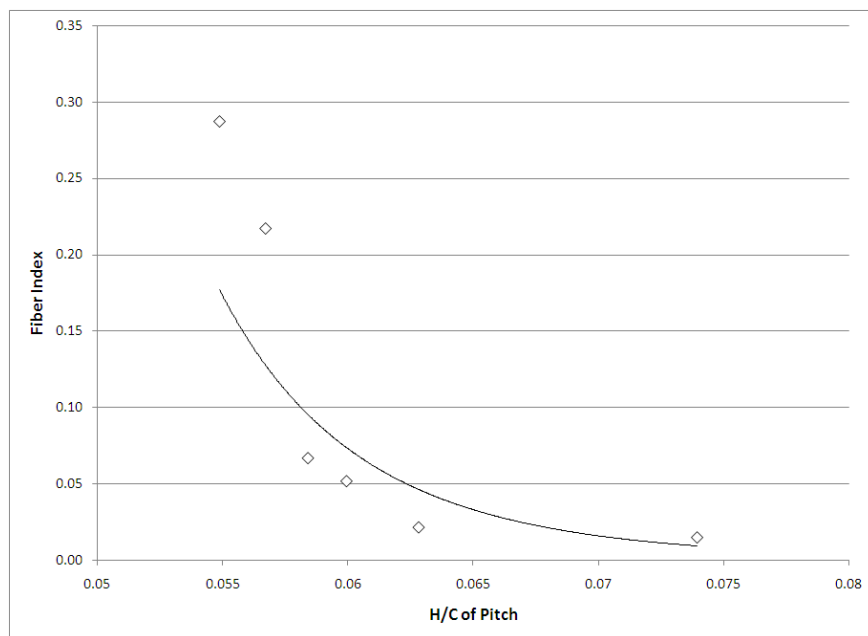


Figure 4.26. Dependence of Coke Fiber Index on Pitch H/C

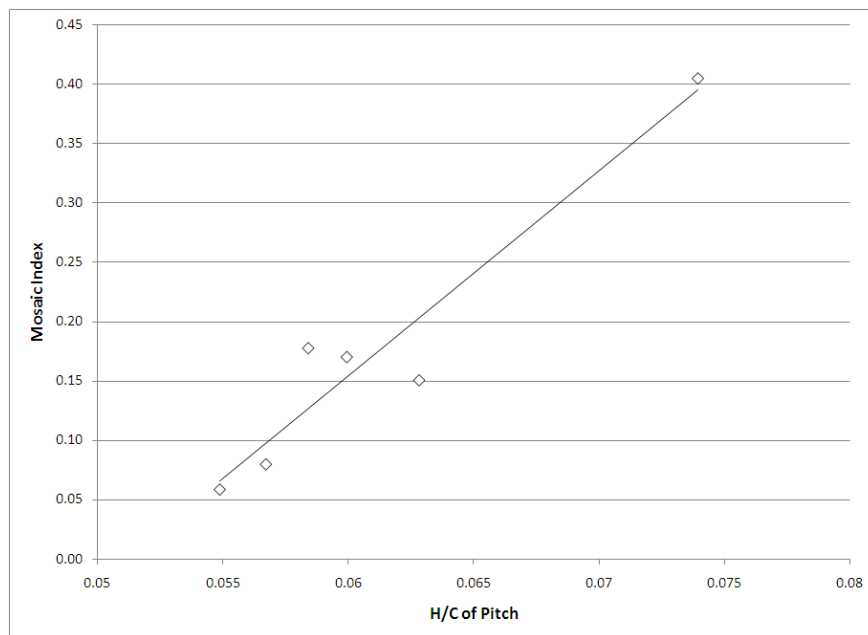


Figure 4.27. Dependence of Coke Mosaic Index on Pitch H/C

As discussed in Chapter 2, development of anisotropy greatly depends on the molecular associations among the aromatic structures known as Local Molecular Orientation (LMO). The Chemical composition dependence of LMO is expressed in terms of the LMO factor given by Equation 4.1 where [O], [S] and [H] are weight percent of Oxygen, Sulfur and Hydrogen respectively.

$$F_{LMO} = \frac{([O] + [S])}{[H]} \quad \text{Eqn 4.1 [43]}$$

The variation of the image analysis indices can give some insight on how the other elements affect the development of anisotropy. Figure 4.28 shows this relationship. Contrary to our expectation, Mosaic Index increases with F_{LMO} while Fiber index decreases. This can be an indication that cokes with lower anisotropy have higher potential for local molecular arrangement but the problems with later association of these arrangements make the texture fine. In other words, mesophase can form readily but difficulty in growth and coalescence of the formed spheres makes the final texture a very fine one with a high mosaic index.

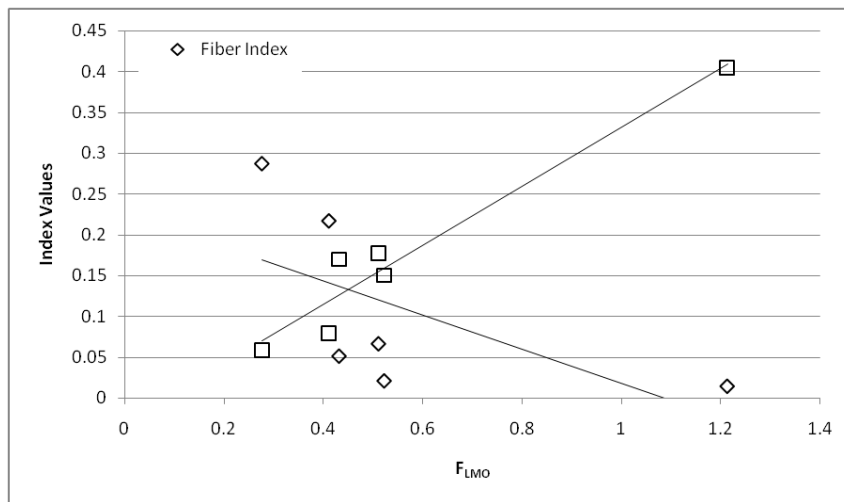


Figure 4.28. Dependence of Coke Anisotropy Indices on F_{LMO} of Pitch

4.5. X-ray diffraction Studies

X-ray diffraction was used to calculate the coke crystalline properties such as crystallite size and micro-strain in different crystallographic planes. X-ray diffraction results also very well show the evolution of crystal structure form raw coal to calcined coke. Figure 4.29 shows the diffraction pattern of coal and residue for run #9. Coal and residue show sharp mineral peaks over a background of nearly amorphous structure. The intensity of background is lower in residue which shows its lower organic content compared to that of coal. Quantitative X-ray diffraction analysis using SiroquantTM on low temperature ashes of coal and residue shows their similar mineral content (Figure 4.30). In pitch, mineral peaks disappear and graphitic structure starts to develop in diffraction patterns of green and calcined coke (Figure 4.31).

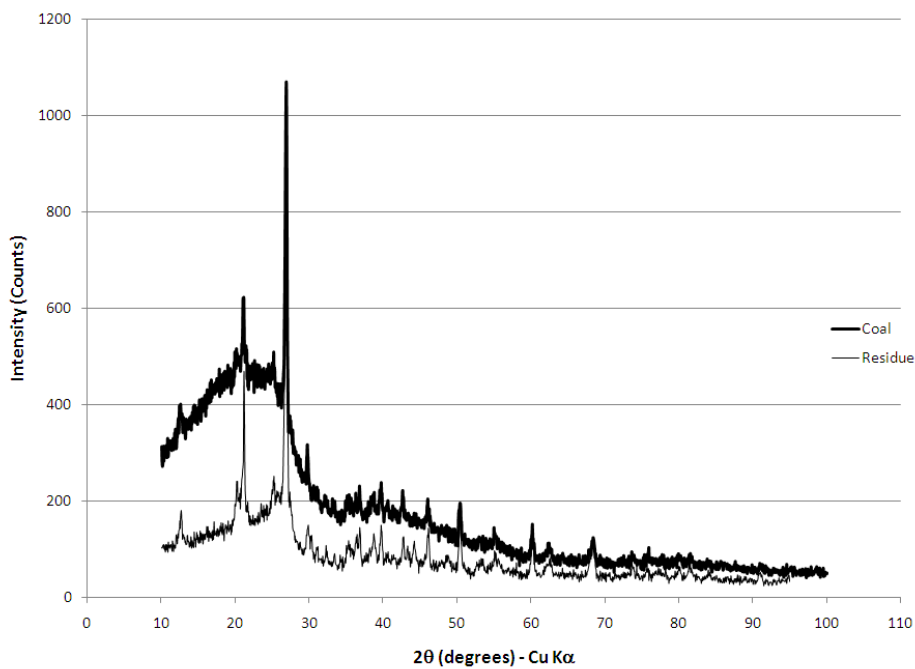


Figure 4.29. X-ray Diffraction Patterns of coal and residue

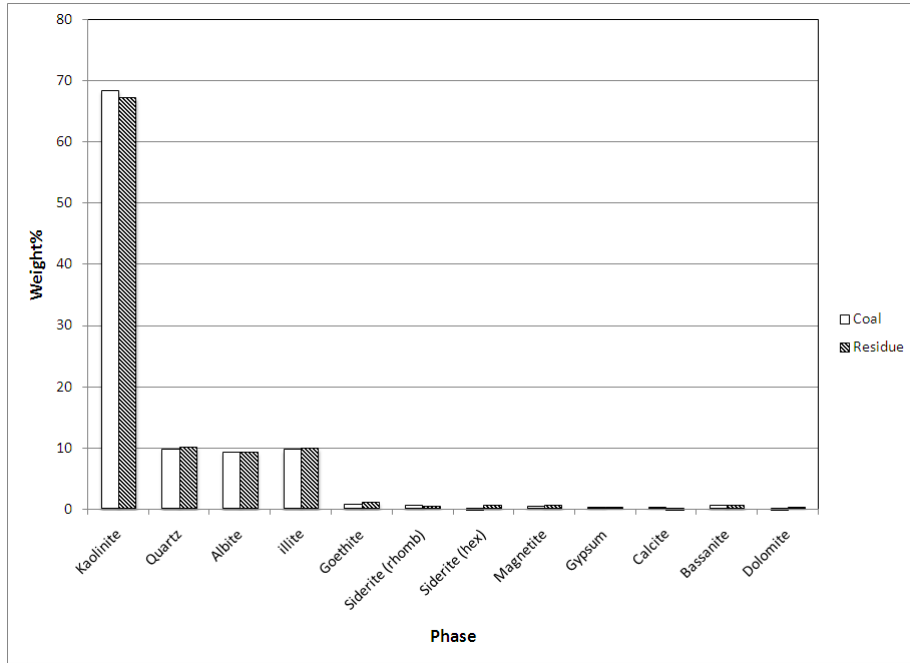


Figure 4.30. Composition of minerals in low temperature ash of coal and residue

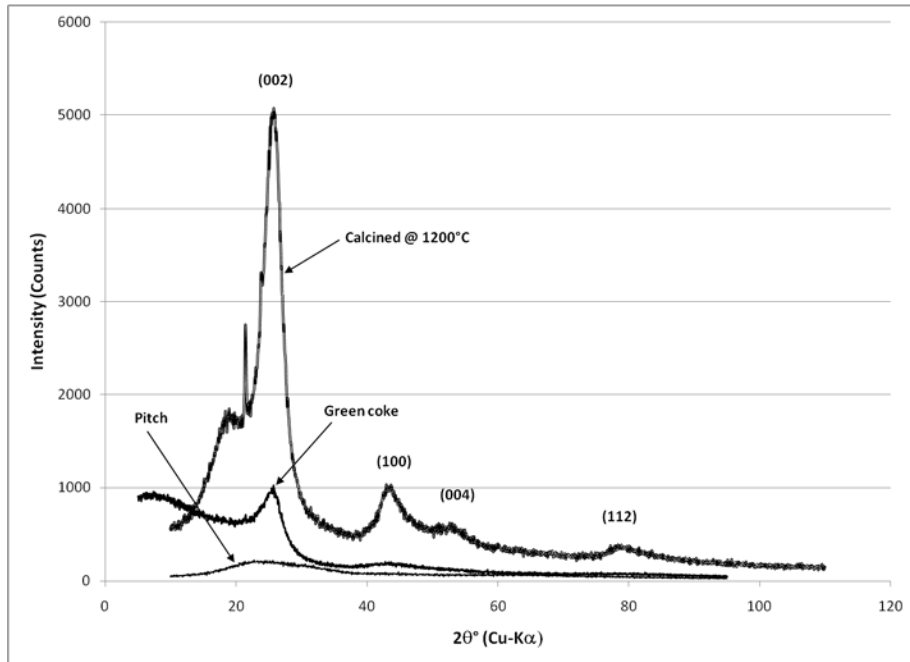


Figure 4.31. Crystal structure evolution of carbon from pitch to calcined coke

Development of crystallinity following a pattern similar to that of graphite is quite clear in Figure 4.31. Peaks (002), (100) and (004) are all typical of carbonaceous materials. For most of the products, another peak at angles smaller than that of (002) is observed that cannot be associated with any crystalline plane in graphite. Prifti et al [63] have reported this peak for cokes heat treated from 1100°C to 1600°C. They use non-stable dwarf term for its description and explain its occurrence as a result of creation of defects in the planar structure of coke at these temperatures. The peak is considered non-stable because it disappears at higher temperatures. In this work, the only significance of this peak is its effect on the accuracy of curve fitting procedure used in line profile analysis of (002) peaks.

Figures 4.32 and 4.33 show the correlation between crystallite height and width calculated using single line analysis and the anisotropy indices calculated from the image analysis. Regardless of the goodness of correlations, the general trend is an increase in crystallite height and width with increase in the anisotropy. Both L_c and L_a show an increasing trend with fiber index while the reverse is true when values are plotted versus mosaic index. This can be explained on the basis that structures with high mosaic index tend to show more isotropic properties. This means that crystallites are too small to create any directionality in the properties. Small crystals show a rather uniform texture which is a characteristic of textures with high fiber index.

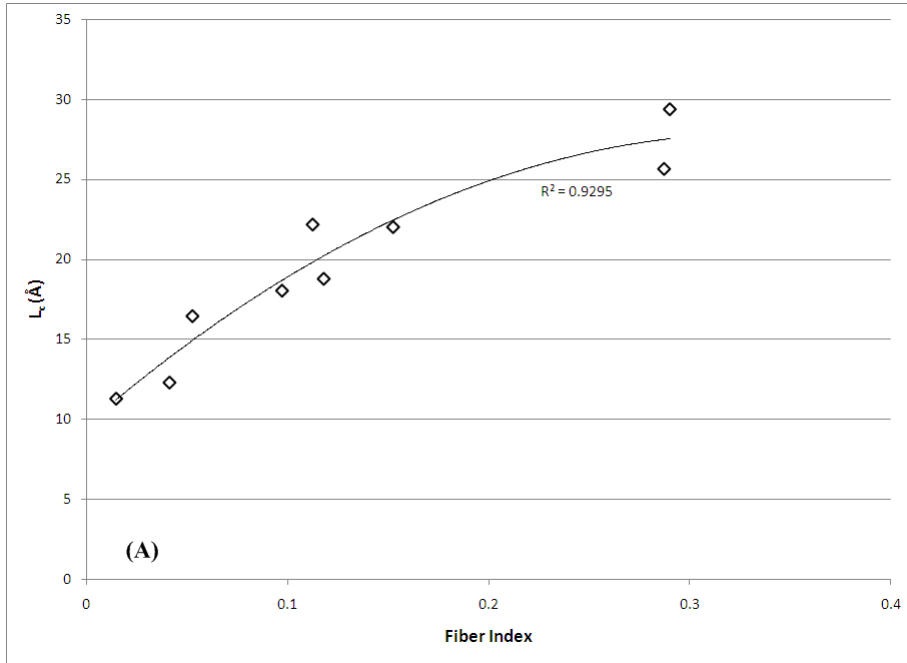


Figure 4.32. Relation between crystallite height (L_c) and Fiber index

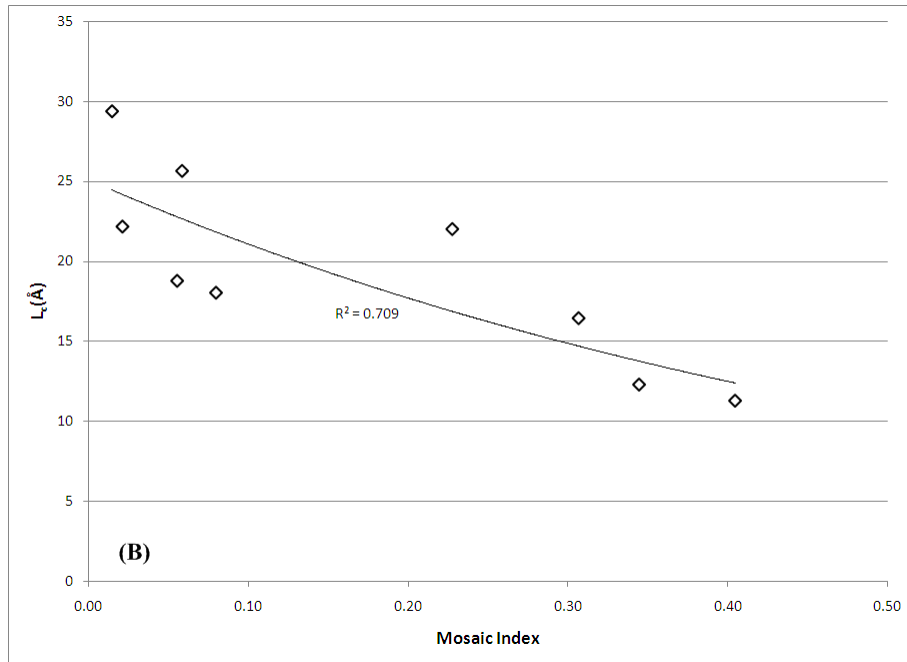


Figure 4.33. Relation between crystallite height (L_c) and Mosaic index

CHAPTER 5

CONCLUSIONS AND RECOMMENDATIONS

The objective of this study was to study the suitability of the coal extract produced by solvent extraction of an Albertan subbituminous coal as a precursor for production of carbon anodes. Tetralin and a coal-derived solvent were the main solvents used in liquefaction experiments. Hydrotreatments were also performed on the coal-derived solvent to provide another set of solvents. Produced coal extracts were undergone a simple heat treatment before being treated in a lab-scale coker. Coal, solvents, coal extracts and cokes were studied by chemical and physical characterization techniques to determine the favorable liquefaction and processing conditions and the suitability of the produced extracts as carbon anode precursor.

5.1. Conclusions

1. The Albertan coal studied is a suitable choice for pitch production using solvent extraction. Its low sulfur content makes it suitable for carbon anode feedstock production and its high oxygen gives it properties favorable for coal liquefaction.
2. Liquefaction reactions under hydrogen atmosphere generally have higher coal conversion compared to Nitrogen when Tetralin is used as a solvent

3. 1 hour seems to be the suitable residence time for liquefaction experiments although the effect was not significant for solvents other than Tetralin.
4. 400°C yields the highest coal conversion. Lower temperatures are not suitable for coal dissolution due to low rate of cracking reactions. The lower conversion at higher temperatures might be an artifact of the experimental procedure.
5. Hydrogen pressure in the range 40-60 bar didn't show a unique effect. Higher pressure favored higher conversion by some solvents while the reverse was observed for some other solvents.
6. The coal-derived solvent and its hydrotreated variations all have liquefaction yields lower than that of Tetralin but hydrotreatment has improved the conversion of coal to liquid extract.
7. Solvents with lower aromatic hydrogen content have yielded higher coal conversion but feedstocks produced by these solvents have more favorable properties as carbon anode precursor as evidenced by optical microscopy and x-ray diffraction.
8. Solvent properties persist through the whole process. For coal-derived solvents, process is basically a coal/solvent co-processing as compared to classic liquefaction. This can have serious technical and economic implications when the amount of solvent consumed to produce a certain amount of coke precursor is considered.
9. Post liquefaction processes can dramatically affect the properties of the produced feedstocks. This can be used to give more flexibility to the

process. A single coal extract produced under certain conditions can be processed to produce feedstocks of different properties. This way, different components of carbon anode (coke, binder pitch, etc.) can be produced from a single resource that is coal.

10. More severe distillation conditions produced products with higher aromaticity while heat treatment on didn't show any significant effect on this factor.
11. Yield of the coke from produced feedstocks was found to be dependent on the aromaticity as well as softening point of them. Softening can represent the molecular size distribution of the pitch therefore showing the effect of this factor in addition to the aromatic content on the coke yield.
12. Anisotropy of coke can be very well described by image analysis of the polarized light optical micrographs. The technique deployed in this work has the advantage of providing a systematic approach to anisotropy estimation preventing human errors in the calculations.
13. The calculated indices very well correlate with feedstock chemistry. High aromatic content of pitch favors high anisotropy while high H/C ratio has the reverse effect.
14. X-ray diffraction of residue shows the effectiveness of mineral matter removal in the liquefaction process as a very well agreement exists between the patterns of coal and residue.

15. X-ray diffraction can provide alternative pathway for anisotropy estimation, however the correlation is too far from perfect to be used as a quantitative tool but it can still show a general trend

5.2. Recommendations

Like any other area of engineering, long-term sustainability of the process requires a fundamental understanding of the ongoing processes. Coal liquefaction involves two complicated components: Coal and the combination of processes occurring during liquefaction. Use of coal or petroleum-derived solvents adds to this complexity. This work can serve as a starting point for development of a technology for production of carbon anode precursor from coal liquefaction products. However, fundamental understanding of the process requires a much better planned and detailed approach. The following recommendations can be helpful for future continuation of the present work:

1. Rate studies using the reactor of the scale used in this study may not provide valid data due to large heating and cooling rates involved. Initial digestion experiments should first be performed in mini-reactors or tube bombs before scaling up to a larger autoclave.
2. Tetralin or other commercial solvents can provide some insight into extractability of the coal but extraction behavior of each industrial solvent should also be studied before any judgment on the choice of operating conditions can be made.

3. Compositional analysis of the off-gas during coal liquefaction is necessary to understand the difference in liquefaction behavior when different solvents are used.
4. Hydrogenation of solvents used in this study was somehow arbitrary. This caused different hydrotreated solvents to have similar properties and therefore making the comparison between them rather difficult or sometimes impossible. An optimization of the hydrogenation process seems to be necessary. This can be done using a parametric study through varying temperature, hydrogen pressure, residence time and even solvent or solvent combination.
5. Solvents from more diverse sources should be tried. Solvent blending or combination can improve liquefaction conversion and optimize the quality of produced pitches.
6. Detailed chemical characterization of the solvents and pitches are highly recommended. Use of C^{13} NMR and molecular weight distribution using simulated distillation can clarify the liquefaction behavior of the solvents and carbonization mechanism of the pitches. Use of a more suitable solvent like carbon disulfide or carbon tetrachloride is also recommended for conduction of H^0 NMR experiments.
7. Coke yields of most of the pitches produced are not as high as desired. This can be due to presence of too much solvent in the coal digest. More severe distillation conditions therefore seem necessary to improve this parameter. In addition to vacuum distillation and heat treatment,

another technique that is useful in improving the coke yield of the coal extract is the air blowing technique [65]. Use of this technique or its combination with the current post-liquefaction processes can improve the coke yield of the digested extracts.

8. The coking technique used seems to be suitable for this stage of study but use of a setup more similar to delayed coking can provide a more realistic means for understanding the suitability of produced feedstocks as carbon anode precursor. A semi-batch tube bomb setup using sand bath is available that can be used for this purpose.
9. Only a limited number of cokes were calcined in this study. More calcination experiments are necessary to understand how the feedstocks behave in the final stage of carbon anode production.
10. Physical and chemical characterization of the calcined cokes is also helpful in this regard. Cross linking Sulfur plays an important role in development of anisotropic structure therefore characterization of this type of sulfur in calcined products is necessary in understanding their behavior. Measurement of electrical conductivity and coefficient of thermal expansion of both green and calcined cokes can provide some insight on the suitability of these products as carbon anode precursor. Measurement of porosity by CO₂ or N₂ absorption is necessary as porosity as it is a key physical property affecting many other qualities like mechanical strength and electrical conductivity.

REFERENCES

1. Biological Abundance of Elements in Internet Encyclopedia of Science, retrieved on July 22, 2009 @ <http://www.daviddarling.info/encyclopedia/E/elbio.html>
2. Song, C. and Schobert, H. H., "Non-fuel uses of coals and synthesis of chemicals and materials", Fuel, Vol. 75, No. 6, pp. 724-736, 1996.
3. B. T. Kelly, Physics of Graphite, Applied Science Publishers, USA, 1981
4. Brian McEnaney, "Structure and Bonding in Carbon Materials" in D. Burchell (Editor), Carbon Materials for Advanced Technologies, Elsevier, USA, 1999
5. International committee for characterization and terminology of carbon. First publication of 30 tentative definitions, Carbon 1982, 20, pp. 445-449.
6. Fathi Habashi (Editor), Handbook of Extractive Metallurgy, Wiley, USA, 1997
7. George E. Totten, D. Scott MacKenzie (Editors), Handbook of aluminum. Volume 2, Alloy production and materials manufacturing, Marcel Dekker, USA, 2003
8. Arnold J. Hoilberg (Editor), Bituminous Materials. Volume 3: Coal Tars and Pitches, Interscience Publishers, USA, 1979
9. Gray, R.J. and Krupinski, K.C. "Pitch Production: Supply, coking, optical microscopy and applications." Introduction to Carbon Technologies. Universidadde Alicante, Secretariado de Publicaciones, p 358, 1997.
10. "Technical Report". "Coal Based Nuclear Graphites for the New Production Gas Cooled Reactor. Task 1: Development of Coal-Derived Isotropic Coke and Nuclear Graphite." West Virginia University, 1994.

11. Peter G. Stansberry et al. "Coal-derived Carbons" in D. Burchell (Editor), Carbon Materials for Advanced Technologies, Elsevier, USA, 1999
12. Isao Mochida, "Chemistry in Production and Utilization of Needle Coke" in Peter A. Throver (Editor), Chemistry and Physics of Carbon, Vol. 24, CRC Press, USA, 1993
13. A. Oberlin, "Carbonization and Graphitization", Carbon, Vol. 22, No. 6, pp. 521- 541, 1984
14. Vorpagel ER, Lavin JG, "Most stable configurations of polynuclear aromatic hydrocarbon molecules in pitches via molecular modeling", Carbon, Vol. 30, No. 7, pp. 1033-1040, 1992
15. R. A. Greinke, "Early Stages of Petroleum Pitch Carbonization" in Peter A. Throver (Editor), Chemistry and Physics of Carbon, Vol. 24, CRC Press, USA, 1993
16. A. Oberlin and S. Bonnamy, "Carbonization and Graphitization" in Pierre Delhaès (Editor) Graphite and Precursors, Gordon & Breach, Australia, 2001
17. I.C. Lewis, "Chemistry of Carbonization, Carbon", Vol. 20, No. 6, pp. 519-529, 1982
18. I. Mochida, "Anisotropy of Needle Cokes", Bulletin of the Chemical Society of Japan, Vol. 49, No. 2, pp. 514 -519, 1996
19. H. P. Klug, X-ray diffraction procedures for polycrystalline and amorphous materials, Wiley, USA, 1974
20. Merrick, D. Coal Combustion and Conversion Technology, Elsevier, USA, 1984
21. Schobert, H. Coal: The Energy Source of the Past and Future. American Chemical Society, USA, 1987.
22. Ergun, S., "Coal Classification and Characterization," in C.Y.Wen (Editor) Coal Conversion Technology, Addison-Wesley Publishing Company, Reading, Mass., 1979.

23. B. R. Cooper and W. A. Ellingson (Editors), Science and Technology of Coal Utilization, Plenum Publishing Corporation, USA, 1984
24. Shirley Cheng Tsai, Fundamentals of Coal Beneficiation and Utilization, Elsevier, USA, 1982
25. Yatish T. Shah, Reaction Engineering in Direct Coal Liquefaction, Addison-Wesley Publishing Company Inc., USA, 1981
26. R. H. Schlosberg, Chemistry of Coal Conversion, Plenum Press, USA, 1985
27. Curran et al, Mechanism of the Hydrogen Transfer Process to Coal and Coal Extract , Ind. Eng. Chem. Process Des. Dev., Vol. 6, pp. 166-173, 1967.
28. D. F. McMillen et al, “Hydrogen-Transfer-Promoted Bond Scission Initiated by Coal Fragments”, Energy & Fuels, Vol. 1, pp. 193-198, 1987
29. R. Malhotra and D. F. McMillen, “A Mechanistic Numerical Model for Coal Liquefaction Involving Hydrogenolysis of Strong Bonds”, Energy & Fuels, Vol. 4, pp. 184-193, 1990
30. J. R. Pullen, Solvent Extraction of Coal, Report No. ICTIS/TR16, IEA Coal Research, UK., 1981
31. Berkowitz, N. An Introduction to Coal Technology. Academic Press, Inc., USA, 1994.
32. Robert A. Keogh and Burtron H. Davis, “Comparison of Liquefaction Pathways of a Bituminous and Subbituminous Coal”, Energy & Fuels, Vol. 8, No. 2, pp. 289-293, 1994
33. Given, P.H. et al, “Dependence of Coal Liquefaction Behavior on Coal Characteristics. 2: Role of Petrographic Composition.” Fuel, Vol. 54, No. 1, pp. 40-49, 1975.
34. J. T. Joseph et al, “Coal Maceral Chemistry. 1. Liquefaction Behavior”, Energy & Fuels, Vol. 5, pp. 724 -729, 1991

35. Whitehurst, D.D., Mitchell, T.O., and Farcasiu, M., "Coal Liquefaction: The Chemistry and Technology of Thermal Processes", Mobil Research and Development Corporation, Central Research Division, Princeton, New Jersey, 1980.
36. Oele, A. P. et al, "Extractive Disintegration of Bituminous Coals", Fuel, Vol. 30, No. 7, pp. 169-178, 1951
37. Wise, W. S., Solvent Treatment of Coal, Mills & Boon, UK, 1971
38. Curtis, C. W. et al, "Effect Solvent Quality on Coal Conversion", American Chemical Society, Division of Fuel Chemistry, Preprints, Vol. 24, No. 3, pp. 185-194, 1979
39. Kouzu, M. et al, "Effect of Solvent Hydrotreatment on Product Yield in the Coal Liquefaction Process", Fuel Processing Technology, Vol. 68, pp. 237-254, 2000.
40. R. J. Diefendorf, Ext. Abstracts 16th Bien. Conf. on Carbon, San Diego, Plenary Lecture, 1983
41. Mochida, I., "Study of carbonization using a tube bomb: Evaluation of lump needle coke, carbonization mechanism and optimization", Fuel, Vol. 67, No. 9, pp. 1171-1181, 1988
42. Mochida, I. et al, "Carbonization in the Tube Bomb Leading to Needle Coke: III. Carbonization Properties of Several Pitches", Carbon, Vol. 27, No. 3, pp. 375-380, 1989
43. Oberlin A. and Rousseaux, F., "Graphitization of Several carbons: Studies using X-ray Diffraction and Transmission Electron Microscopy", Journal of Applied Crystallography, Vol. 1, pp. 218-226, 1968
44. Marsh, H.; Walker, P. L. "The formation of graphitizable carbons via mesophase: chemical and kinetic considerations" In Thrower, P. A. (Editor) Chemistry and Physics of Carbon, Vol. 15, Marcel Dekker, USA, 1979

45. Marsh, H. and Forrest, M., "Theoretical and experimental approaches to the carbonization of coals and coal blends" In Coal and Coal Products: Analytical Characterization Techniques, ACS symposium series, American Chemical Society, USA, 1982
46. Mochida, I. and Korai, Y., "Carbonization in the tube bomb leading to needle coke: I. Cocarbonization of a petroleum vacuum residue and FCC-decant oil into better needle coke, Carbon", Vol. 27, No. 3, pp. 359-365, 1989.
47. Oya, A. et al, "Structural Studies of Coke Using Optical Microscopy and X-ray Diffraction", Fuel, Vol. 62, No. 3, pp. 275-278, 1983
48. Rørvik et al, "Characterization of Optical Texture in Cokes by Image Analysis", Light Metals: Proceedings of TMS Annual Meeting, USA, pp. 549-554, 2000
49. J. L. Eilertsen et al, "An Automatic Image Analysis of coke Texture", Carbon, Vol. 34, No. 3, pp. 375 – 385, 1996
50. B. D. Cullity, Elements of X-ray Diffraction, 2nd Edition, Addison-Wesley, USA, 1978
51. L. V. Azaroff, Elements of X-ray Crystallography, McGraw-Hill, USA, 1968
52. H. G. Jiang et al, "On the applicability of the x-ray diffraction line profile analysis in extracting grain size and micro-strain in nano-crystalline materials", Journal of Materials Research, Vol. 14, No. 2, pp. 549-559, 1999
53. Peter J. F. Harris, "Rosalind Franklin's Work on Coal, Carbon, and Graphite", Interdisciplinary Science Reviews, Vol. 26, No. 3, pp. 204-210, 2001
54. Rosalind E. Franklin, "The Interpretation of Diffuse X-ray Diagrams of Carbon", Acta Crystallographica, Vo. 3, pp. 107-120, 1950
55. R. Diamond et al, "New X-Ray Data on Coals" , Nature, Vol. 177, pp. 500–502, 1956

56. B. E. Warren and P. Bodenstein, "The Diffraction Pattern of Fine Particle Carbon Blacks", *Acta Crystallographica*, Vol. 18, pp. 282-289, 1965
57. Jinggeng Zhao et al, "Structural evolution in the graphitization process of activated carbon by high-pressure sintering", *Carbon*, Vol. 47, No. 3, pp. 744-751, 2009
58. ASTM D3461: Standard test method for Softening Point of Asphalt and Pitch (Mettler Cup-and-Ball Method), American Society for Testing and Materials, 2007.
59. F. Sanchez-Bajo and F. L. Cumbera, "The Use of the Pseudo-Voigt Function in the Variance Method of X-ray Line-Broadening Analysis", *Journal of Applied Crystallography*, Vol. 30, pp. 427 – 430, 1997
60. Iwashita, N. et al, "Specification for a standard procedure of X-ray diffraction measurements on carbon materials", *Carbon*, Vol. 42, No. 4, pp. 701-714, 2004
61. NIH Website @ <http://rsbweb.nih.gov/ij/download.html> retrieved on August 28, 2009
62. ImageJ Documentation @ <http://rsbweb.nih.gov/ij/docs/index.html> retrieved on August 28, 2009
63. I. S. Prifti and J. Dode, "A dwarf nonstable x-ray peak near the 002 line for cokes heat treated from 1100°C to 1600°C", Letter to Editor, *Carbon*, Vol. 25, No. 3, pp. 435-436, 1997
64. Kurganova, V. M. et al, "Conversion of Petroleum Product Boiling Points from Reduced Pressure to Atmospheric Pressure", *Chemistry and Technology of Fuels and Oils*, Vol. 15, No. 1-2, pp. 25-28, 1979
65. Blanco C. et al, "A comparative study of air-blown and thermally treated coal-tar pitches", *Carbon*, Vol. 38, No. 4, pp. 517-523, 2000

Appendix A
MASS BALANCES

Table A1. Digestion & Filtration Mass Balance							
Run	Coal In (g)	Solvent In (g)	THF In (g)	Samp. (g)	THF_S Out (g)	THF_Ins Out (g)	Digestion Balance
27	50	150	371.45	0.37	436.51	20.85	-24.84%
28	50	150	358.82	0.63	455.23	18.93	-17.70%
30	50	150	241.24	0	291.03	21.14	-41.35%
31	50	150	265.54	0.48	338.78	21.86	-28.92%
32	50	150	271.17	0.39	307.68	20.51	-43.40%
37	50	150	300.99	2.03	379	23.96	-23.70%
38	50	150	304.6	0.74	350.08	20.38	-35.94%
39	50	150	269.27	0.82	329.33	23.88	-32.55%
40	50	150	100	0.61	70.42	45.53	-157.38%
41	50	150	256.26	0.45	300.43	25.36	-39.85%
42	50	150	200	0.54	337.36	25.36	-10.11%
43	50	150	150	1.9	236.37	27.72	-31.58%
44	50	150	170	0.6	259.16	35.53	-25.30%
45	50	150	183.53	0.67	314.89	32.9	-10.06%
46	50	150	255.98	0.47	329.79	27.12	-27.59%
47	50	150	258.58	0.53	369.09	22.2	-17.04%
48	50	150	171.64	0.65	270.11	23.71	-26.21%
49	50	150	220.67	0.37	314.48	23.37	-24.38%
50	50	150	240	0.63	312.78	25.78	-29.72%

Table A2. Soxhlet Extraction Mass Balance					
Run	THF_Ins In(g)	THF In (g)	THF_S out(g)	THF_Ins Out (g)	Soxhlet Balance
27	20.85	240.49	207.17	15.02	-14.98%
28	18.93	255.06	226.14	12.77	-12.80%
30	21.14	199.84	162.34	17.74	-18.51%
31	21.86	226.03	179.01	16.92	-20.96%
32	20.51	230.78	180.85	13.32	-22.73%
37	23.96	293.97	208.86	14.54	-29.73%
38	20.38	323.33	271.96	17.36	-15.82%
39	23.88	199.96	176.43	18.23	-13.04%
40	45.53	196.02	171.39	27.02	-17.86%
41	25.36	338.42	205.62	16.29	-39.00%
42	25.36	236.79	207.73	18.76	-13.60%
43	27.72	219.61	205.04	13.08	-11.81%
44	35.53	283.23	222.21	25.85	-22.18%
45	32.9	236.68	187.55	25.68	-20.90%
46	27.12	210.43	173.1	17.8	-19.64%
47	22.2	220.25	191.14	15.37	-14.82%
48	23.71	274.82	214.68	22.46	-20.56%
49	23.37	251.96	200.33	21.63	-19.38%
50	25.78	250.14	259.62	15.09	-0.44%

Table A3. Distillation Mass Balance							
Run	Dist-Feed In(g)	Samp. (g)	Rec THF Out (g)	Oil Out (g)	Pitch Out (g)	THF Balance	Distillation Balance
27	643.68	4.74	300.97	192.53	135.37	-50.82%	-1.56%
28	681.37	0	355.44	184.64	128.95	-42.10%	-1.81%
30	453.37	7.19	158.2	143.06	75.46	-64.13%	-15.32%
31	517.79	5.68	182.6	222.98	88.67	-62.85%	-3.45%
32	488.53	0	248.48	133	88.35	-50.50%	-3.83%
37	587.86	0	321.59	126.92	131.8	-45.95%	-1.28%
38	622.04	0	283.81	95.27	115.47	-54.80%	-20.50%
39	505.76	0	321.23	206.58	33.41	-31.54%	10.97%
40	241.81	0	109.1	109.64	102.51	-63.14%	32.85%
41	506.05	0	358.11	52.11	87.46	-39.78%	-1.65%
42	545.09	0	359.85	82.43	92.36	-17.61%	-1.92%
43	441.41	0	263.47	49.97	102.36	-28.72%	-5.80%
44	481.37	0	296.4	121.48	59.74	-34.60%	-0.78%
45	502.44	0	315.35	117.93	61.3	-24.95%	-1.56%
46	502.89	0	325.66	44.37	105.74	-30.18%	-5.39%
47	560.23	0	368.95	30.12	124.95	-22.95%	-6.46%
48	484.79	0	299.03	127.57	33.28	-33.02%	-5.14%
49	514.81	0	345.78	115.96	42.52	-26.84%	-2.05%
50	572.4	0	332.79	12.36	191.16	-32.10%	-6.31%

Table A4. Overall Mass Balance					
Run	Coal In (g)	Solvent In (g)	Oil Out (g)	Pitch Out (g)	Product Balance
27	50	150	192.53	135.37	74.02%
28	50	150	184.64	128.95	63.50%
30	50	150	143.06	75.46	21.73%
31	50	150	222.98	88.67	67.37%
32	50	150	133	88.35	17.53%
37	50	150	126.92	131.8	37.65%
38	50	150	95.27	115.47	14.42%
39	50	150	206.58	33.41	29.52%
40	50	150	109.64	102.51	19.89%
41	50	150	52.11	87.46	-21.85%
42	50	150	82.43	92.36	-2.96%
43	50	150	49.97	102.36	-22.89%
44	50	150	121.48	59.74	-9.09%
45	50	150	117.93	61.3	-10.05%
46	50	150	44.37	105.74	-24.71%
47	50	150	30.12	124.95	-22.20%
48	50	150	127.57	33.28	-19.25%
49	50	150	115.96	42.52	-20.57%
50	50	150	12.36	191.16	2.07%

Table A5. Ash Balance

Run	Weight of coal in (g)	%Ash of coal	Ash in Coal (g)	Weight of Residue Out (g)	%Ash of Residue	Ash in Residue (g)	(Out - IN)/IN
7	60	15.54%	9.324	27.34	32.57%	8.9046	-4.50%
8	60	15.54%	9.324	19.82	35.61%	7.0579	-24.30%
9	60	15.54%	9.324	19.25	40.00%	7.7000	-17.42%
11	60	15.54%	9.324	45.63	15.23%	6.9494	-25.47%
12	60	15.54%	9.324	46.1	18.47%	8.5168	-8.66%
13	60	15.54%	9.324	23.64	35.67%	8.4324	-9.56%
14	60	15.54%	9.324	19.81	40.33%	7.9892	-14.32%
15	60	15.54%	9.324	28.97	36.31%	10.5185	12.81%
16	60	15.54%	9.324	26.85	33.84%	9.0862	-2.55%
17	60	15.54%	9.324	19.96	45.73%	9.1286	-2.10%
18	60	15.54%	9.324	23.16	33.95%	7.8628	-15.67%
19	60	15.54%	9.324	27.67	32.61%	9.0242	-3.22%
20	60	15.54%	9.324	30.76	21.34%	6.5642	-29.60%
21	50	15.54%	7.77	26.65	16.48%	4.3919	-43.48%
22	45	15.54%	6.993	19.62	15.25%	2.9921	-57.21%
23	60	15.54%	9.324	40.22	16.87%	6.7851	-27.23%
24	50	15.54%	7.77	20.89	19.66%	4.1070	-47.14%
25	50	15.54%	7.77	19.98	30.27%	6.0479	-22.16%
26	50	15.54%	7.77	19.06	42.32%	8.0662	3.81%
27	50	15.54%	7.77	15.02	28.74%	4.3167	-44.44%
28	50	15.54%	7.77	12.77	41.85%	5.3442	-31.22%
30	50	15.54%	7.77	17.74	32.60%	5.7839	-25.56%
31	50	15.54%	7.77	16.92	30.73%	5.1987	-33.09%
32	50	15.54%	7.77	13.32	32.47%	4.3250	-44.34%
37	50	15.54%	7.77	14.54	39.17%	5.6955	-26.70%
38	50	15.54%	7.77	17.36	33.18%	5.7599	-25.87%
39	50	15.54%	7.77	18.23	35.74%	6.5146	-16.16%
40	50	15.54%	7.77	27.02	25.56%	6.9063	-11.12%
41	50	15.54%	7.77	16.29	33.36%	5.4340	-30.06%
42	50	15.54%	7.77	18.76	35.36%	6.6335	-14.63%
43	50	15.54%	7.77	13.08	0.4817	6.300636	-18.91%
44	50	15.54%	7.77	25.85	21.37%	5.5241	-28.90%
45	50	15.54%	7.77	25.68	23.21%	5.9603	-23.29%
46	50	11.36%	5.68	17.8	35.25%	6.2745	10.47%
47	50	11.36%	5.68	15.37	39.68%	6.0988	7.37%
48	50	11.36%	5.68	23.71	28.60%	6.7811	19.38%

Appendix B
SELECTED OPTICAL MICROGRAPHS

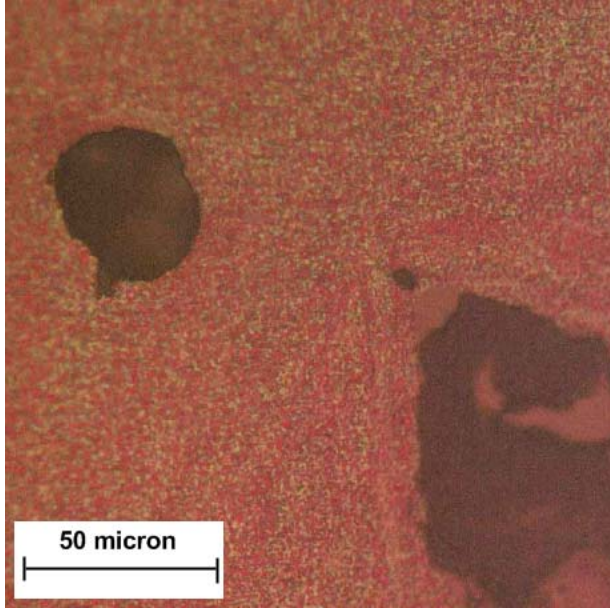


Figure B1.
Optical Micrograph of Coke #6

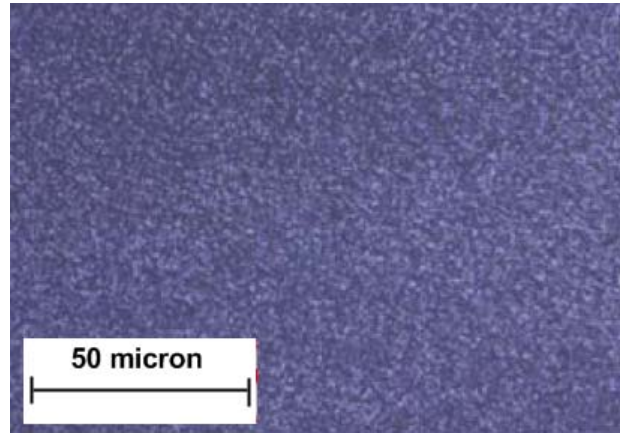


Figure B2.
Optical Micrograph of Coke #7

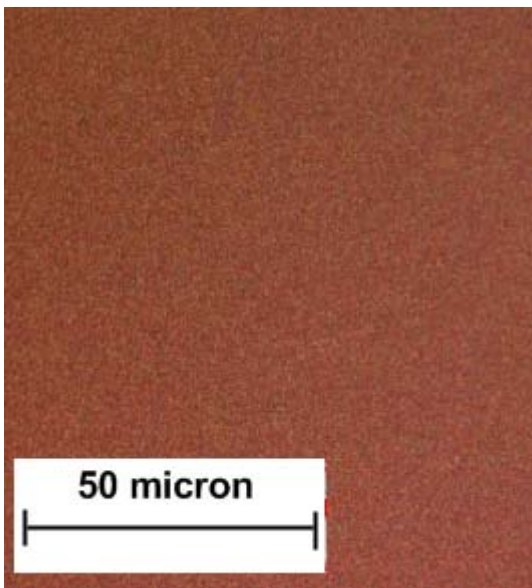


Figure B3.
Optical Micrograph of Coke #8

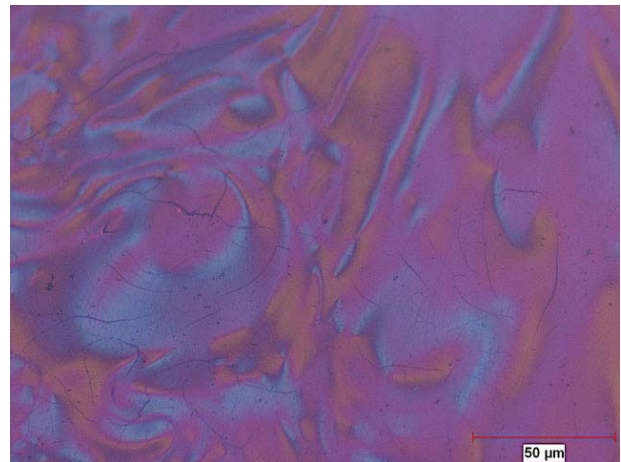


Figure B4.
Optical Micrograph of Coke #9B2

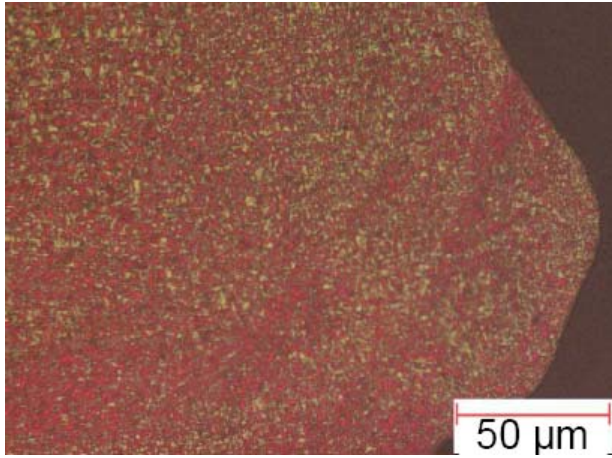


Figure B5.
Optical Micrograph of Coke #11B2

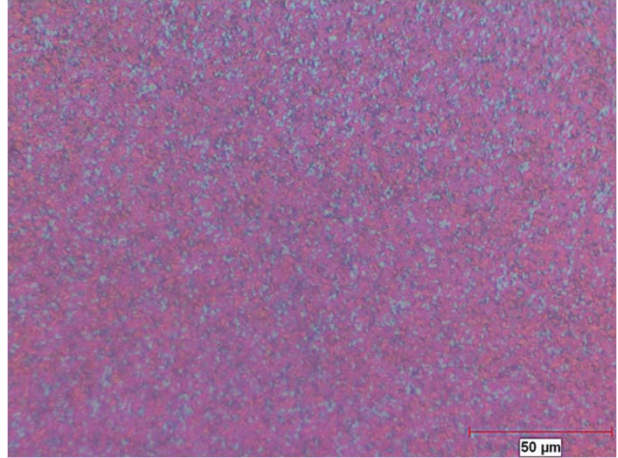


Figure B6.
Optical Micrograph of Coke #21B2

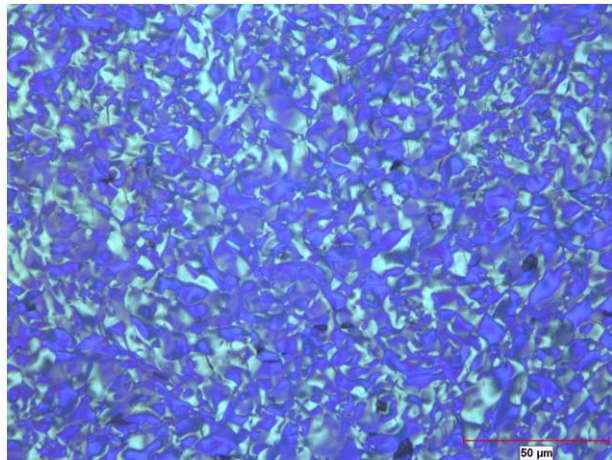


Figure B7.
Optical Micrograph of Coke #22B1

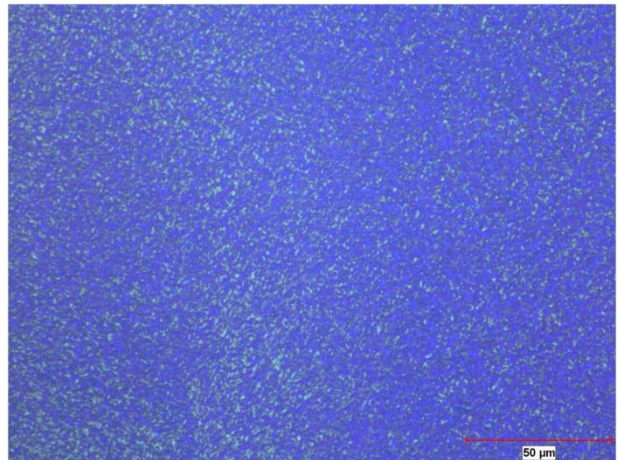


Figure B8.
Optical Micrograph of Coke #23B2

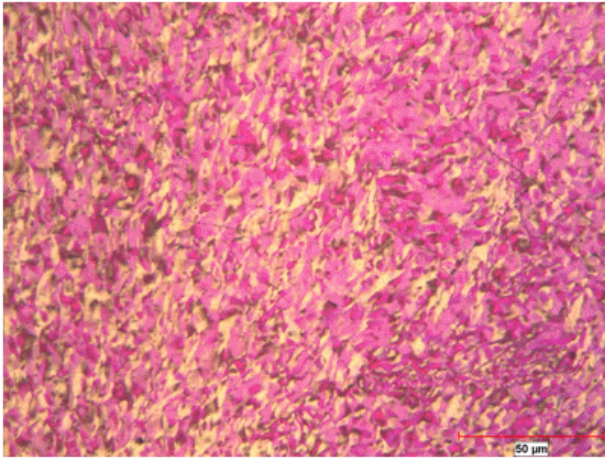


Figure B9.
Optical Micrograph of Coke #24B1

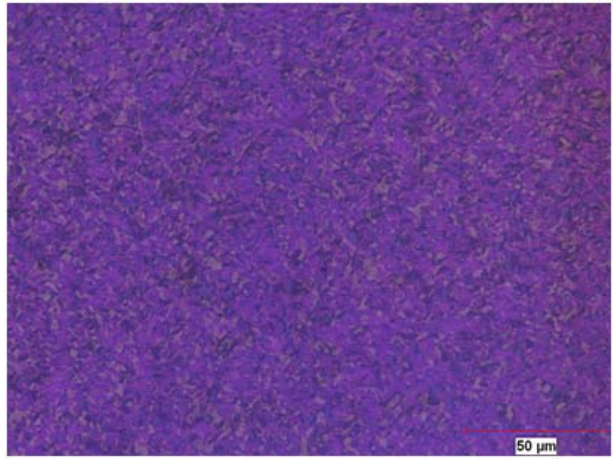


Figure B10.
Optical Micrograph of Coke #25

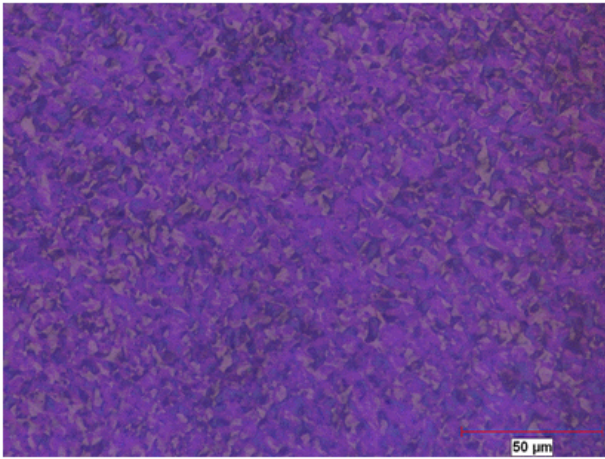


Figure B11.
Optical Micrograph of Coke #22B1

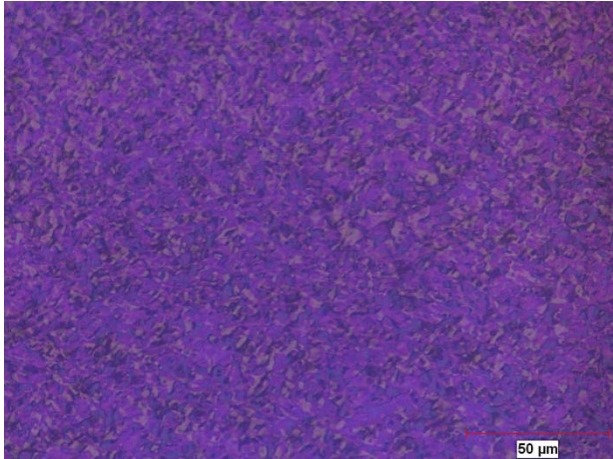


Figure B12.
Optical Micrograph of Coke #28B1

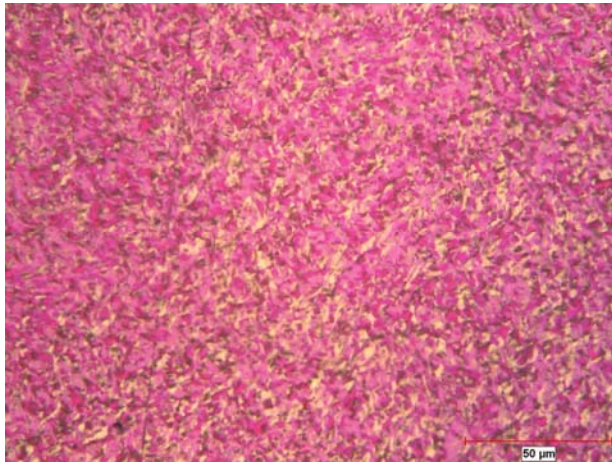


Figure B13.
Optical Micrograph of Coke #28B2

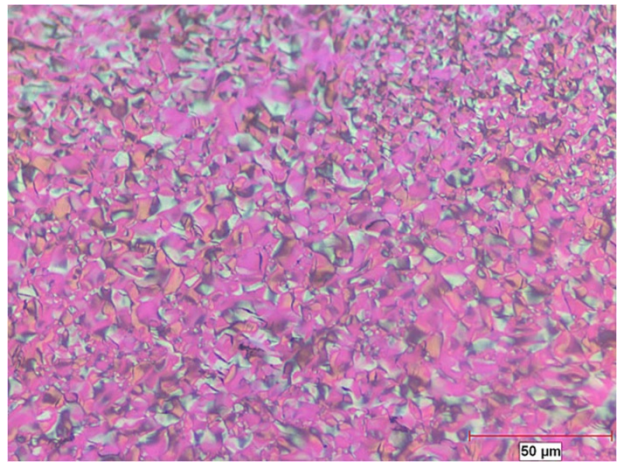


Figure B14.
Optical Micrograph of Coke #30B2

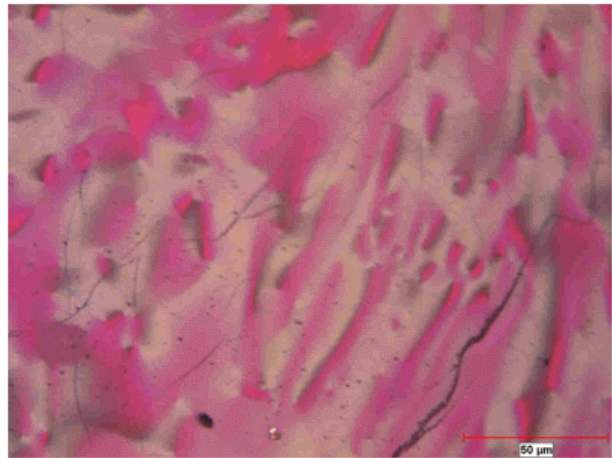


Figure B15.
Optical Micrograph of Coke #31B1

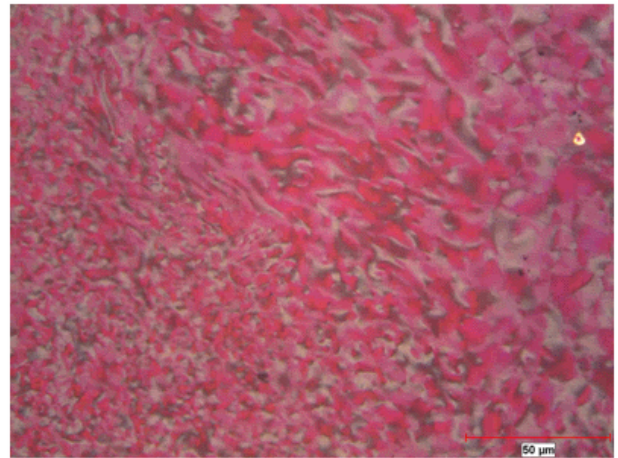


Figure B16.
Optical Micrograph of Coke #37

APPENDIX C
TYPICAL X-RAY DIFFRACTION CALCULATIONS

Table C1. Line profile analysis of (002) reflection of several cokes							
Coke	$2\theta^\circ$	η	β_c	β_g	R^2	$L_c(\text{\AA})$	Strain(ϵ)
7	25.69	0.3963	7.225316	8.49811	95.41%	11	0.162617
9B2	25.58	0.4312	3.177102	3.359752	93.17%	26	0.064577
21	25.65	0.9123	6.110672	1.272791	96.27%	13	0.024395
24	25.89	0.7338	3.703939	1.638628	98.12%	22	0.031106
31B1	25.98	0.9828	4.343633	0.413636	91.27%	19	0.007824
31B2	25.88	0.4621	2.235847	2.166198	85.13%	36	0.041137
38B1	25.37	0.503919	3.673951	3.127663	94.72%	22	0.060631
37	25.92	0.5614	4.959436	3.57989	97.36%	16	0.067875